THE REGULATION OF PHYTOPLANKTON PRODUCTIVITY IN A SHALLOW, TURBID, OLIGOTROPHIC LAKE

VOLUME II: FIGURES AND TABLES

By

EDWARD GORDON JOHN

AKHURST

VOLUME 2

CONTENTS

Chapter 1 Introduction

Page No.

Figures

1.1. Bathymetric map of Lake Midmar showing location of meteorological (M) and sampling station (S) in main basin. 1

Chapter 2 Materials and Methods

Figures

2.1 Mgeni river catchment and its location in southern Africa. 2

2.2 a) Lake Midmar showing extent of main basin for heat budget purposes and position of transect (A.A) used to construct a cross-sectional profile of main basin.
b) Cross-sectional profile of main basin. 3

Tables

2.1 Morphometric and hydrological characteristics of Lake Midmar at Full Supply Level (FSL). 4

Chapter 3 Thermal characteristics and mixing regime of Lake Midmar

Figures

3.1 Annual variation of daily integrals of global radiation reaching the ground on clear days in the southern hemisphere. 5

3.2 Average annual number of days, a) with no sunshine (overcast days); b) with 10% or less of the possible sunshine duration (dull days); c) with 50% or more of the possible sunshine duration (sunny days) and d) with 90% or more of the possible sunshine duration (bright days). 6

3.3 Annual variation in daily values ($J/m^2/d$) for the period November 1980 to October 1981 of : a) net incoming solar radiation (Qs - Qr) and b) latent heat (Qe). 7

c) net longwave radiation (Qb) and d) sensible heat exchange (Qh). 8

3.4 Annual changes in the heat content (kJ/m^2) for the period November 1980 to October 1981. 9

3.5 Annual variation in daily values ($J/m^2/d$) for the period November 1980 to October 1981 of a) heat storage (Qt) and b) net advection. 10

3.6 Annual variation in monthly mean daily values ($J/m^2/d$) for components of the energy balance equation in three lakes

a) Lake Mendota 11

b) Lake le Roux 12

c) Lake Midmar 13

3.7 Annual variation in a) Mean daily air (A), surface water (0-3m, S) and bottom water (b) temperatures for the interval between successive sampling days for the period November 1980 to October 1981. 14

b) Monthly mean daily air (A), surface water (S) and bottom water (B) temperatures for the period November 1980 to October 1981. 15

3.8 Annual variation in mean daily wind speed (m/sec) for the period November 1980 to October 1981. 16

3.9 Annual diel variation in hourly mean wind speed (m/sec) in relation to diel variation in selected months

a) August, September, October and November; 17

b) December, January, February and March. 18

3.10 Wind roses to show daily mean angular distribution of wind for selected months, August through to January. 19

3.11 Annual variation in daily values of stability (J/m^2) for the period November 1980 to October 1981. 20

3.12 Annual variation in work of the wind (J/m^2) for the period November 1980 to October 1981. 21

3.13 Examples of direct work curves used to determine the mixing depth . 22

3.14 Annual variation in mixing depth in relation to lake bottom at main basin station, for the period November 1980 to October 1981. 23

3.15 a) Temperature profiles on two sampling days, 2nd December 1980 and 14th July 1981. 24
b) Corresponding direct work curves for 2nd December 1981 and 14th July 1981. 24

3.16 Hypsographic curve for Lake Midmar. 25

3.17 Diurnal variation in depth distribution of density gradients measured on 23rd December 1980 at 06.00, 10.00, 14.00 and 18.00 hours. 26

3.18 Annual variation in Wedderburn number (log10) for the period November 1980 to October 1981. 27

3.19 Isotherm plot for Lake Midmar for the period November 1980 to October 1981. 28

3.20 Annual variation in stability (J/m^2) in Hartbeespoort dam (solid line) and Lake Midmar (dotted line) for the period November 1980 to October 1981. 29

3.21 Isotherm plot for Lake Midmar for the period November 1977 to October 1978. 30

Tables

3.1 Selected morphometric and thermal characteristics of some southern African impoundments. 31

3.2 Heat budget characteristics for a range of lakes from different latitudes. 32

3.3 Annual range of energy flux values for incident solar radiation, latent heat and heat storage; the Birgean Annual Heat Budget and maximum heat storage flux for Lakes Mendota and Midmar. 32

3.4 Mean annual sunshine duration (hours) and number of days with no sun, overcast (1-10%), dull (11-49%), sunny (50-89% or bright (90-100% of possible sunshine duration) conditions at two meteorological stations, Fauresmith (F) and Cedara (C). 33

3.5 The maximum fetch (km) for winds from a particular direction at Lake Midmar. 33

3.6 Range of wind speeds used in Weather Bureau and Beaufort classification schemes. 33

Chapter 4 Underwater light and phosphorus dynamics in Lake Midmar

Figures

4.1 Relative size of the major phosphorus pools in a lake water - sediment system. 34

4.2 Changes in monthly mean lake volume (x10^6 m^3) and monthly mean river flow (x10^6 m^3) in the Mgeni river for the period October 1980 to September 1982. 35

4.3 Annual variation in depth of the euphotic zone (m) and river loading of total suspended solids (kg TSS/wk) for the period November 1980 to October 1981. 36

4.4 Annual variation in a) the vertical attenuation coefficient for downwelling PAR irradiance (K_d(PAR), ln units/m) and b) depth of the euphotic zone (m), for the period October 1980 to September 1981 and October 1982 to September 1983. 37

4.5 Absorbance scans over the PAR spectral range (400-700nm) for filtered and unfiltered lake water after correction for absorption by distilled water. 38

4.6 Annual variation in the vertical attenuation coefficient for downwelling blue (B), green (G) and red (R) light for the period October 1982 to September 1983. 39

4.7 Histograms to show distribution of $Z_{eu}:Z_m$ ratio values in 1980-81 and 1982-83. 40

4.8 Annual variation in the total phosphorus content of the water column and river inputs of total phosphorus for the period November 1980 to October 1981. 41

4.9 Annual variation in the net external load (NEL), sediment flux (SF) and net internal load (NIL) of total phosphorus for the period November 1980 to October 1981. 42

4.10 Annual variation in mean total phosphorus (TP) and soluble reactive phosphorus (SRP) concentrations in the water column for 1980-81 and 1982-83. 43

4.11 Sources of inorganic particulate material (solid boxes) and processes influencing inorganic turbidity in Lake Midmar. 44

Tables

4.1 Means, ranges and coefficients of variation for the vertical attenuation coefficient for downwelling PAR irradiance K_d(PAR) and depth of the euphotic zone in 1980-81 and 1982-83. 45

4.2 Regression constants for regression analysis of K_d(PAR) with phytoplankton standing crop (as B, mg Chl $\underline{a}/m^3$, and ΣB, mg Chl $\underline{a}/m^2$), total suspended solids and mean wind speed on the day prior to sampling. 45

4.3 Means and ranges of vertical attenuation coefficients for downwelling blue, green and red light in 1980-81 and 1982-83. 46

4.4 Planimetrically determined amounts of total phosphorus exchanged with sediments for the period November 1980 to October 1981. 46

Chapter 5 Factors influencing phytoplankton productivity in Lake Midmar.

Figures

5.1 General form of productivity-depth profile in lakes. 47

5.2 a) The relationship between the productivity-depth profile and the rectangle of equivalent area generated by Talling's model to predict ΣA, the area under the productivity-depth profile. 48

b) General relationship between specific productivity (mgC/mg Chl a/h) and irradiance to show derivation of P_e, the photosynthetic efficiency, l_K, the photosynthetic saturation parameter and l_{opt}, the optimum irradiance required for the light saturated rate of production (P_{max}). 48

c) Diagrams to show the influence on values of l_K of changes in i) P_e, (with maximum specific productivity constant) and ii) maximum specific productivity (with P_e constant). 48

5.3 Changes in productivity parameters, P_{max} (the light saturated rate of production) and ΣA (planimetrically determined integral rate of production) in relation to changes in river inputs of suspended solids (TSS) for the period November 1980 to May 1981. 49

5.4 Histograms to show number of occasions (as frequency) when P_{max} was measured at a particular depth in 1980-81 and 1982-83. 50

5.5 Annual variation in planimetrically determined values of ΣA (ΣA_p) in 1980-81 and 1982-83. 51

5.6 Annual variation in planimetrically determined values of ΣA (ΣA_p) and predicted values of ΣA, using Talling's model (ΣA_T) in a) 1980-81 52
b) 1982-83. 53

5.7 Annual variation in the subsurface irradiance (I'_0) during incubation period (10.00 to 14.00 hours) in 1980-81 and 1982-83. 54

5.8 Annual variation in values of the photosynthetic saturation parameter (I_K) in 1980-81 and 1982-83 55

5.9 Annual variation in values of photosynthetic efficiency (P_e) in 1980-81 and 1982-83. 56

5.10 Annual variation in a) phytoplankton standing crop (as mean chlorophyll concentration in the euphotic zone (B)) and b) assimilation number in 1980-81 and 1982-83 57

5.11 The relationship between productivity and irradiance determined by incubating samples collected at 5m, at 0.5m for different periods of time (one, two, three or four hours) on two different occasions. 58

5.12 Annual variation in actual values of ΣA obtained using static incubation flasks (ΣA_p) and calculated values for mixed samples (ΣA_{MIXED}) in a) 1980-81 59
b) 1982-83. 60

5.13 Annual variation in mean irradiance at depth where the light saturated rate of production was measured (I_{opt}) in 1980-81 and 1982-83. 61

5.14 Annual variation in mean water temperature of the euphotic zone in 1980-81 and 1982-83. 62

5.15 Matrix to show the range of possible physiological states in phytoplankton, on any sampling day, as a result of the influence of exposure to favourable light and/or nutrient conditions prior to sampling. 63

Tables

5.1 Means, ranges and coefficients of variation (CV) for the ratio $Z_{eu}:Z_m$ and depth of the euphotic zone (Z_{eu}) in 1980-81 and 1982-83. 64

5.2 Variation in predictive capability of Talling's model in relation to I_K value on selected occasions. 64

5.3 Regression constants for simple and stepwise regression analysis of I_K with P_e. assimilation number, mean irradiance during incubation (I_{IN}) and one day (I_{PRE1}), two (I_{PRE2}) or three (I_{PRE3}) days prior to estimation of I_K, and temperature in 1980-81 and 1982-83. 65

5.4 Regression constants for simple regression analysis of P_e with assimilation number, mean irradiance during incubation (I_{IN}) and one day (I_{PRE1}), two (I_{PRE2}) or three (I_{PRE3}) days prior to estimation of P_e, and temperature in 1980-81 and 1982-83. 66

5.5 Regression constants for stepwise regression analysis of predicted values of ΣA (ΣA_T) with individual components of Talling's model in 1980-81 and 1982-83. 66

5.6 Regression constants for stepwise regression analysis of the light saturated rate of production (P_{max}) with assimilation number and phytoplankton standing crop (as mean chlorophyll concentration in the euphotic zone, B), in 1980-81 and 1982-83. 67

5.7 Variation in predictive capability of Talling's model in relation to values of assimilation number, phytoplankton standing crop (as mean chlorophyll concentration in the euphotic zone, B), I_K and K_d(PAR) on selected occasions. 67

5.8 Regression constants for simple regression analysis of assimilation number with mean irradiance during incubation (I_{IN}) and one day (I_{PRE1}), two (I_{PRE2}) or three days (I_{PRE3}) prior to sampling, temperature and K_d(PAR) in 1980-81 and 1982-83. 68

5.9 Regression constants for simple regression analysis of mean irradiance at depth where the light saturated rate of production was measured (I_{opt}) with mean irradiance during incubation (I_{IN}) and one day (I_{PRE1}), two (I_{PRE2}) or three days (I_{PRE3}) prior to sampling, in 1980-81 and 1982-83. 68

5.10 A comparison of Lake Midmar primary productivity data (as values of P_{max} and ΣA) with a range of African lakes. 69

5.11 Regression constants for simple regression analysis of actual values of ΣA, assimilation number, the photosynthetic saturation parameter (I_K) and the photosynthetic efficiency (P_e) with the ratio $Z_{eu}:Z_m$ and water column stability in 1980-81 and 1982-83. 70

Chapter 6 Discussion

Figures

6.1 Stylised seasonal progression of change in standing populations of three species of phytoplankton in relation to the cycle of stratification and destratification of the water column in a) a classicical stratified lake and b) a stratified lake exhibiting atelomixis. 71

6.2 Stylised seasonal progression of changes in standing populations of summer phytoplankton assemblqages in relation to energy associated with wind-induced vertical mixing events in four different lake types. a) Continuous polymictic tropical lake; b) Classical warm monomictic lake; c) Classical warm monomictic lake exhibiting atelomixis; d) Lake Midmar, a discontinuous polymictic lake. 72

6.3 a) A hypothetical 3-D matrix with axes defined by i) mixing /stability, ii) the concentrations of nitrogen (N) and phosphorus (P) and iii) the N/P ratio which accommodates most phytoplankton assemblages. 73

b) The three directions of periodic progression from one dominant assemblage to another 73

6.4 Annual average solar irradiance (300-2200nm) reaching the earth's surface. 74

6.5 Diagrammatic representation of the three directions of periodic progression from one dominant phytoplankton assemblage to another.

a) as proposed by Reynolds (1984b). 75

b) as proposed by this study. 75

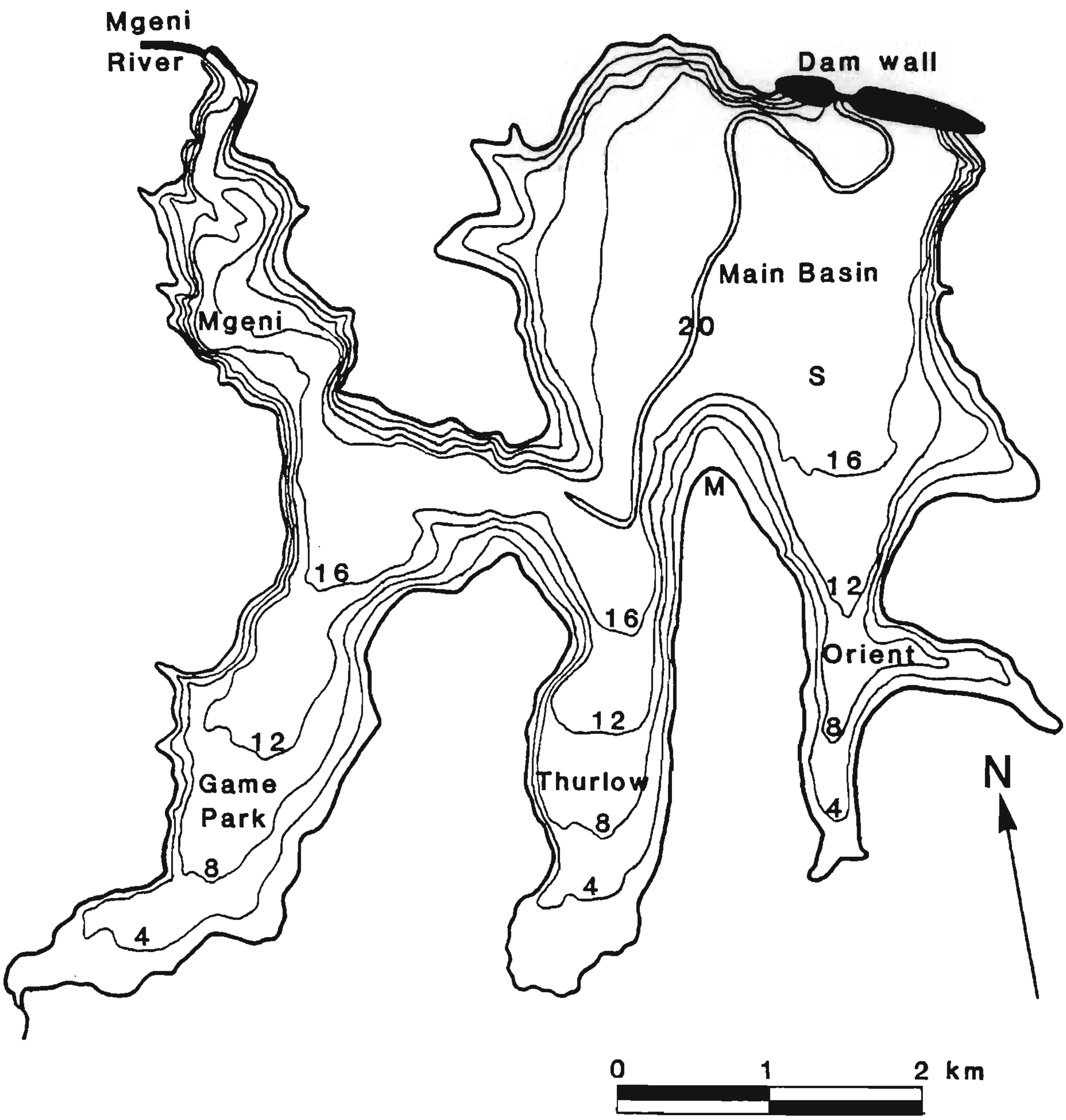

Figure 1.1. Bathymetric map of Lake Midmar showing location of meteorological (M) and sampling station (S) in main basin. Contour lines at 4m intervals.

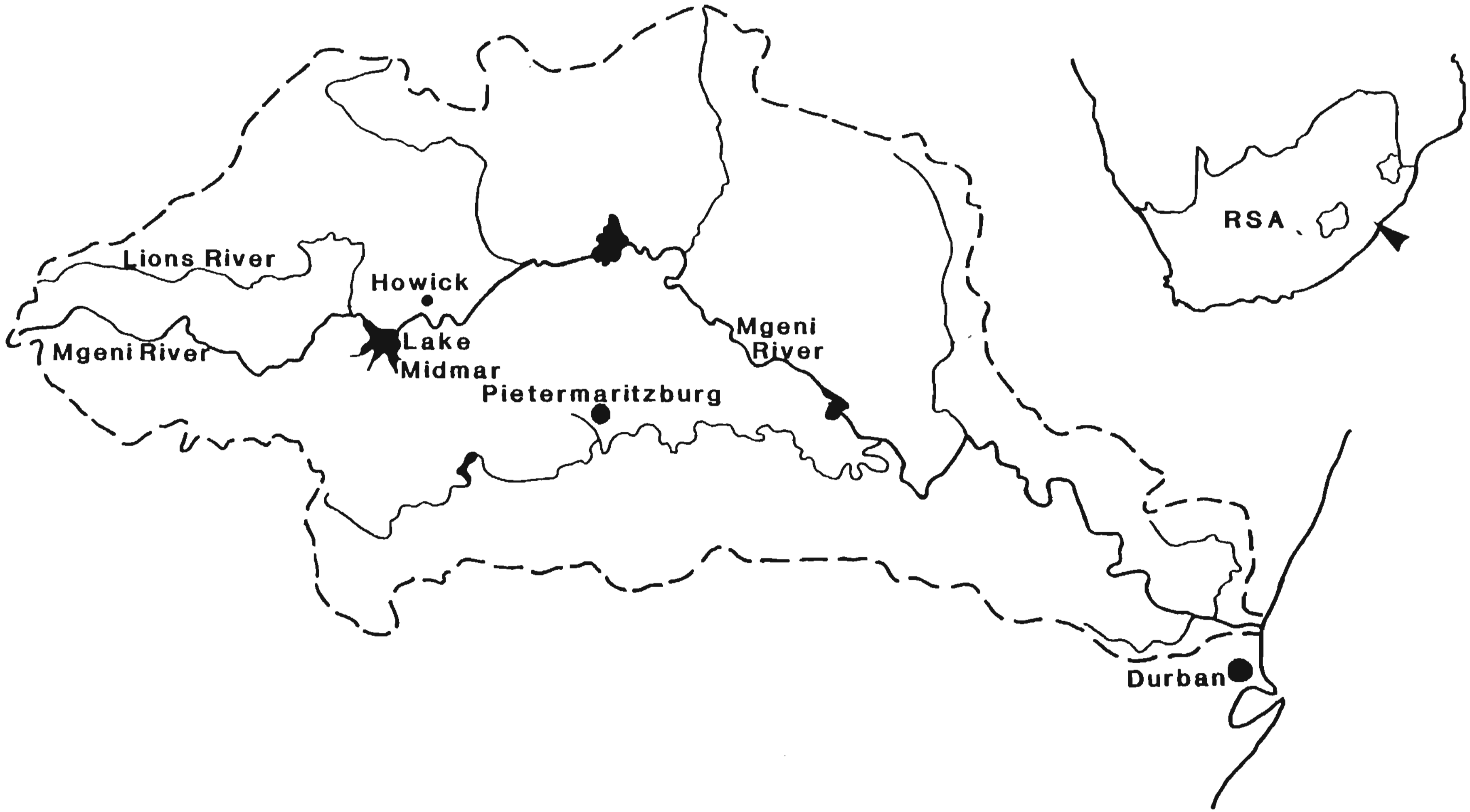

Figure 2.1. Mgeni river catchment and its location in southern Africa.

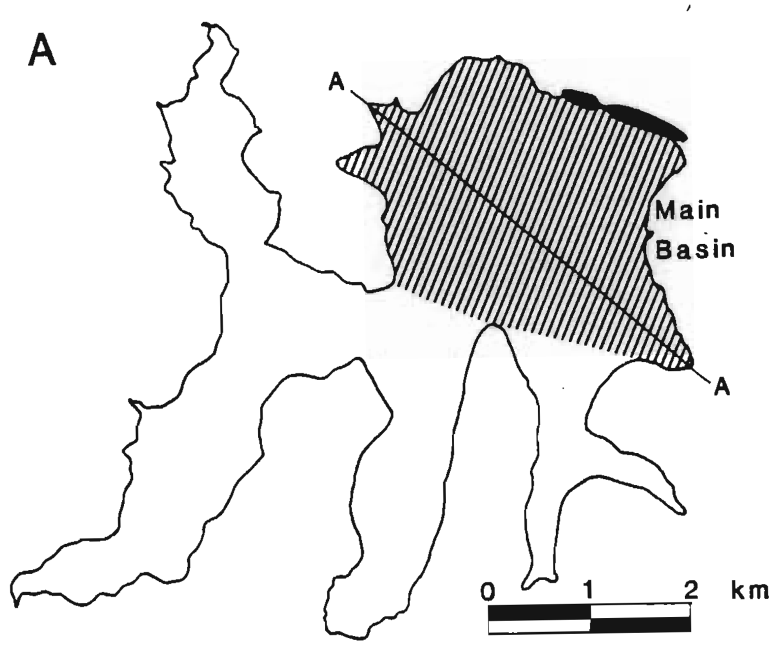

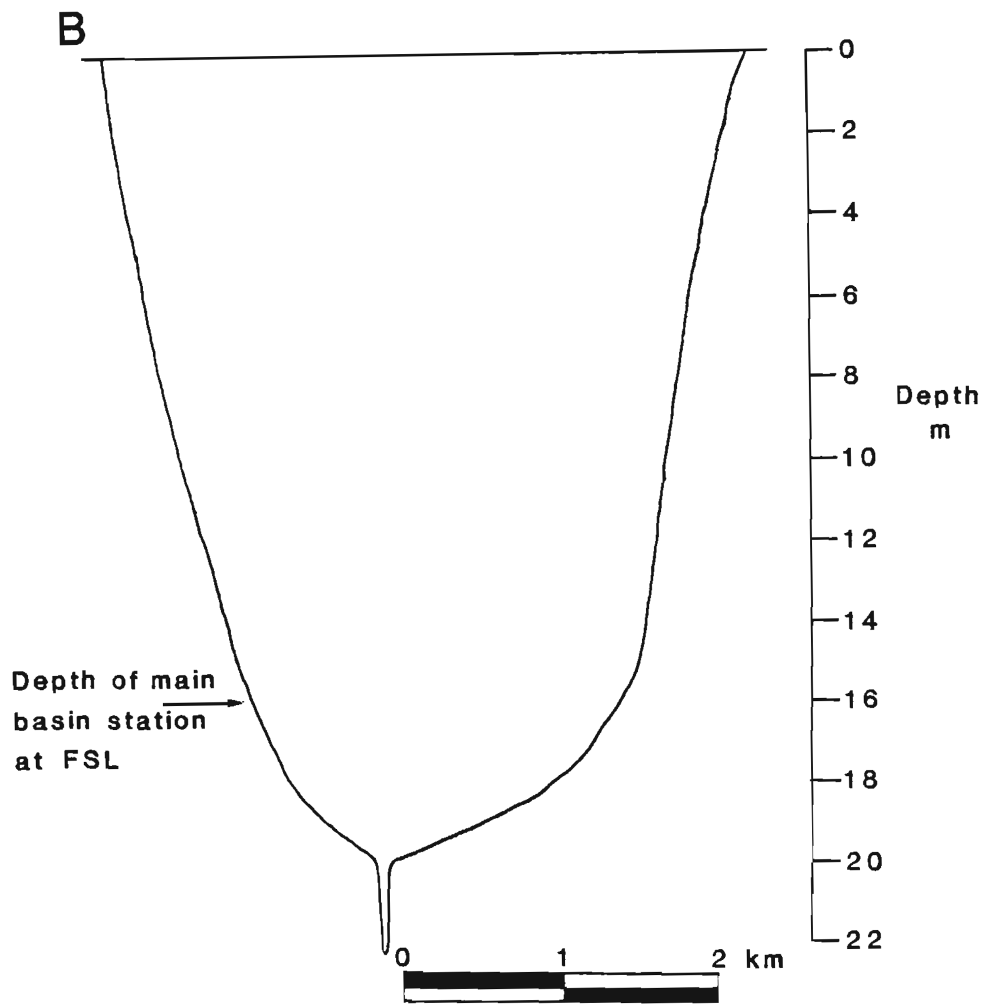

Figure 2.2. a) Lake Midmar showing extent of main basin for heat budget purposes and position of transect (A.A) used to construct a cross-sectional profile of main basin.

b) Cross-sectional profile of main basin.

Table 2.1. Morphometric and hydrological characteristics of Lake Midmar at Full Supply Level (FSL). From: Archibald et al (1980).

Catchment area	928 km^2
Volume	117.2 $x10^6$ m^3
Surface area	15.59 km^2
Maximum depth	22.3 m
Mean depth	11.4 m
Mean retention time	0.87 year

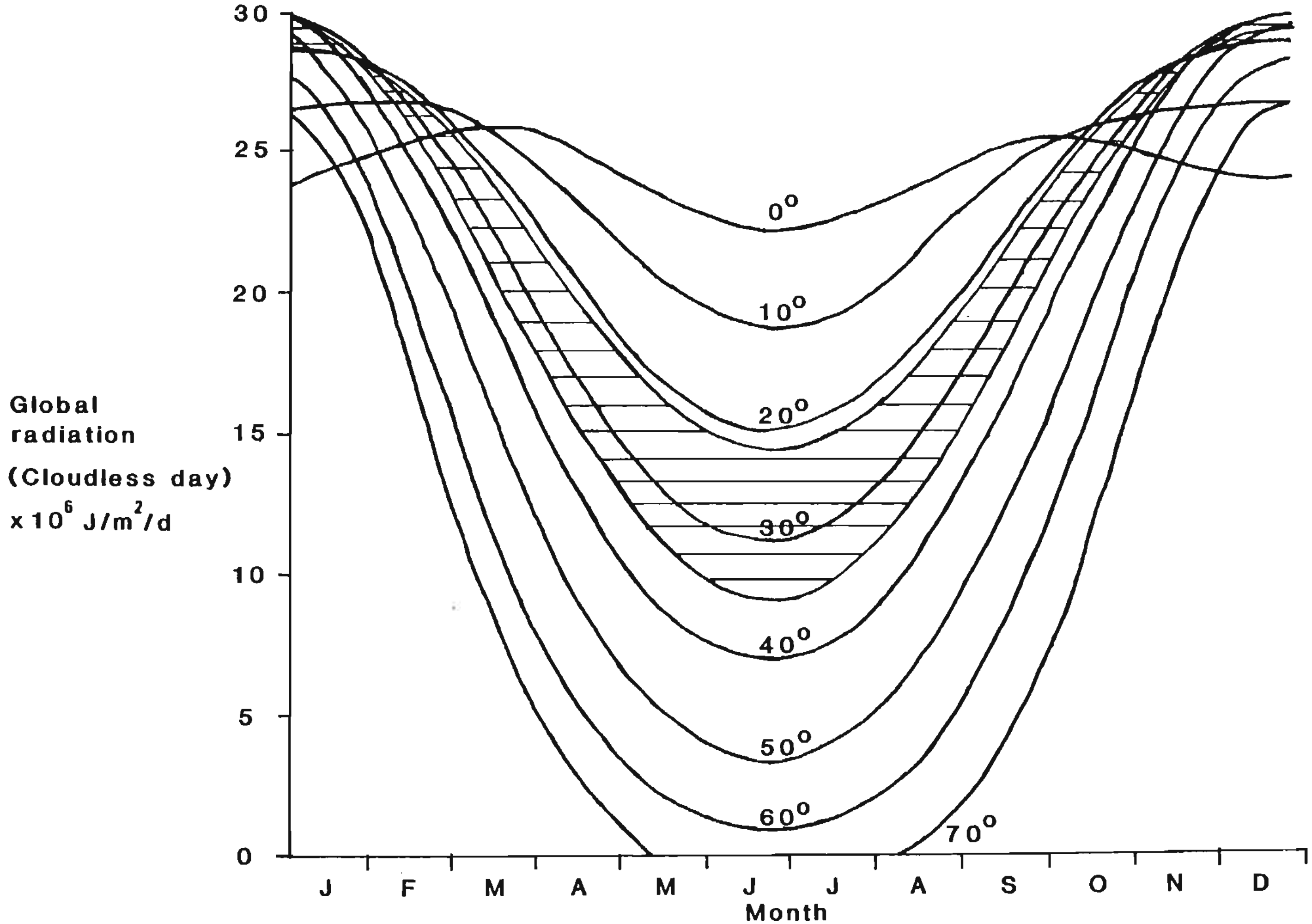

Figure 3.1. Annual variation of daily integrals of global radiation reaching the ground on clear days in the southern hemisphere. Shaded area corresponds to the latitudinal range of South Africa. From: Straskraba (1980).

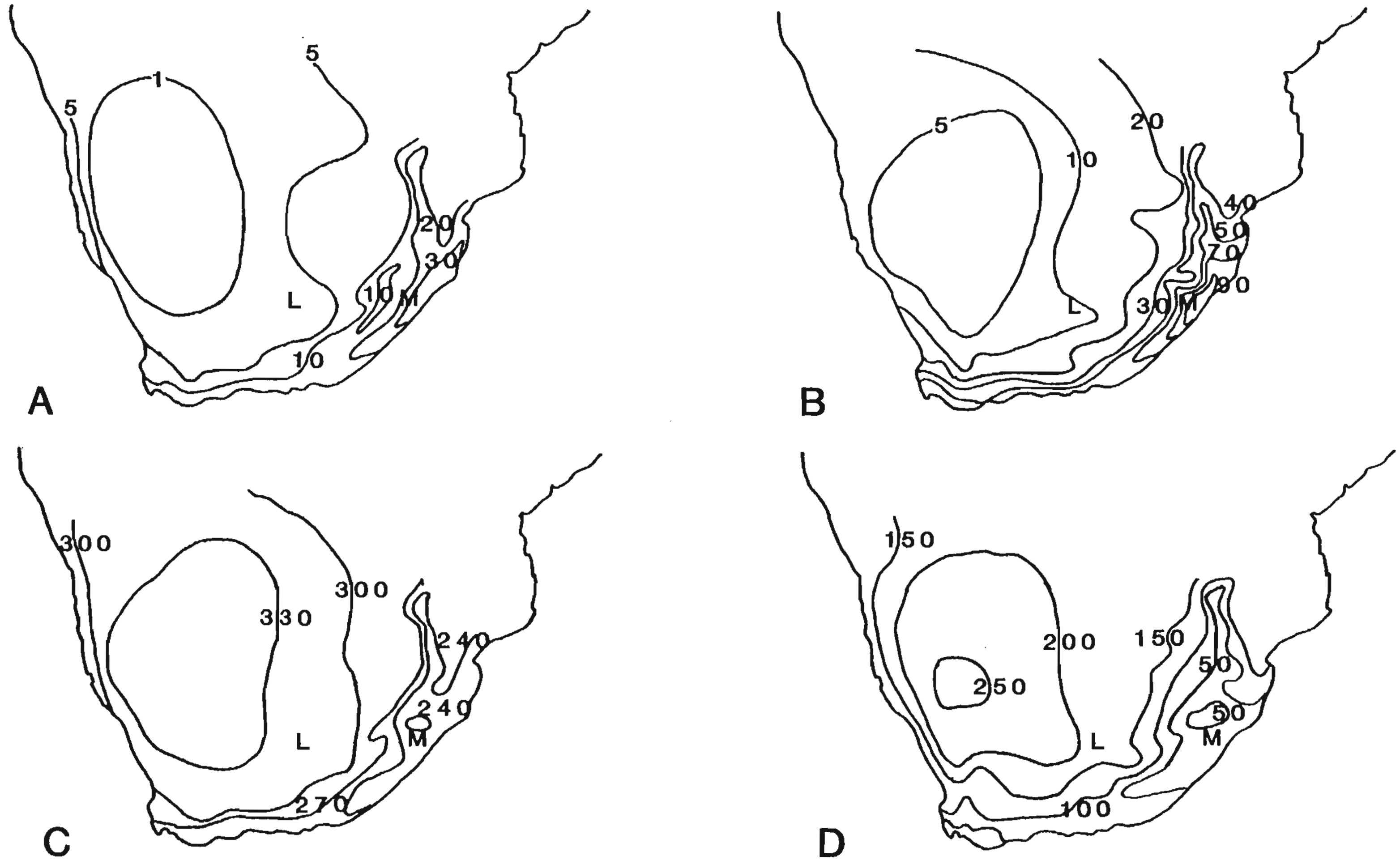

Figure 3.2. Average annual number of days, **a)** with no sunshine (overcast days); **b)** with 10% or less (dull days); **c)** with 50% or more (sunny days) and **d)** with 90% or more (bright days), of the possible sunshine duration. Location of Lakes le Roux and Midmar indicated by L and M respectively. From: Schulze (1965).

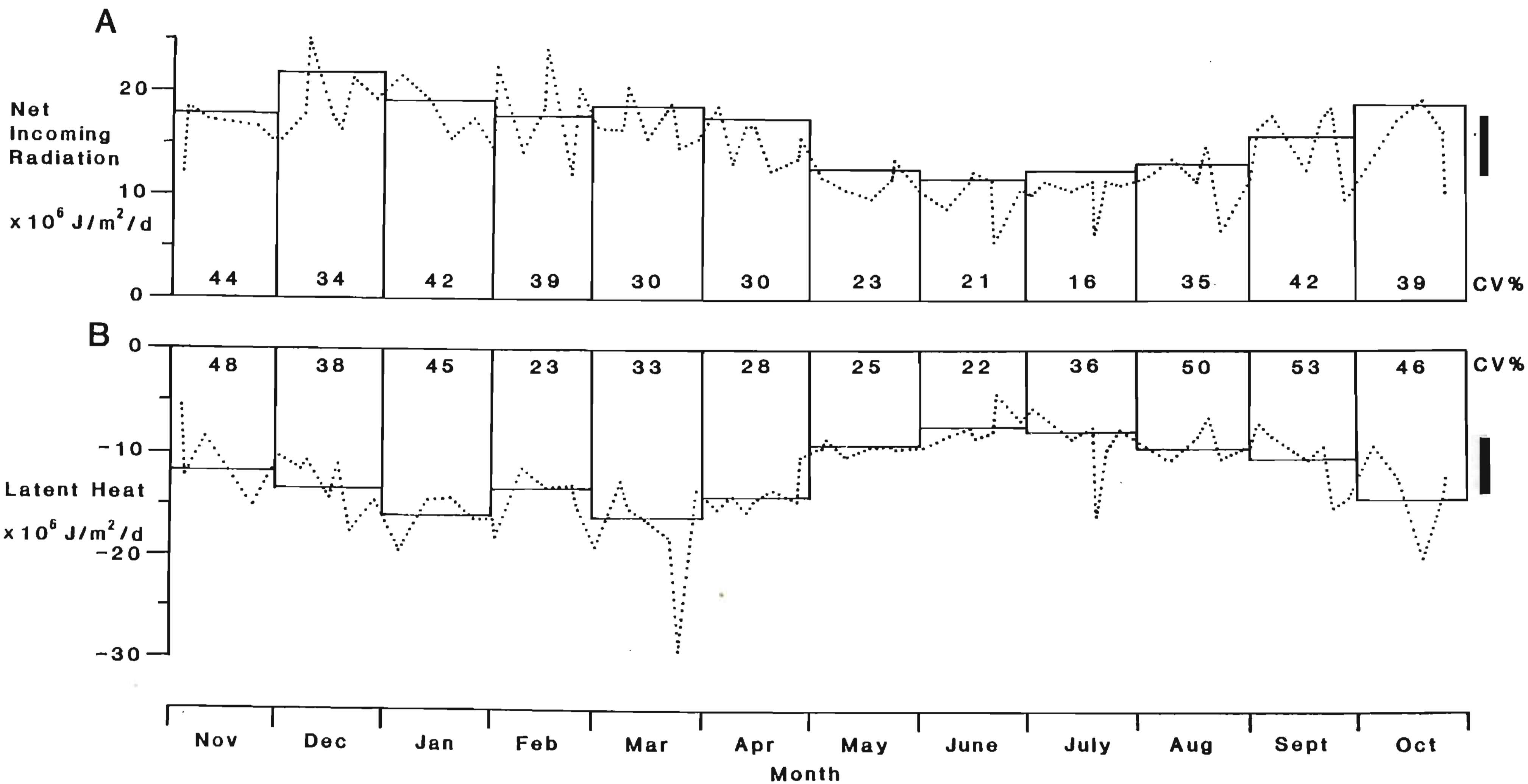

Figure 3.3. Annual variation in daily values ($J/m^2/d$) of **a)** net incoming solar radiation (Qs - Qr); **b)** latent heat (Qe) for the period November 1980 to October 1981. Solid line = monthly mean daily value; Dotted line = mean daily value for the interval between successive sampling days; CV = Coefficient of variation (%) for monthly mean; Vertical bar = Least Significant Difference (LSD) at the <0.05 probability level for monthly means.

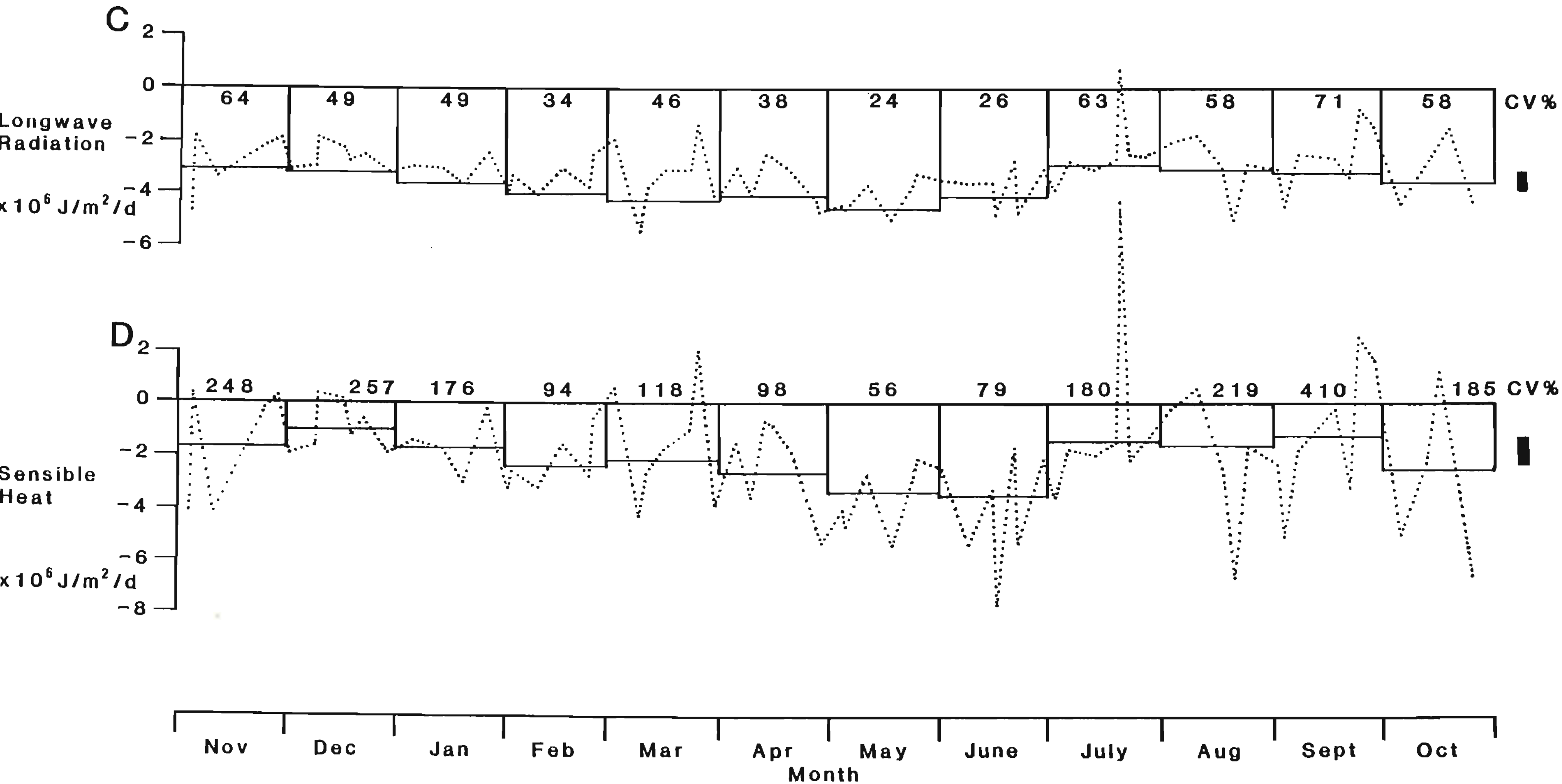

Figure 3.3. Annual variation in daily values ($J/m^2/d$) of **c)** net longwave radiation (Q_b) and **d)** sensible heat exchange (Q_h) for the period November 1980 to October 1981. Solid line = monthly mean daily value; Dotted line = mean daily value for the interval between successive sampling days; CV = Coefficient of variation (%) for monthly mean; Vertical bar = Least Significant Difference (LSD) at the <0.05 probability level for monthly means.

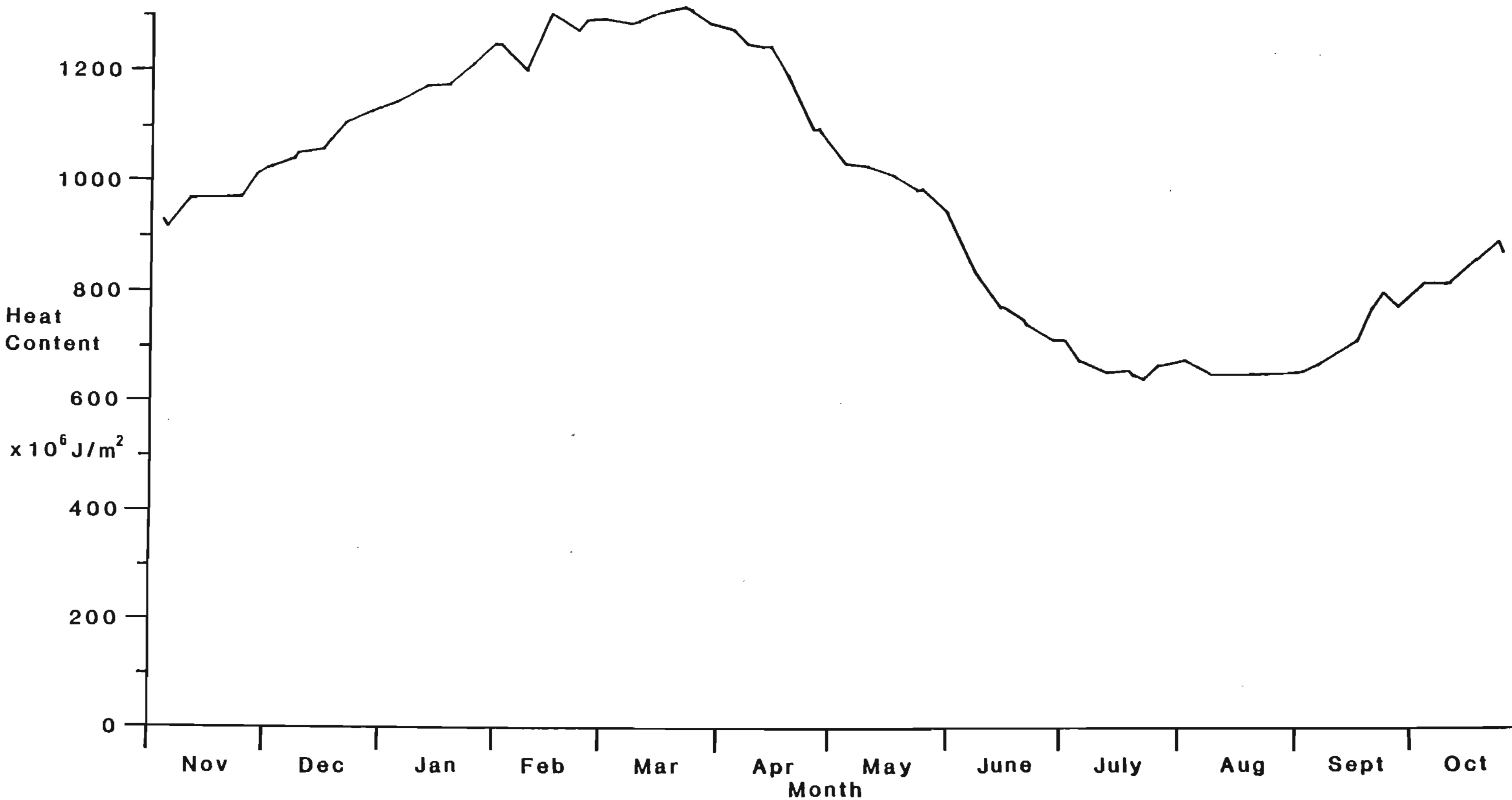

Figure 3.4. Annual changes in the heat content (kJ/m^2) for the period November 1980 to October 1981.

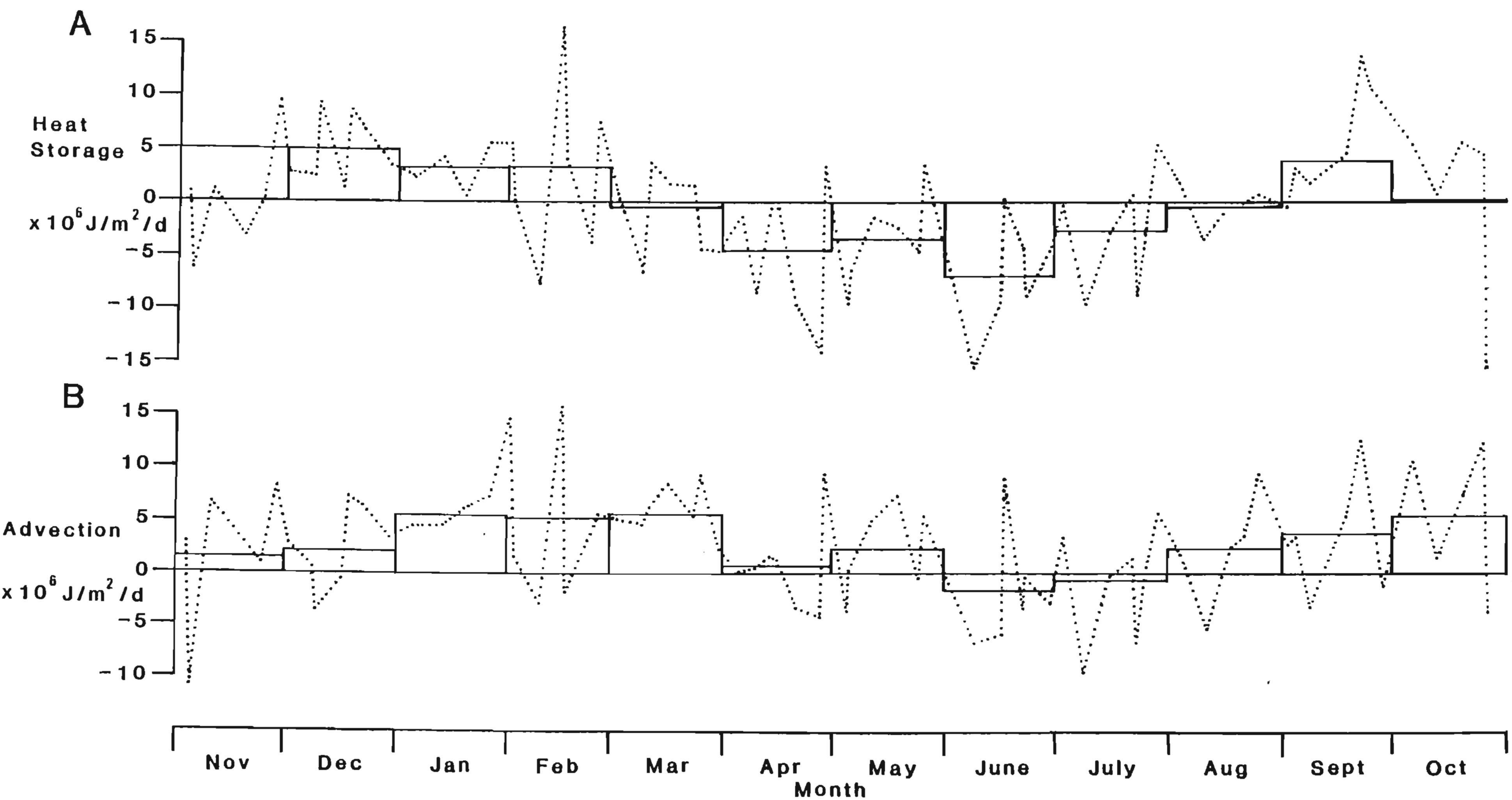

Figure 3.5. Annual variation in daily values ($J/m^2/d$) of **a)** heat storage (Q_t) and **b)** net advection for the period November 1980 to October 1981. Solid line = monthly mean daily value; Dotted line = mean daily value for interval between successive sampling days.

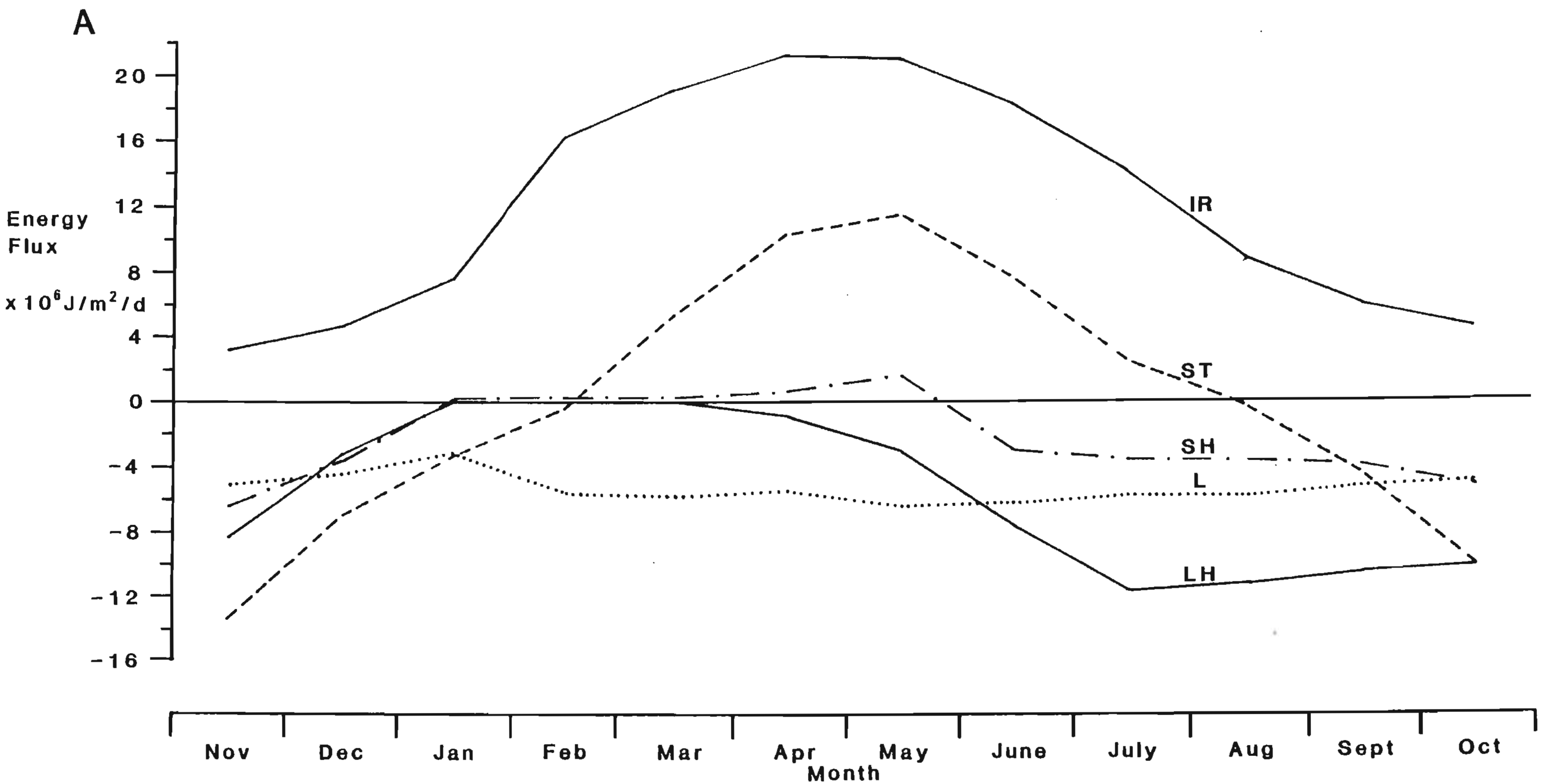

Figure 3.6. a) Annual variation as monthly mean daily values ($J/m^2/d$) in components of the energy balance equation in Lake Mendota.
IR = incident solar radiation; LH = latent heat; L = net longwave; SH = sensible heat; ST = heat storage. From: Dutton & Bryson (1962).

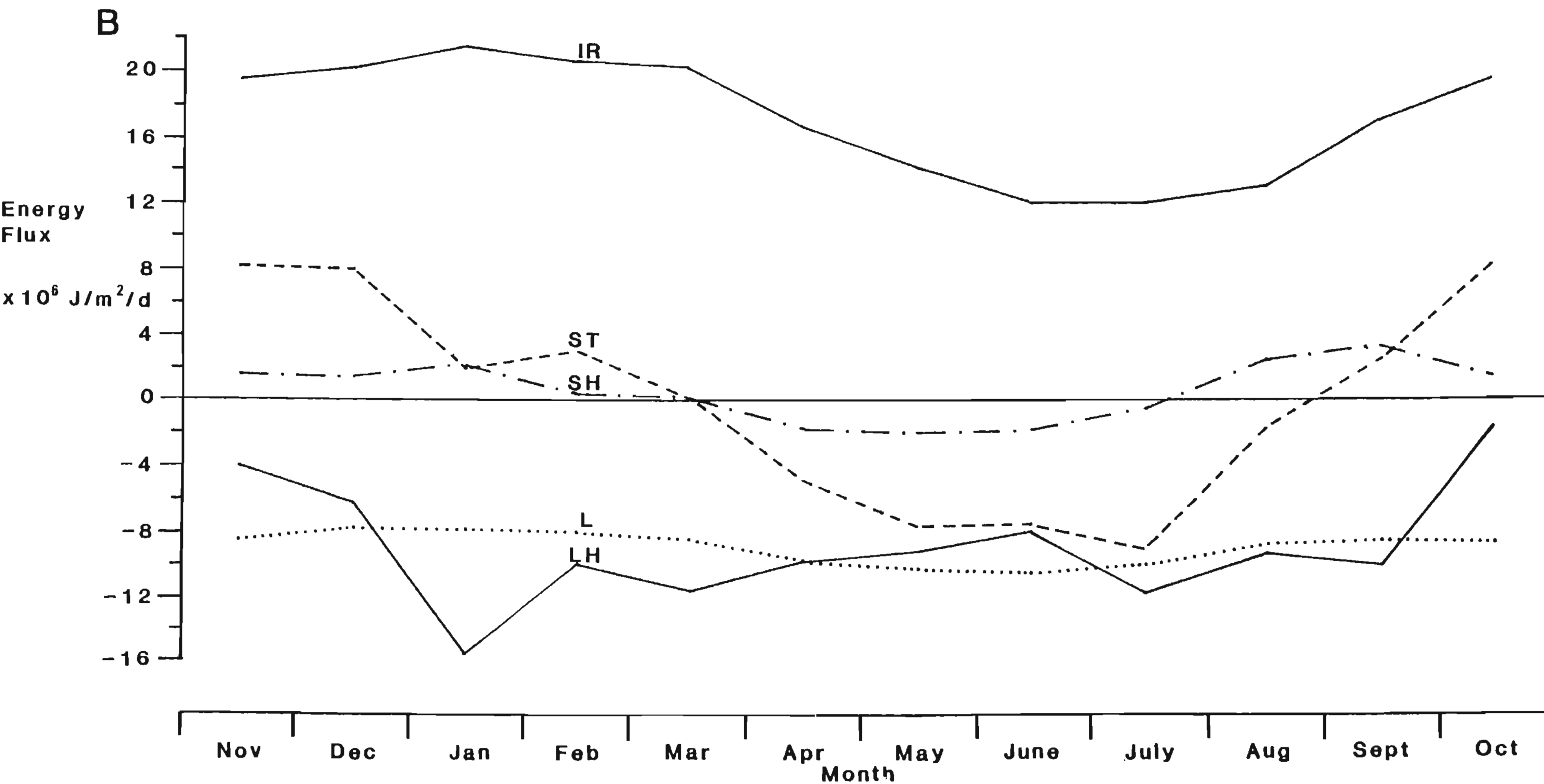

Figure 3.6. b) Annual variation as monthly mean daily values (J/m^2/d) in components of the energy balance equation in b) Lake le Roux.
IR = incident solar radiation; LH = latent heat; LO = net longwave; SH = sensible heat; ST = heat storage. From: Allanson <u>et al</u> (1983).

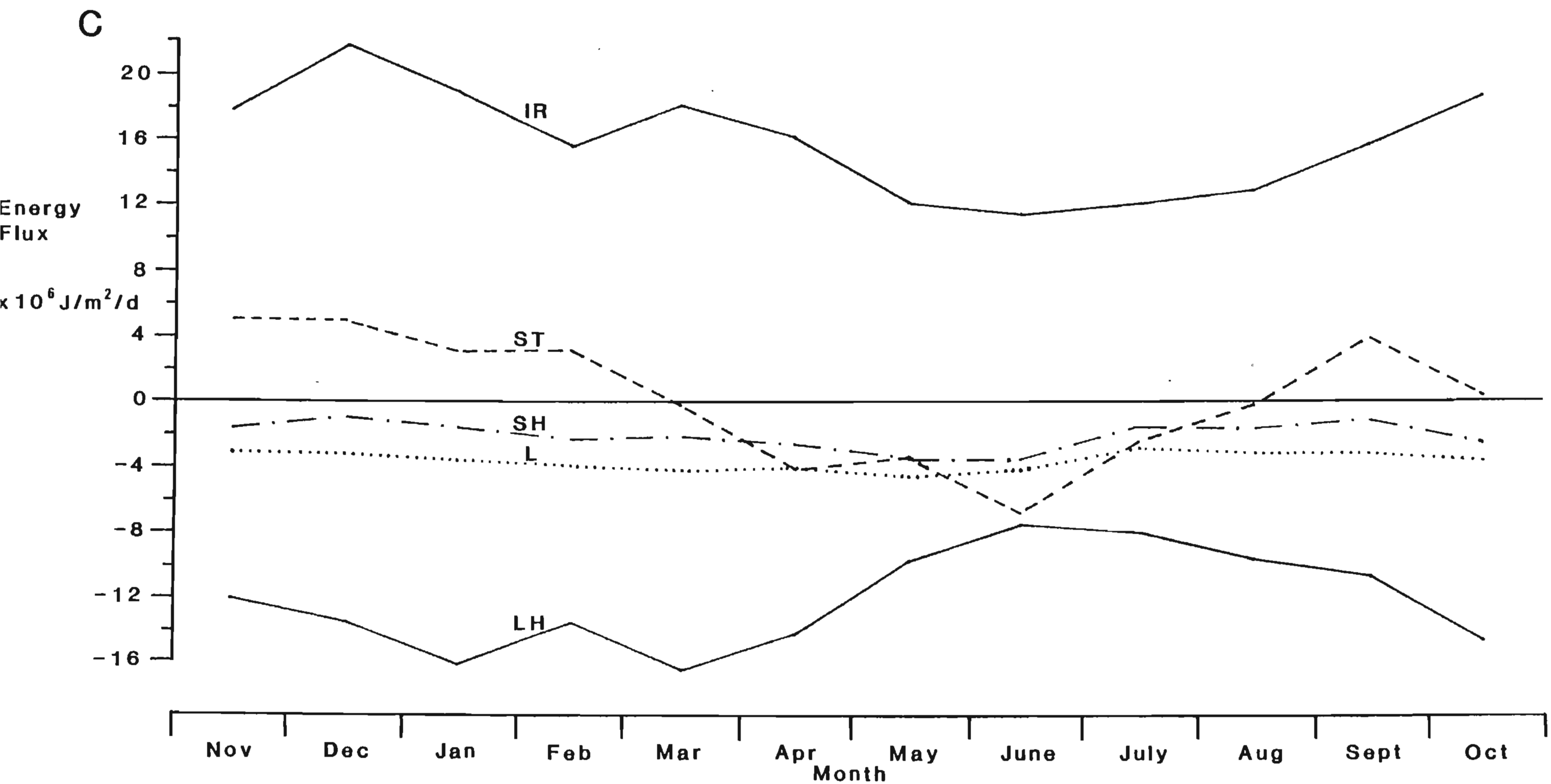

Figure 3.6. **c)** Annual variation as monthly mean daily values (J/m^2/d) in components of the energy balance equation in Lake Midmar.
IR = incident solar radiation; LH = latent heat; LO = net longwave; SH = sensible heat; ST = heat storage, (this study).

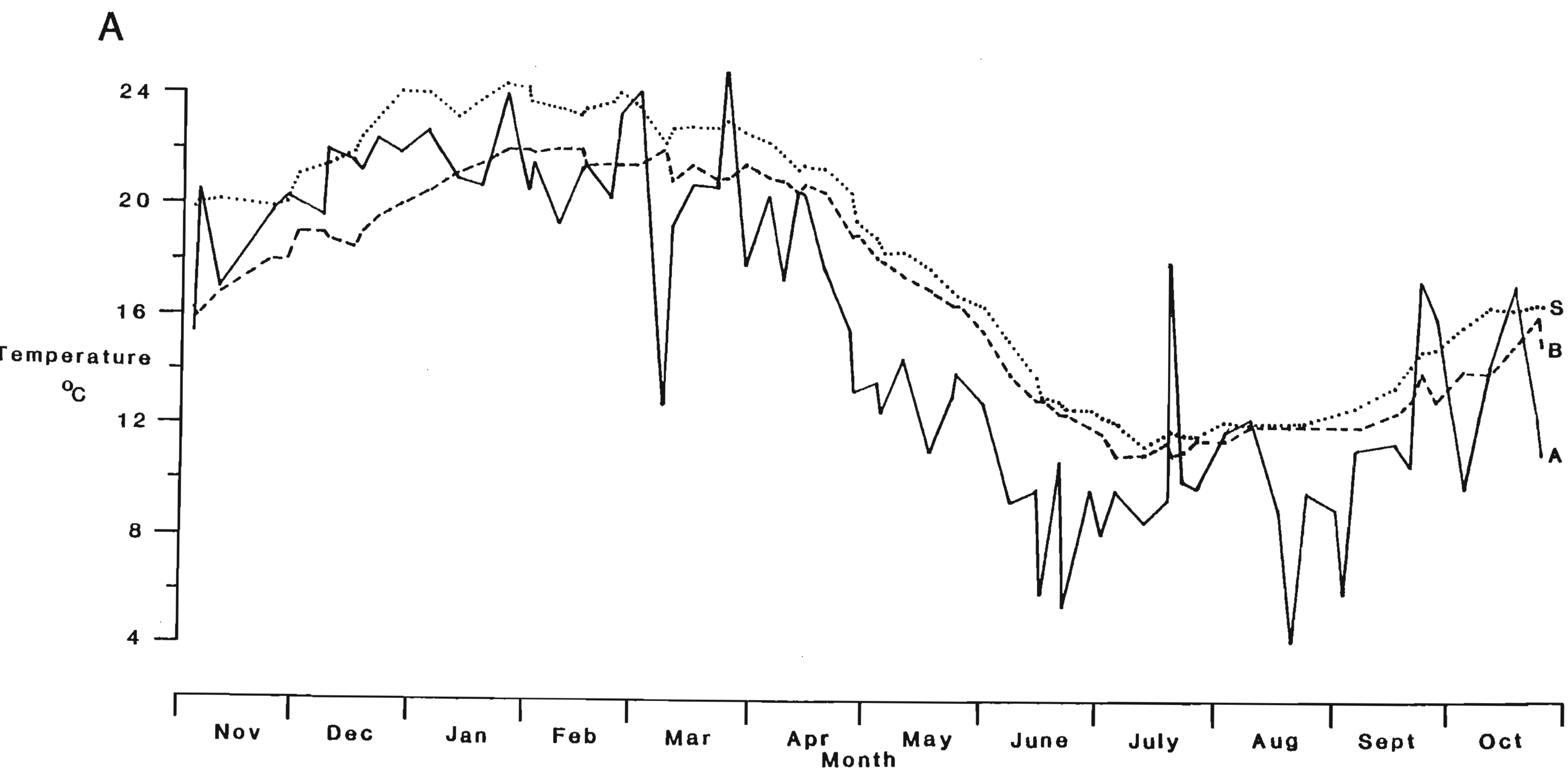

Figure 3.7. Annual variation in **a)** Mean daily air (A), surface water (0-3m, S) and bottom water (B) temperatures for the interval between successive sampling days for the period November 1980 to October 1981.

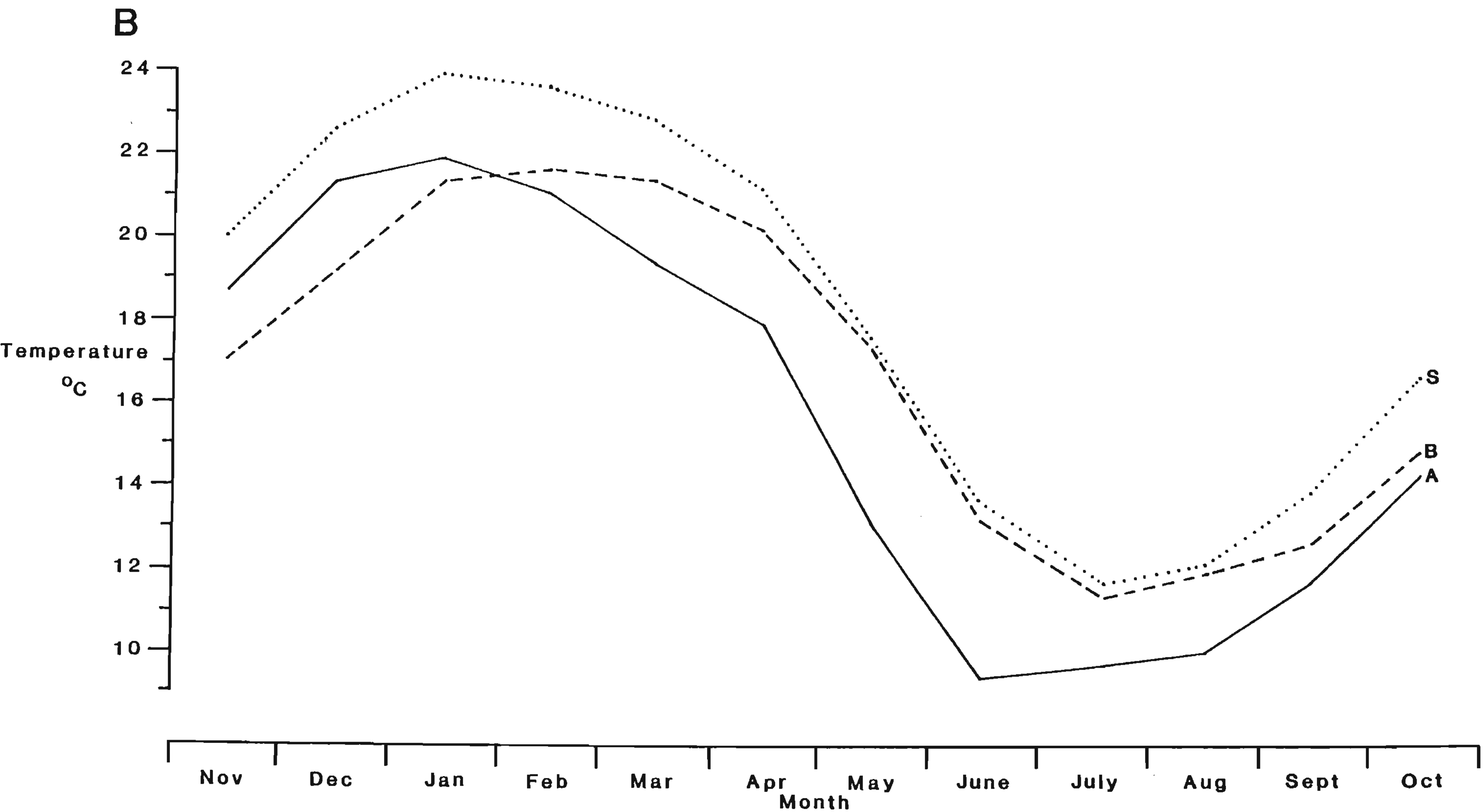

Figure 3.7. Annual variation in **b)** Monthly mean daily air (A), surface water (S) and bottom water (B) temperatures for the period November 1980 to October 1981.

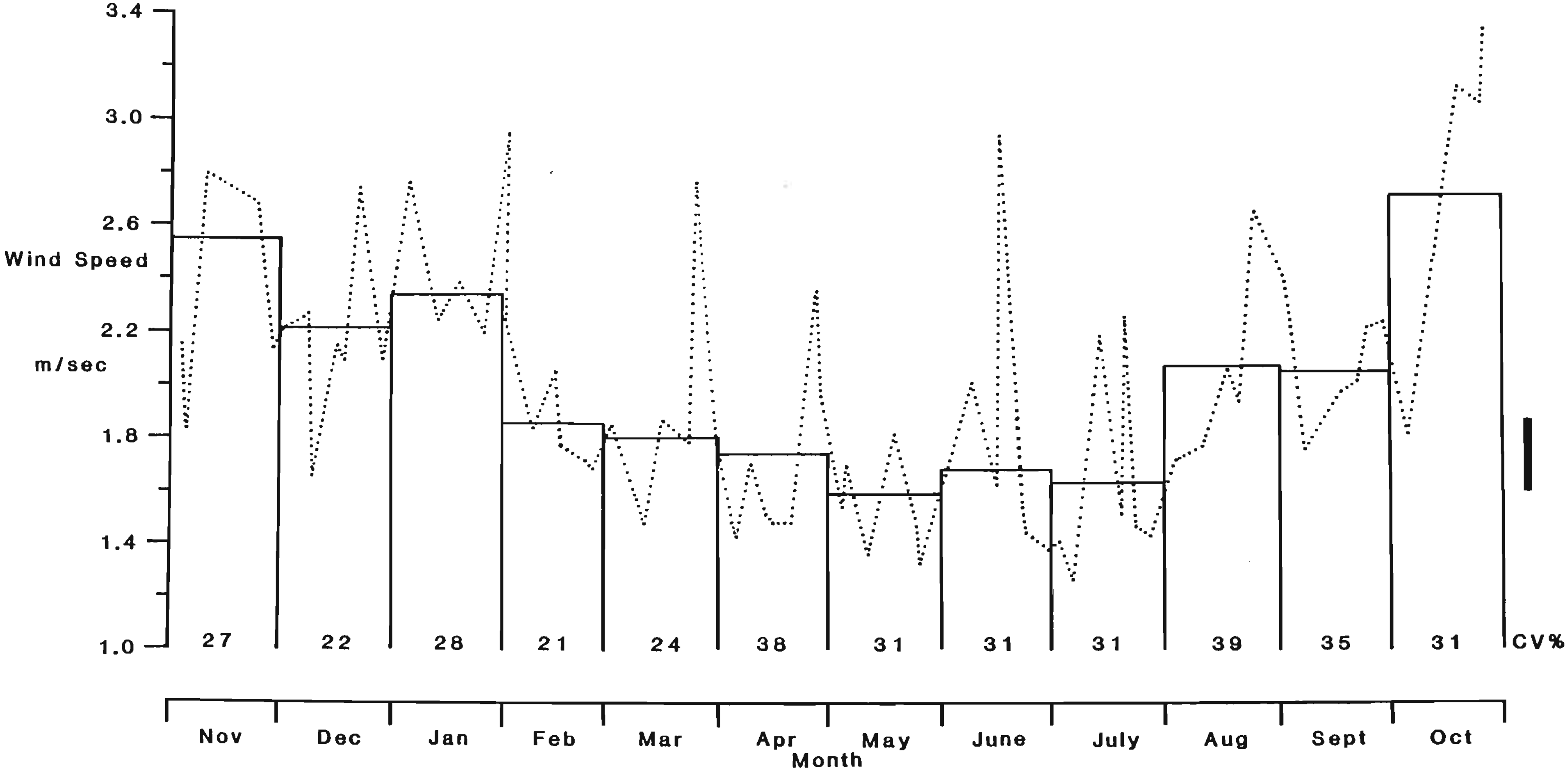

Figure 3.8. Annual variation in mean daily wind speed (m/sec) for the period November 1980 to October 1981. Solid line = monthly mean daily value; Dotted line = mean daily value for the interval between successive sampling days; CV = Coefficient of variation (%) for monthly mean; Vertical bar = LSD at the <0.05 probability level for monthly means.

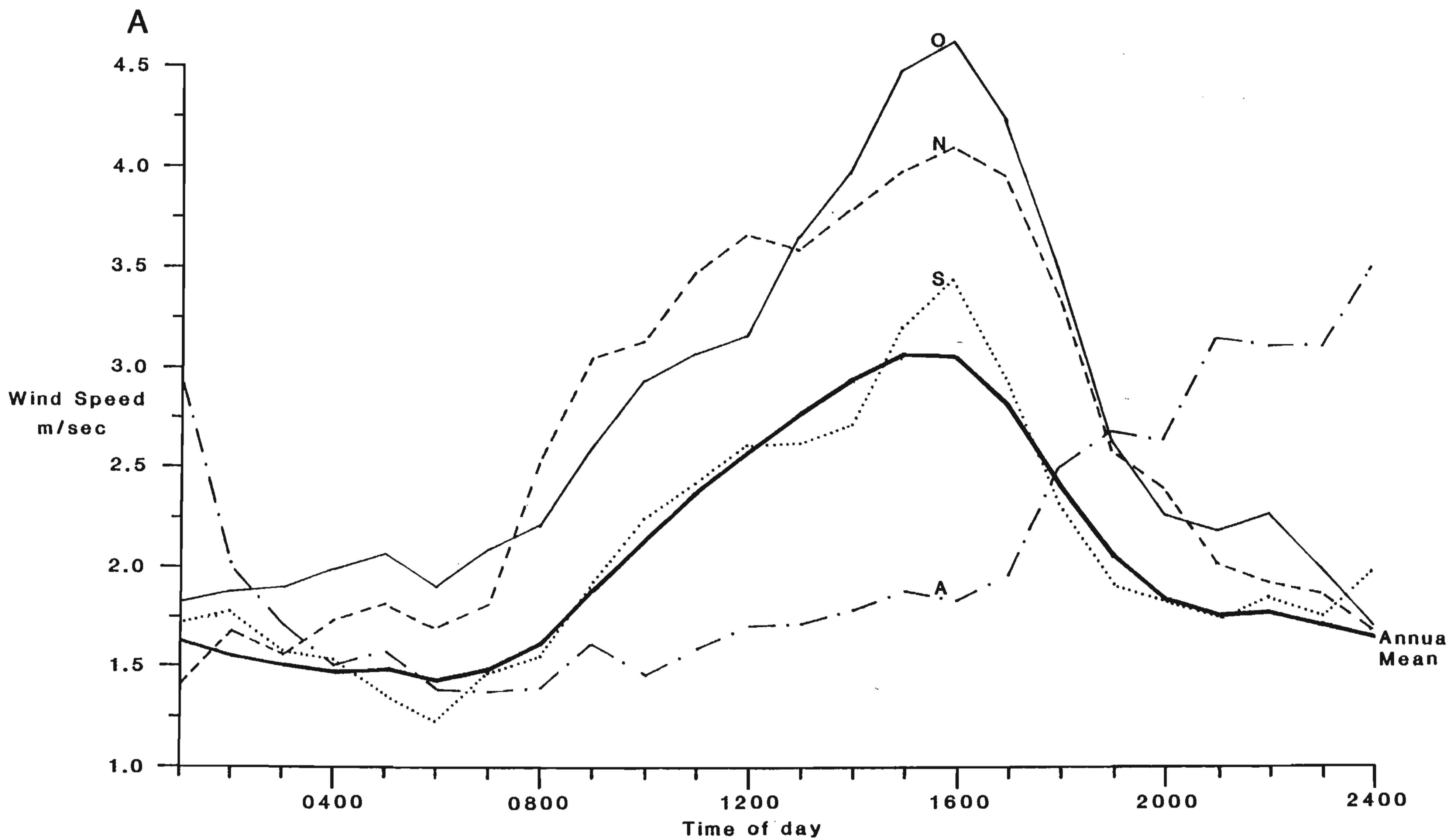

Figure 3.9. a) Annual diel variation in hourly mean wind speed (m/sec) in relation to diel variation in selected months, August, September, October and November.

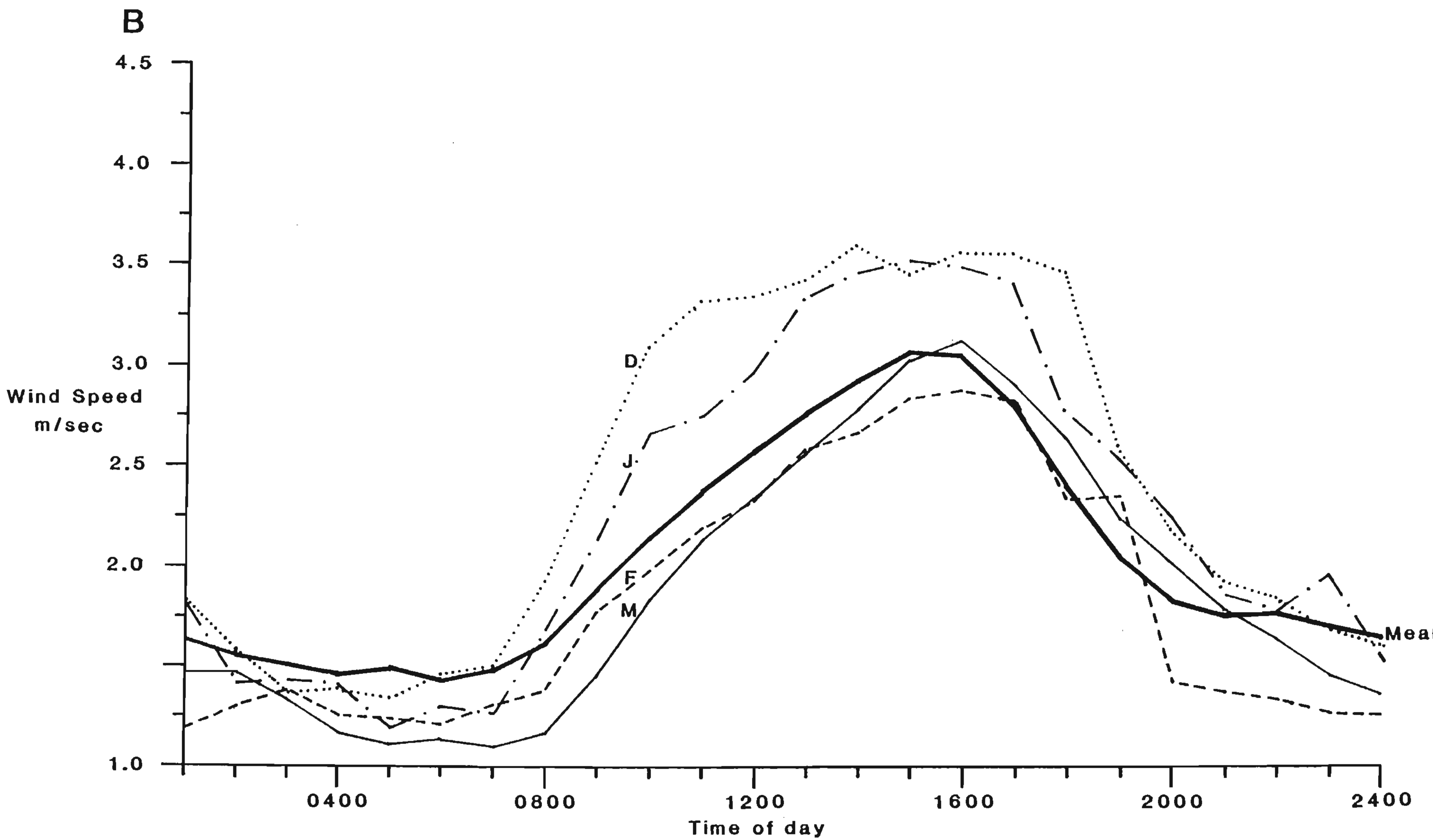

Figure 3.9. b) Annual diel variation in hourly mean wind speed (m/sec) in relation to diel variation in selected months, December, January, February and March.

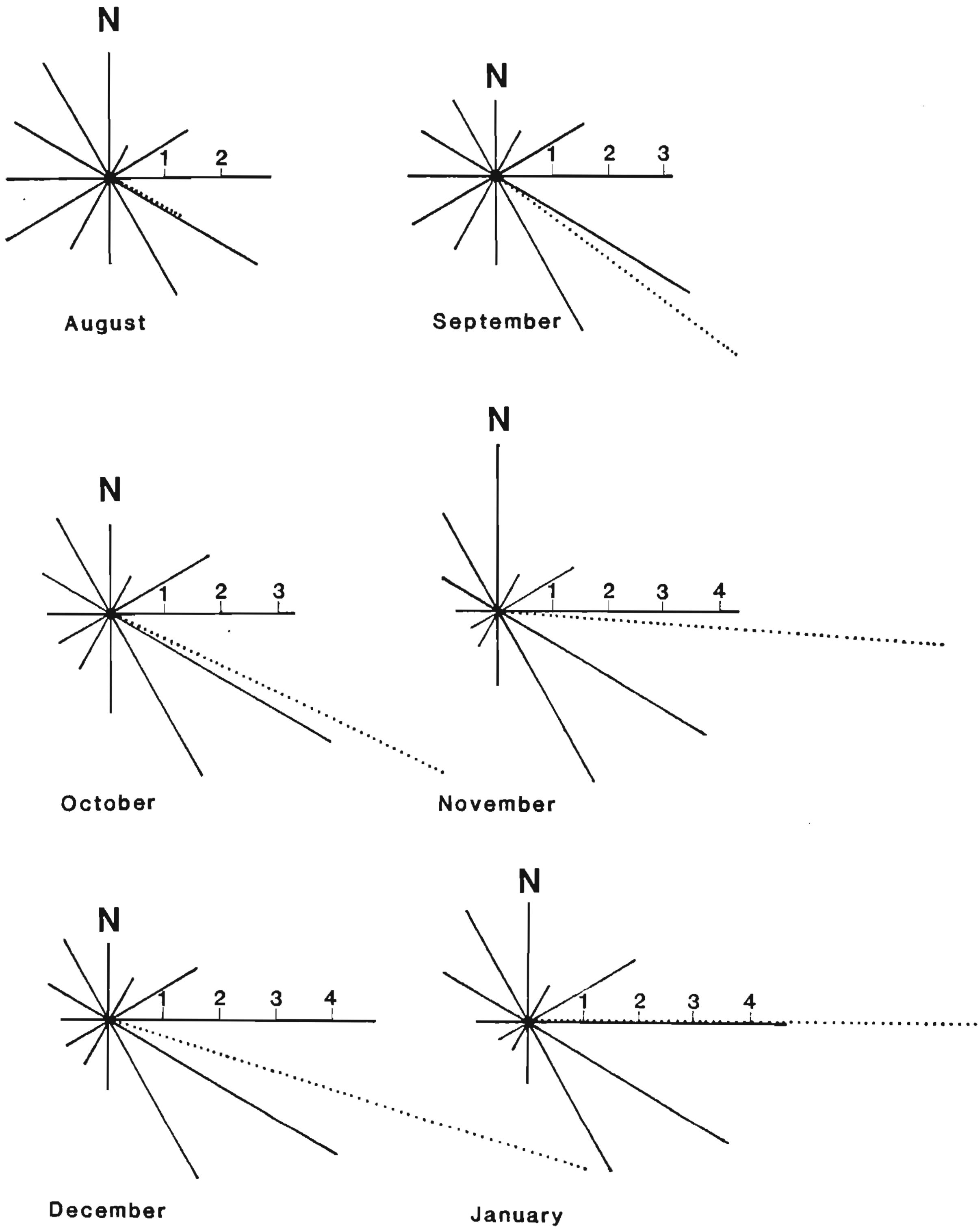

Figure 3.10. Wind roses to show daily mean angular distribution of wind (hours, indicated by solid lines) for selected months, August to January. Dotted line = resultant direction obtained by vector analysis.

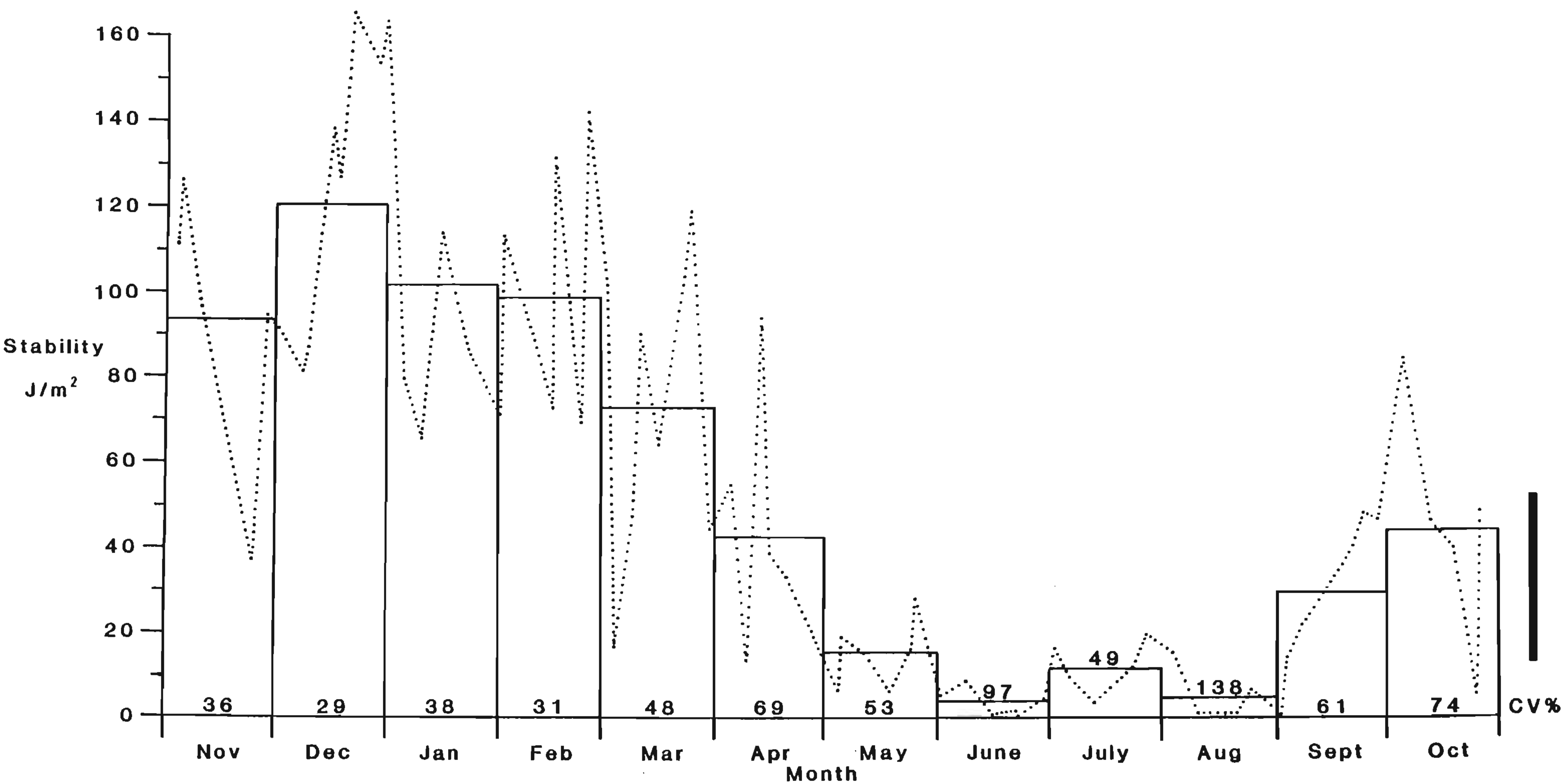

Figure 3.11. Annual variation in daily values of stability (J/m^2) for the period November 1980 to October 1981. Solid line = monthly mean daily value; Dotted lines = mean daily value for the interval between successive sampling days; CV = Coefficient of variation (%) for monthly mean; Vertical bar = LSD at the the <0.05 probability level for monthly means.

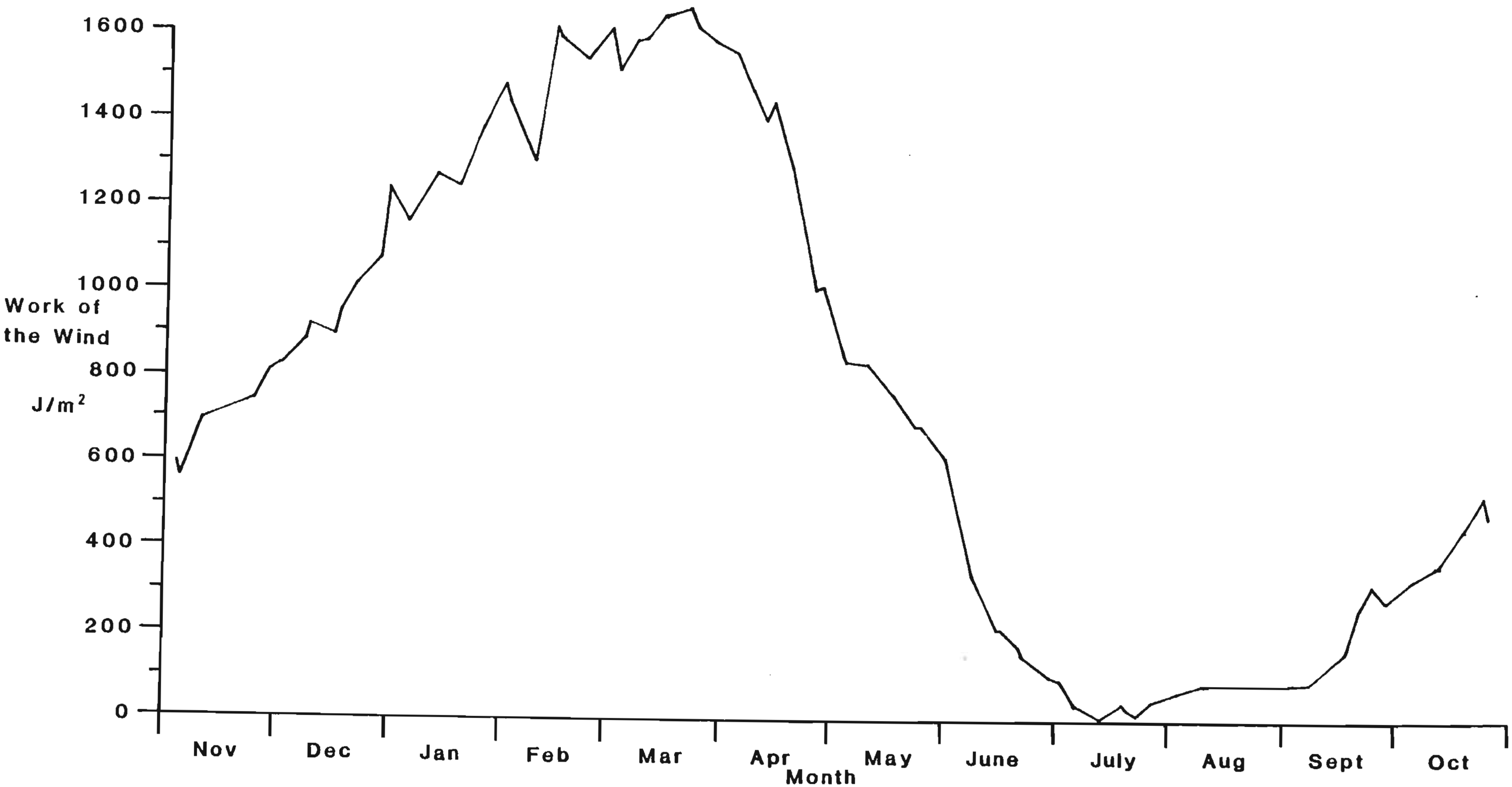

Figure 3.12. Annual variation in work of the wind (J/m^2) for the period November 1980 to October 1981.

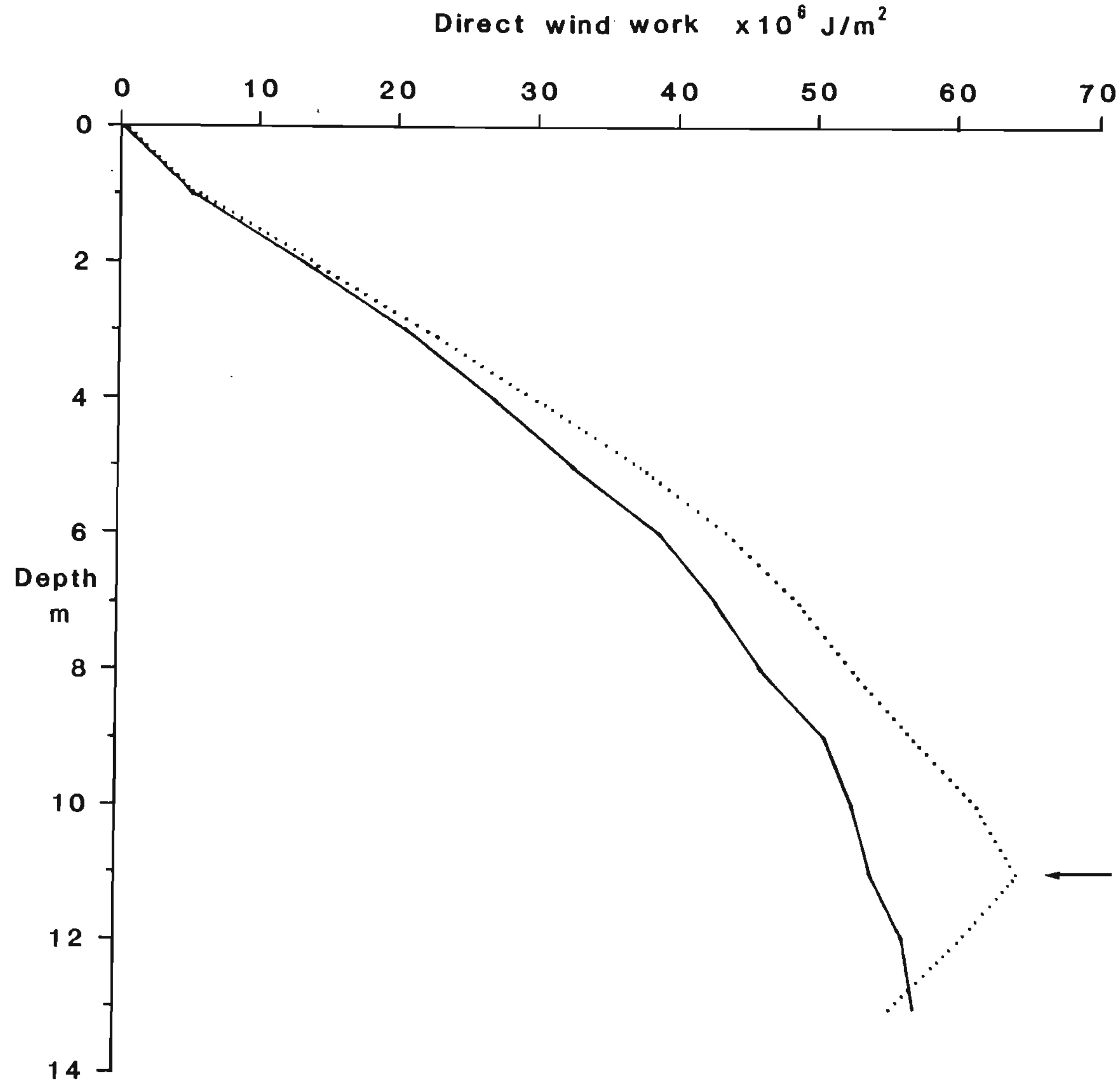

Figure 3.13. Examples of direct work curves used to determine the mixing depth (as the point of maximum inflection), to show mixing to the lake bottom (2nd December, solid line) and partial mixing to 11m (arrow on curve for 10 December, dotted line).

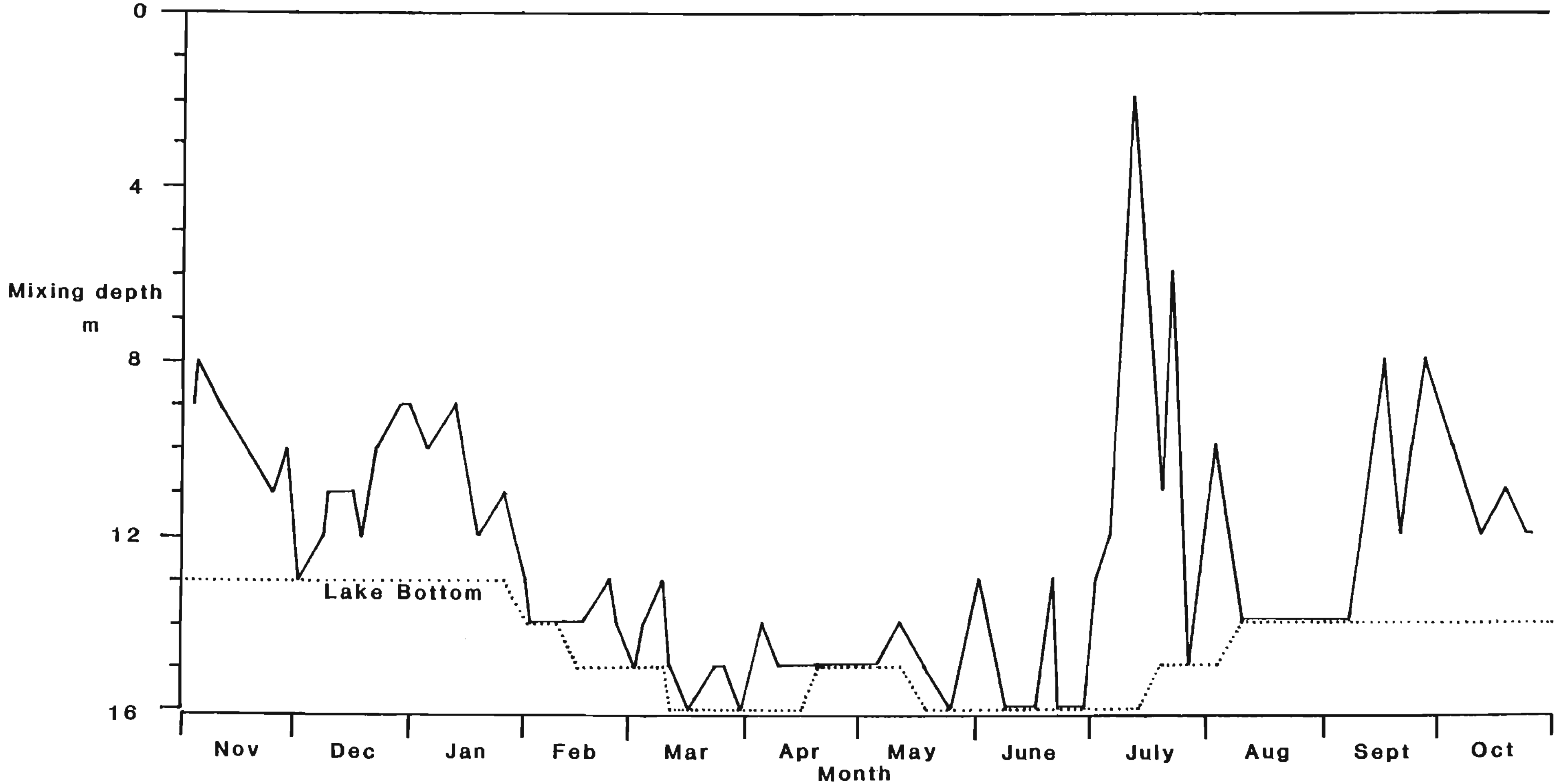

Figure 3.14. Annual variation in mixing depth (solid line) in relation to lake bottom (dotted line) at main basin station, for the period November 1980 to October 1981.

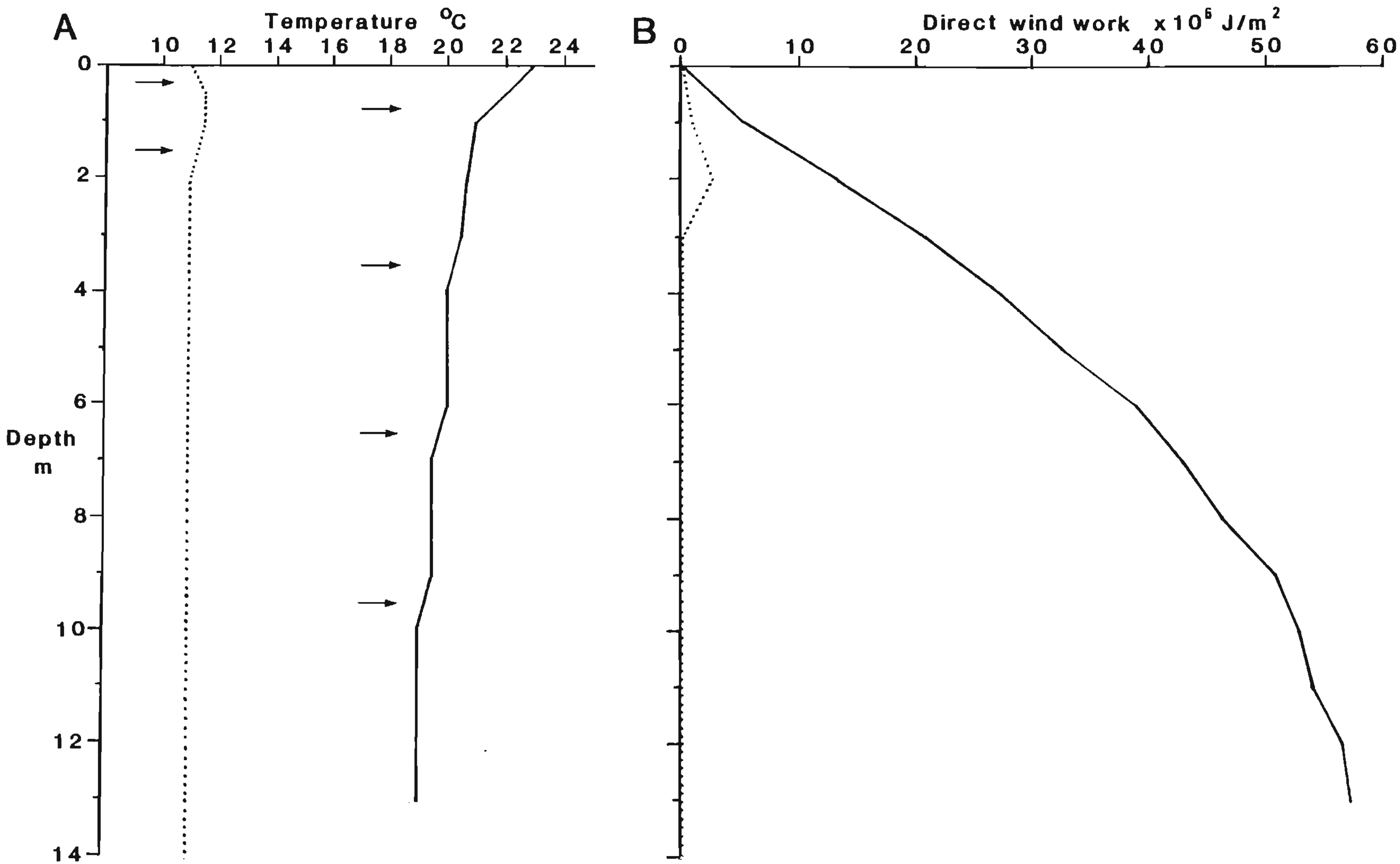

Figure 3.15 a) Temperature profiles on two sampling days, 2nd December 1980 (solid line) and 14th July 1981 (dotted line). Arrows indicate depths where temperature gradient was equal to or greater than 0.5°C/m.

b) Corresponding direct work curves for 2nd December 1981 (solid line) and 14th July 1981 (dotted line).

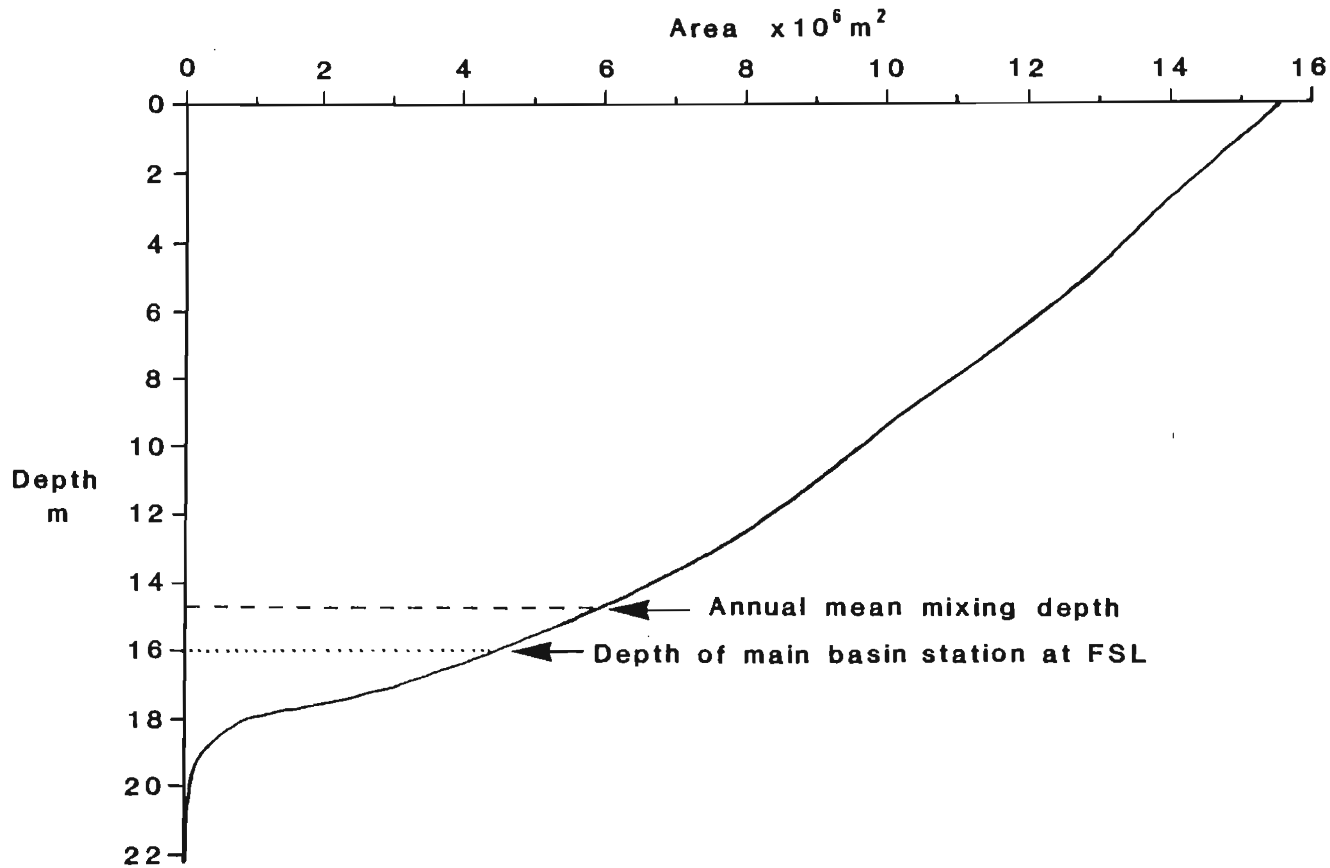

Figure 3.16. Hypsographic curve for Lake Midmar.

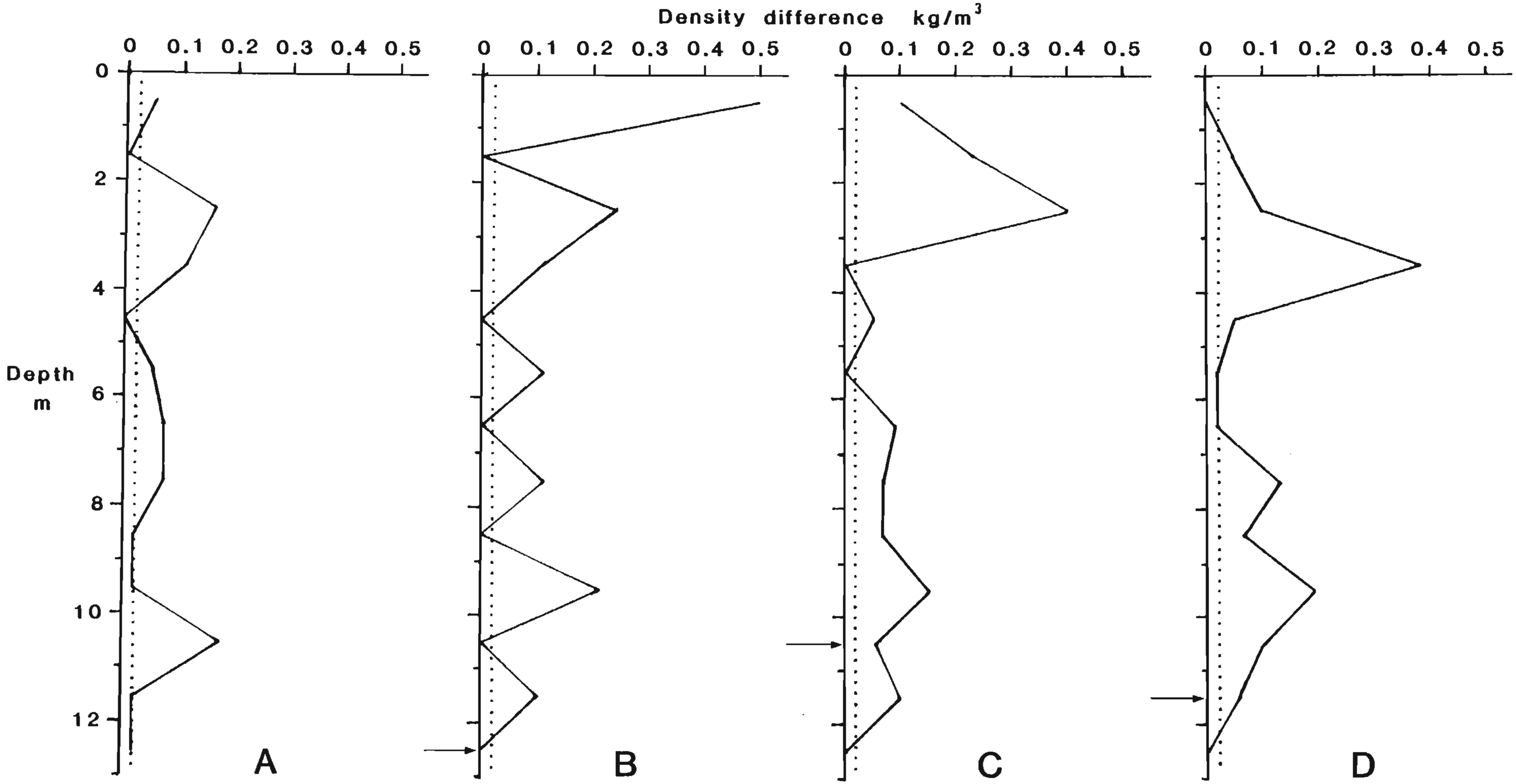

Figure 3.17. Diurnal variation in depth distribution of density gradients measured on 23rd December 1980 at 06.00, 10.00, 14.00 and 18.00 hours. Arrows indicate limit of mixed zone.

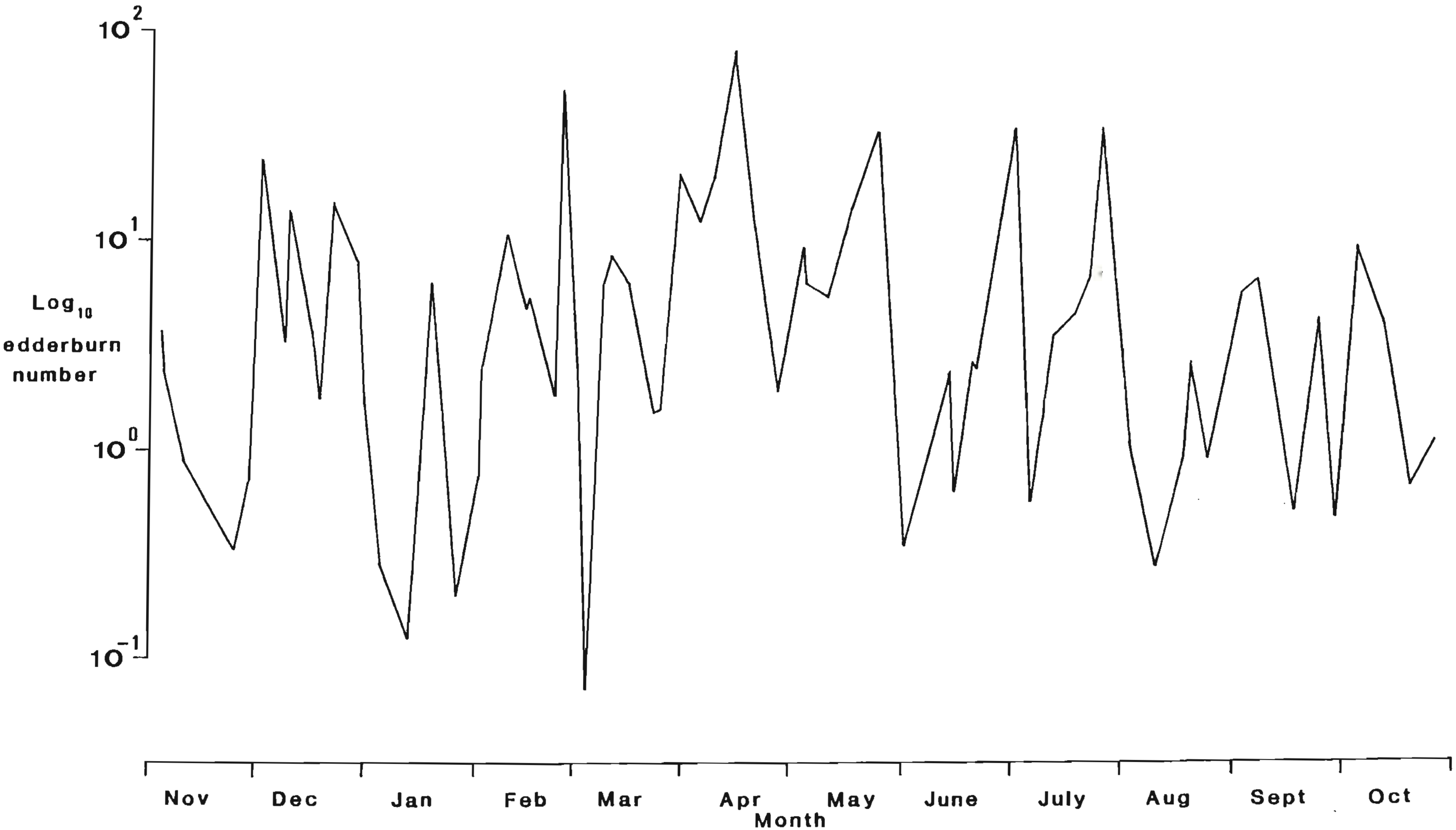

Figure 3.18. Annual variation in Wedderburn number ($\log_{10}$) for the period November 1980 to October 1981.

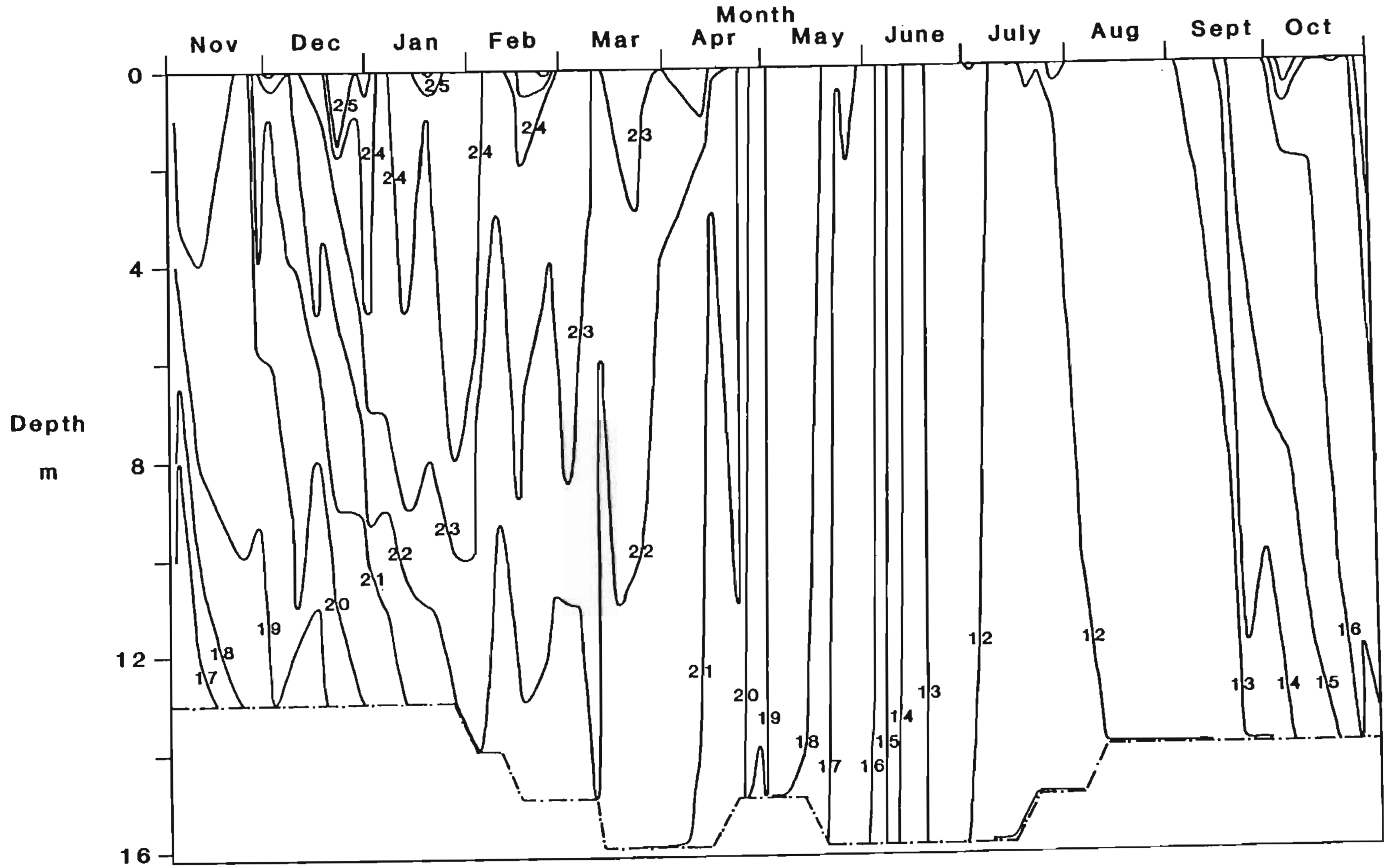

Figure 3.19. Isotherm plot for Lake Midmar for the period November 1980 to October 1981.

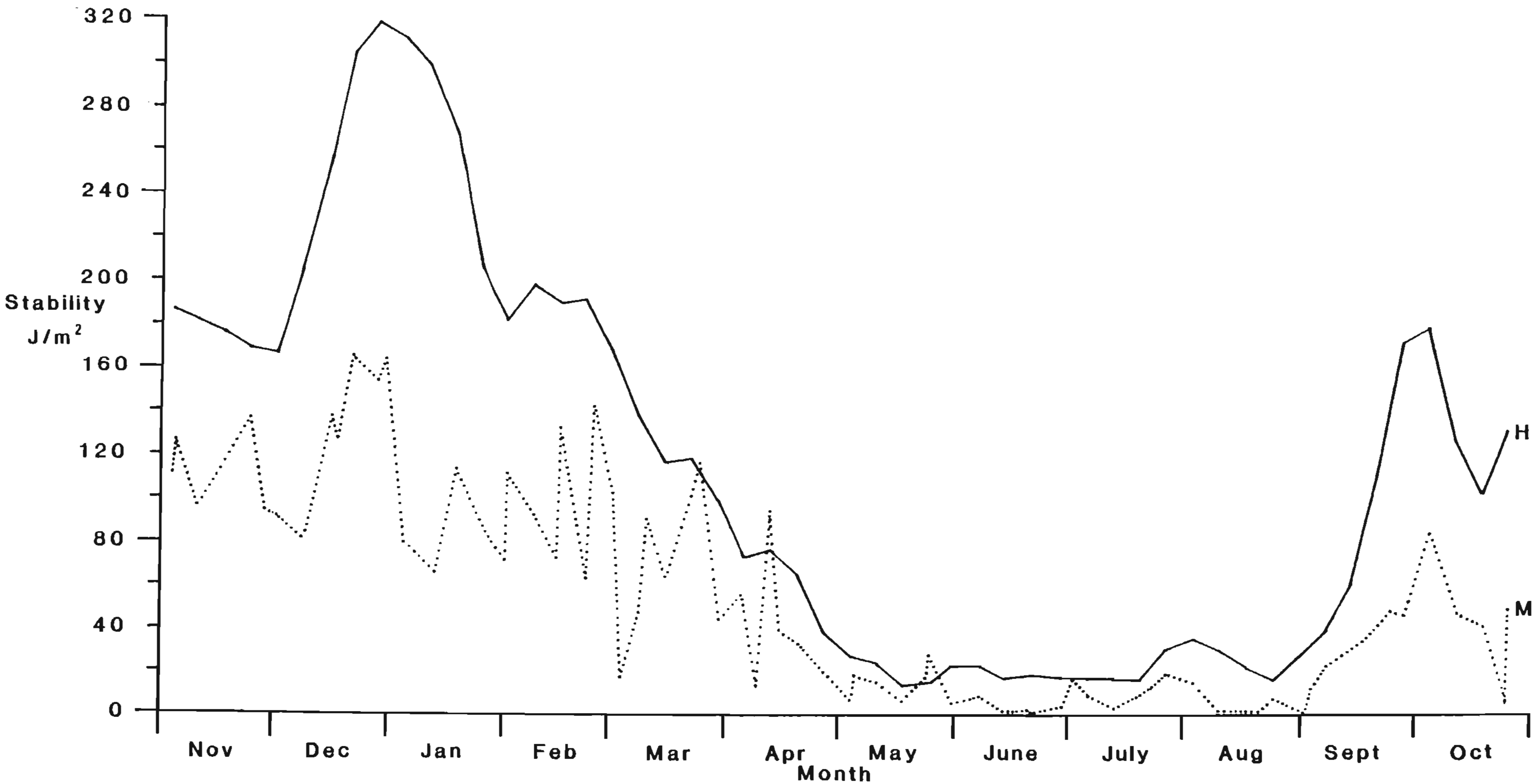

Figure 3.20. Annual variation in stability (J/m^2) in Hartbeespoort dam (solid line) and Lake Midmar (dotted line) for the period November 1980 to October 1981. From: NIWR (1985) and this study.

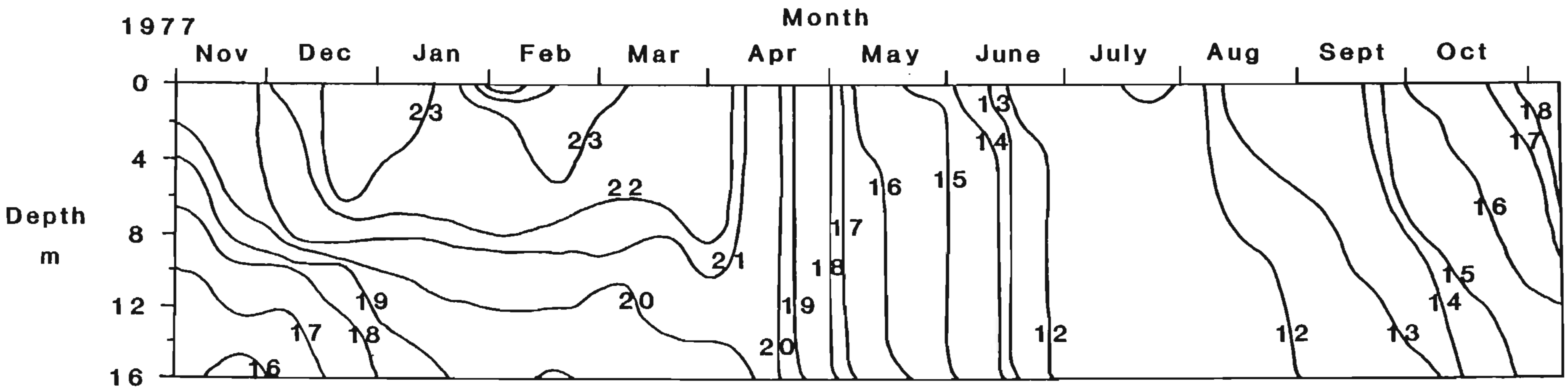

Figure 3.21. Isotherm plot for Lake Midmar for the period November 1977 to October 1978. From: Archibald et al (1980).

Table 3.1. Selected morphometric and thermal characteristics of some South African impoundments. From: Allanson et al (1983), Pieterse and Keulder (1982), Walmsley and Butty (1980) and this study.

Impoundment	Maximum depth m	Mean depth m	Nature of thermocline	Max. summer temperature °C	Max. thermal gradient °C
Wuras	5.0	1.95	Absent	27.3	4
Tonteldoos	10.5	3.9	Unstable	26.0	10
Bloemhof	18.0	4.5	Absent	24.0	4
Bospoort	14.4	5.3	Absent	28.0	5
Olifantsnek	13.6	5.5	Absent	25.0	3
Rust der Winter	20.0	5.7	Present	27.5	9
Rietvlei	17.2	6.4	Unstable	24.8	6
Bronkhorstspruit	19.5	6.8	Absent	27.0	6
Nahoon	18.4	7.2	Absent	26.7	4
Buffelspoort	23.0	7.9	Present	25.4	9
Lindleyspoort	22.2	8.1	Present	24.0	9
Henley	18.8	8.2	Present	24.0	9
Vernon Hooper	16.2	8.8	Present	27.5	6
Laing	37.5	10.4	Present	26.9	8
New Doringpoort	36.0	10.6	Present	26.0	10
Roodeplaat	43.0	10.6	Present	28.4	15
Loskop	36.0	10.7	Present	28.0	11
Hazelmere	30.6	10.8	Present	28.6	7
Midmar	**22.3**	**11.4**	**Unstable**	**25.5**	**6**
Albert Falls	24.6	12.3	Present	29.0	11
Bridle Drift	40.9	12.3	Present	26.8	8
Nagle	38.1	15.2	Present	28.5	8
le Roux	73.0	23.0	Present	22.0	8

Table 3.2. Heat budget characteristics for a range of lakes from different latitudes. From: Allanson et al (1983), Coche (1974), Hutchinson (1957) and this study.

Lake	Latitude	Mean depth m	BAHB	RH	TI	MHC	RH:BAHB	Type
Victoria	1° S	40	41.9	318	7.9	356	7.6	Tropical
Guija	14°13'N	16.5	22.6	134	8.1	156.6	5.9	
Kariba (Basin 2)	17°30'S	24	83.7	163	6.8	246.9	1.95	
Galilee	32°50'N	24	140.1	110.4	4.6	250.5	0.8	Intermed.
Midmar	29°30'S	11.4	67.5	40.4	3.5	107.9	0.6	
le Roux	30°10'S	29	91.6	68.8	2.4	160.4	0.75	
Mead	36°12'N	59	193.3	92	1.6	285.3	0.48	
Mendota	43°07'N	12.1	98.3	22	1.8	120.3	0.22	Temperate
Greiffen	47°23'N	17	66.9	8.4	0.5	75.3	0.13	
Staffel	47°42'N	10.7	63.6	8.8	0.8	72.4	0.14	
Fureso	55°47'N	12.3	71.5	11.3	0.92	82.8	0.16	

BAHB = Birgean annual heat budget; RH = Residual Heat;
TI = Tropicality Index; MHC = Maximum heat content, units 10^4 kJ/m^2

Table 3.3. Annual range of energy flux values for incident solar radiation, latent heat and heat storage, the Birgean Annual Heat Budget (BAHB) and maximum heat storage in Lakes Mendota and Midmar. From: Dutton and Bryson (1962) and this study.

Component	Mendota	Midmar	units
Incident solar radiation	3.1 - 21.8	11.5 - 21.9	x10^3 kJ/m^2/d
Latent heat	0 - 11.6	-7.4 - 16.5	x10^3 kJ/m^2/d
Heat storage	-13.5 - 11.6	-6.1 - 5.1	x10^3 kJ/m^2/d
BAHB	98.3	67.5	x10^4 kJ/m^2
Maximum heat storage	11.6	5.1	x10^3 kJ/m^2/d

Table 3.4. Mean annual sunshine duration (hours) and number of days with no sun, overcast (1-10%), dull (11-49%), sunny (50-89%) or bright (90-100% of possible sunshine duration) conditions at two meteorological stations, Fauresmith (F) and Cedara (C). From: Schulze (1965).

	Mean hours	Daily % of poss. duration	Number of days with				
			No sun	Overcast	Dull	Sunny	Bright condns.
F	9.3	77	3.8	5.3	32.7	199.6	123.8
C	6.6	55	34.8	59.7	40.7	198.4	31.4

Table 3.5. The maximum fetch (km) for winds from a particular direction at Lake Midmar.

Direction	Compass Bearing	Fetch
N - S	0 - 180	5.06
NNE - SSW	30 - 210	6.18
NEE - SWW	60 - 240	4.58
E - W	90 - 270	4.5
EES - WWN	120 - 300	4.22
ESS - WNN	150 - 330	4.08

Table 3.6. Range of wind speeds used in Weather Bureau and Beaufort classification schemes. From: Schulze (1965) and Bodin (1978).

Weather Bureau	Light winds 0 - 4.4	Moderate winds 4.5 - 6.7 m/sec	
Beaufort Scale	Class1 0 -1.6	Class2 1.7 - 3.3	Class3 3.4 - 5.4 m/sec

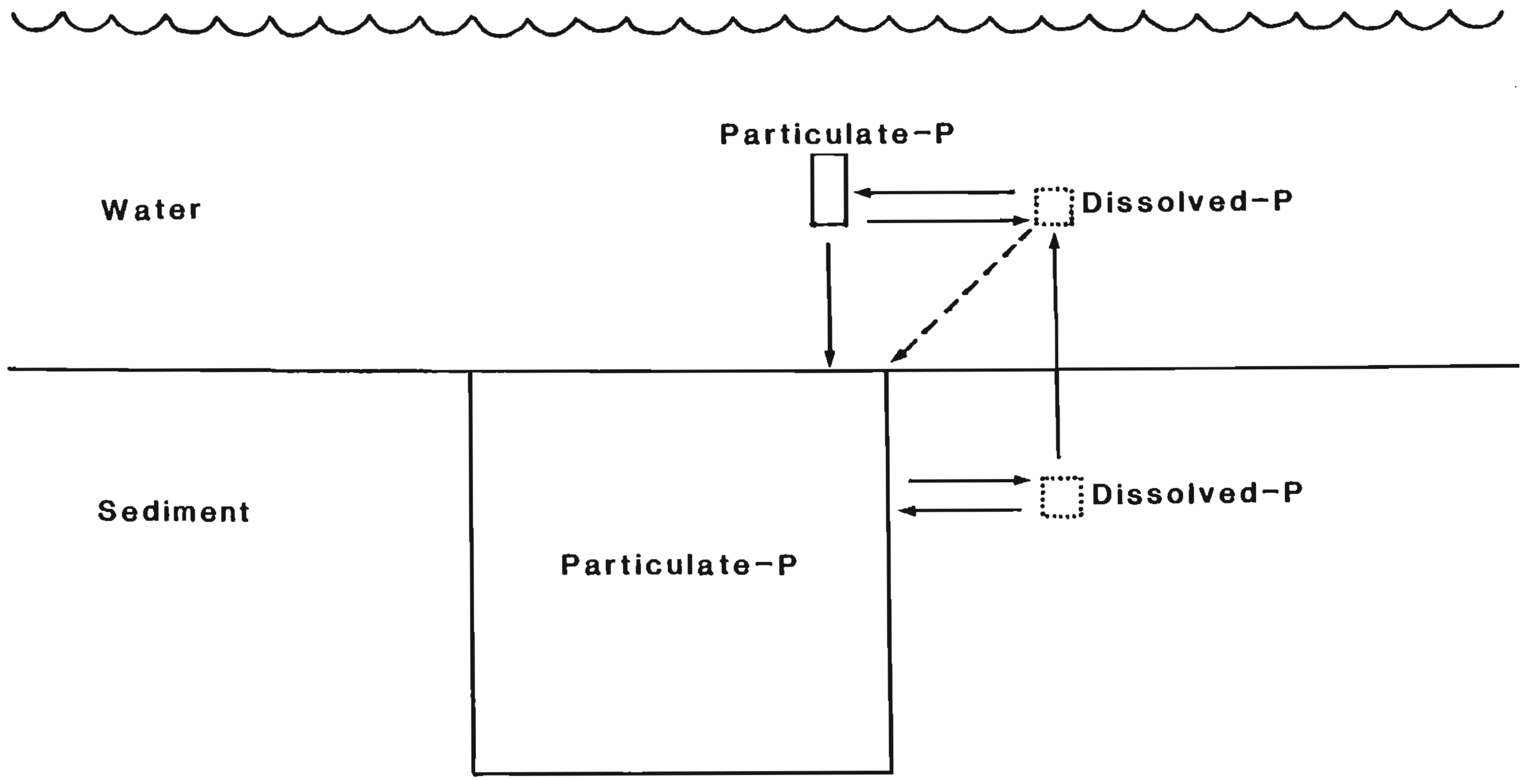

Figure 4.1. Relative size of the major phosphorus pools in a lake water - sediment system. From: Bostrom _et al_ (1982).

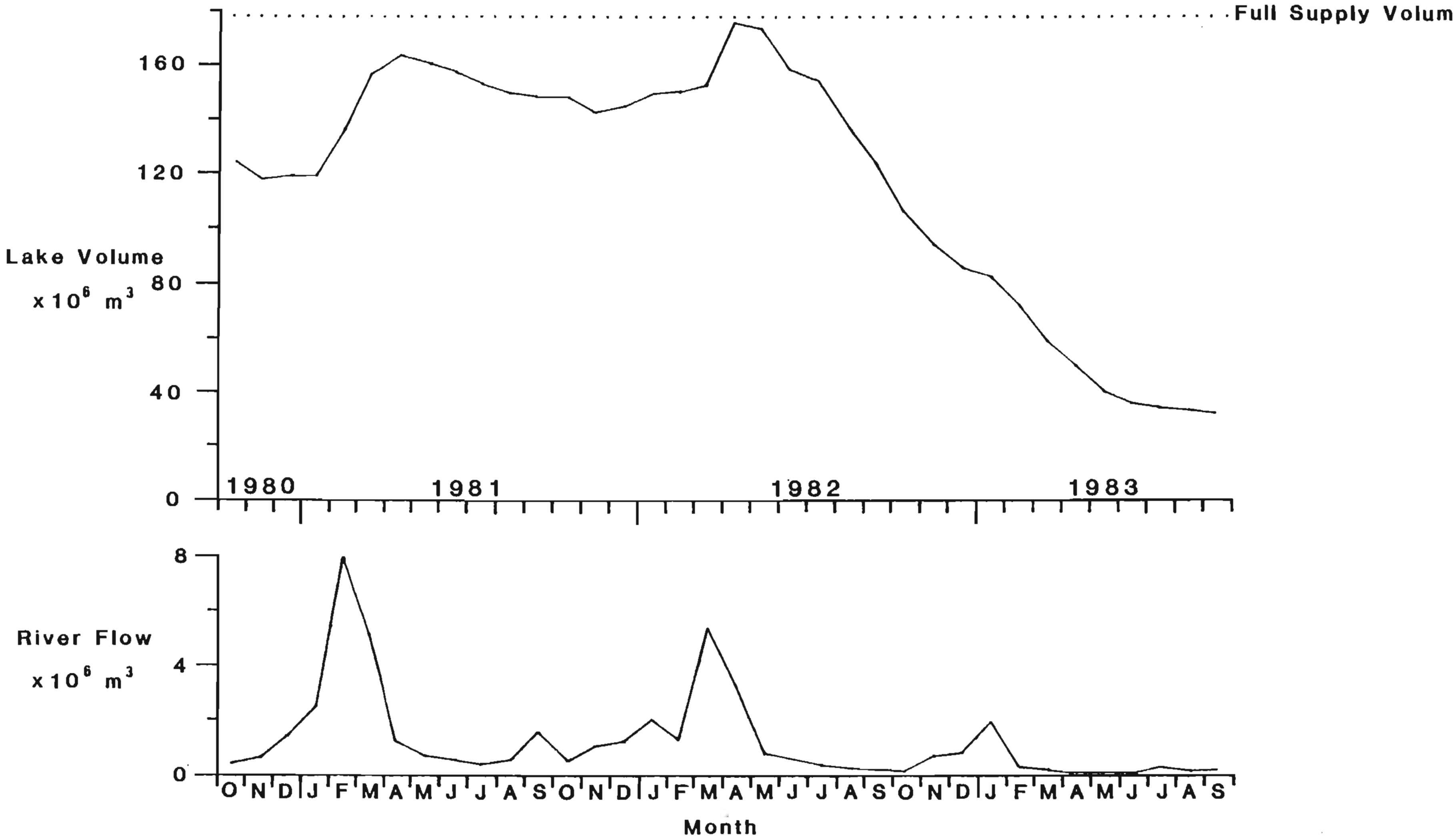

Figure 4.2. Changes in monthly mean lake volume (x10^6 m^3) and monthly mean river flow (x10^6 m^3) in the Mgeni river for the period October 1980 to September 1982. Dotted line = lake volume at full supply level.

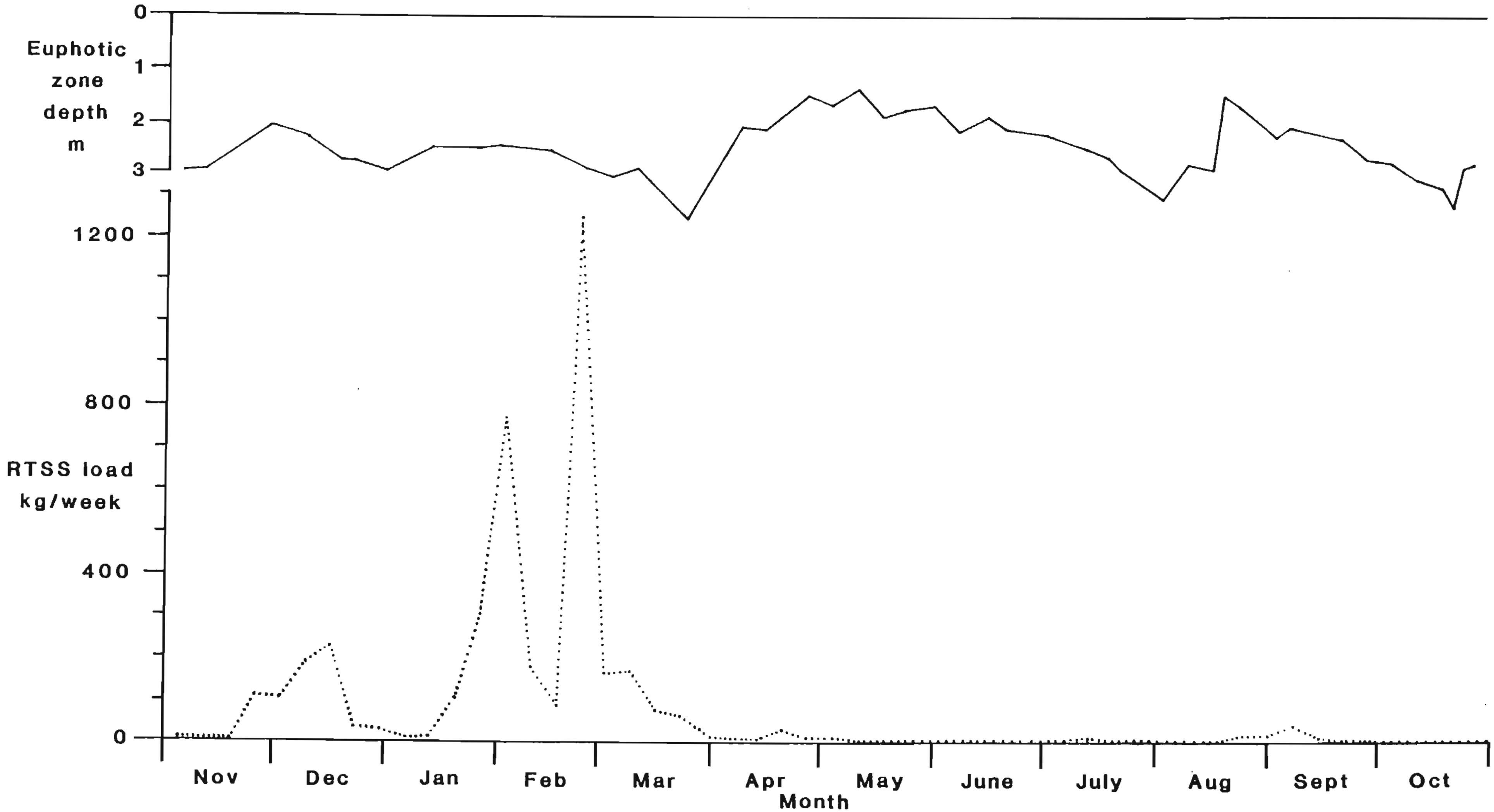

Figure 4.3. Annual variation in depth of the euphotic zone (m) and river loading of total suspended solids (kg TSS/wk) for the period November 1980 to October 1981.

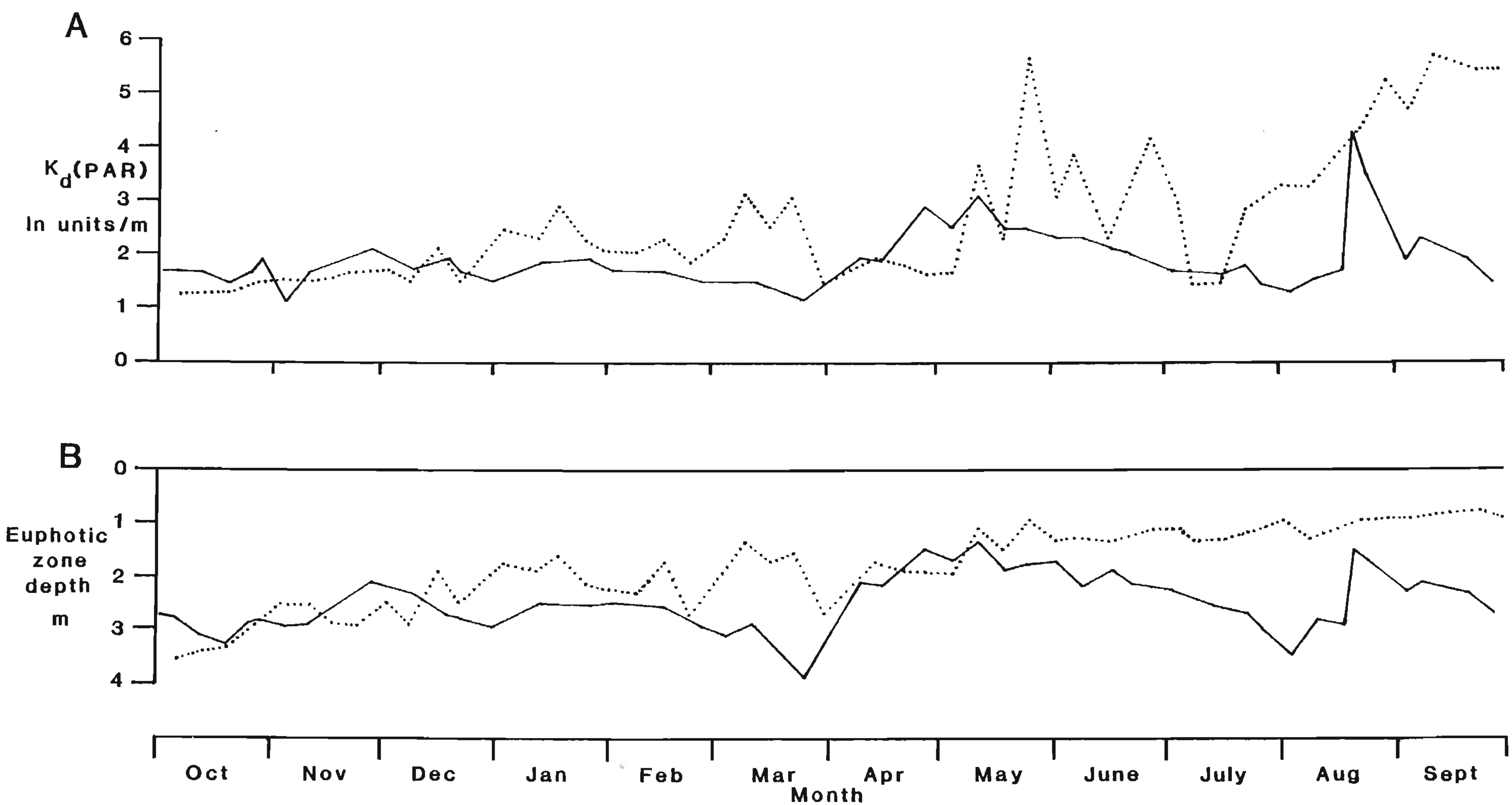

Figure 4.4. Annual variation in a) the vertical attenuation coefficient for downwelling PAR irradiance (K_d(PAR), ln units/m) and b) depth of the euphotic zone (m), for the period October 1980 to September 1981 (solid line) and October 1982 to September 1983 (dotted line).

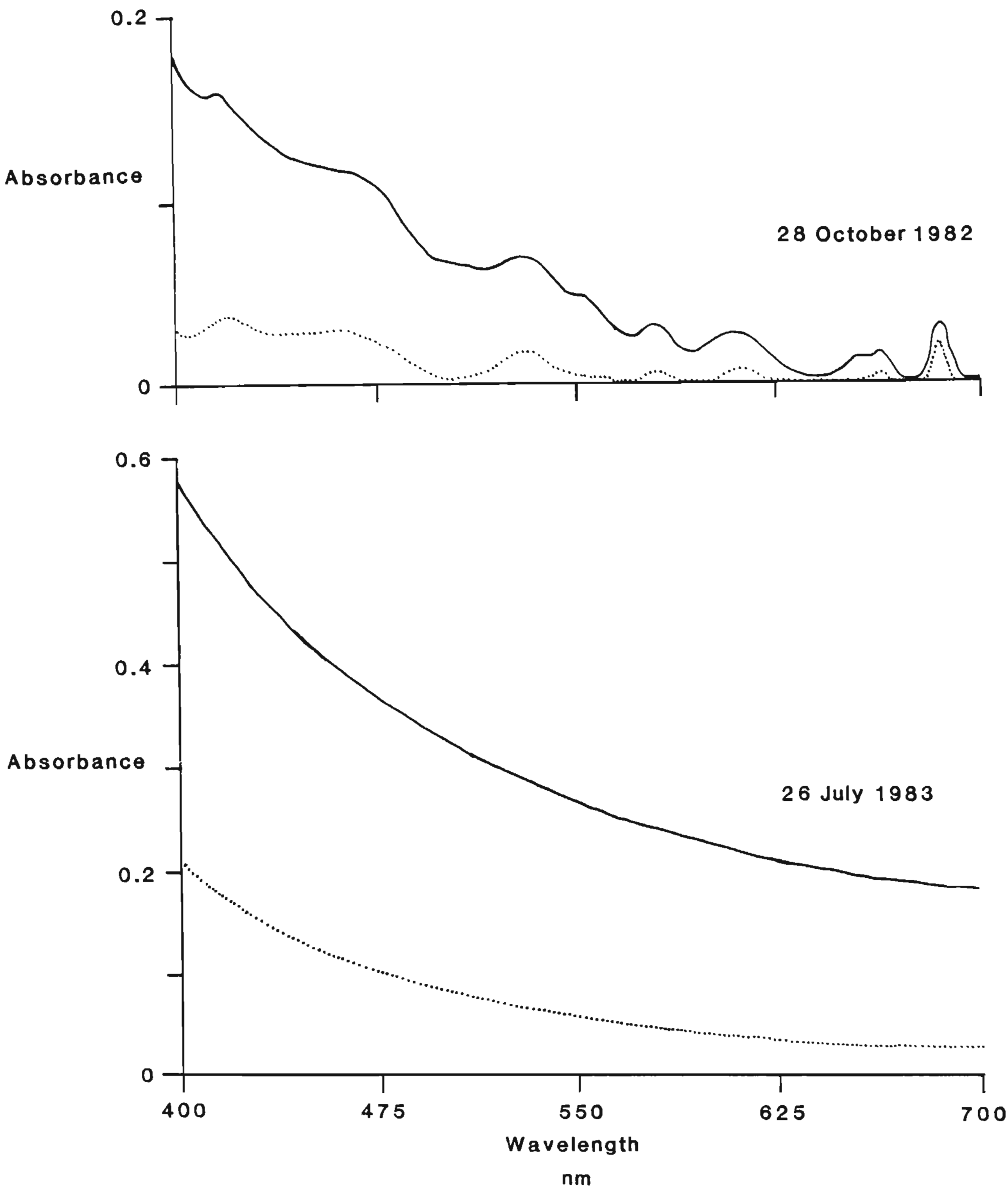

Figure 4.5. Absorbance scans over the PAR spectral range (400-700nm) for filtered (dotted line) and unfiltered lake water (solid line), after correction for absorption by distilled water.

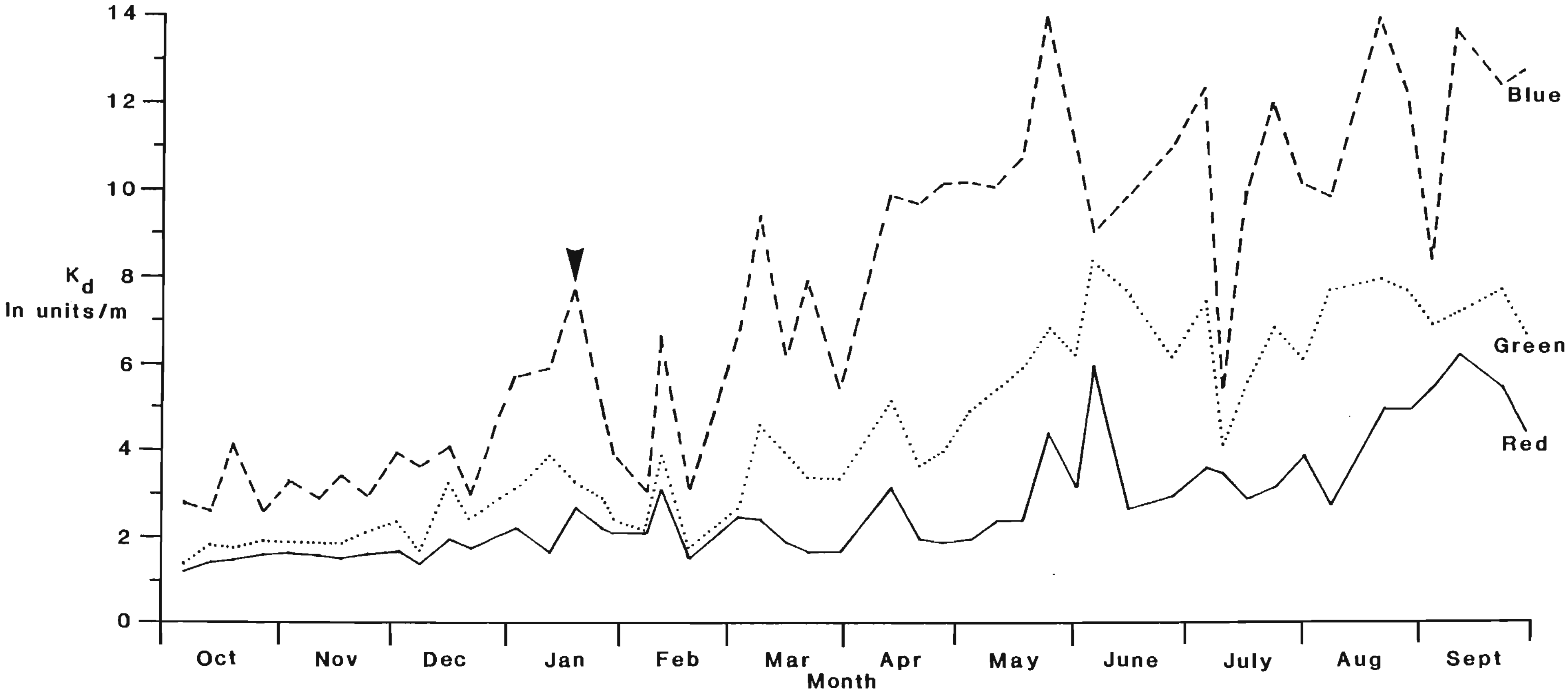

Figure 4.6. Annual variation in the vertical attenuation coefficient for downwelling blue (B), green (G) and red (R) light for the period October 1982 to September 1983. Arrow indicates sampling day when maximum phytoplankton standing crop was measured.

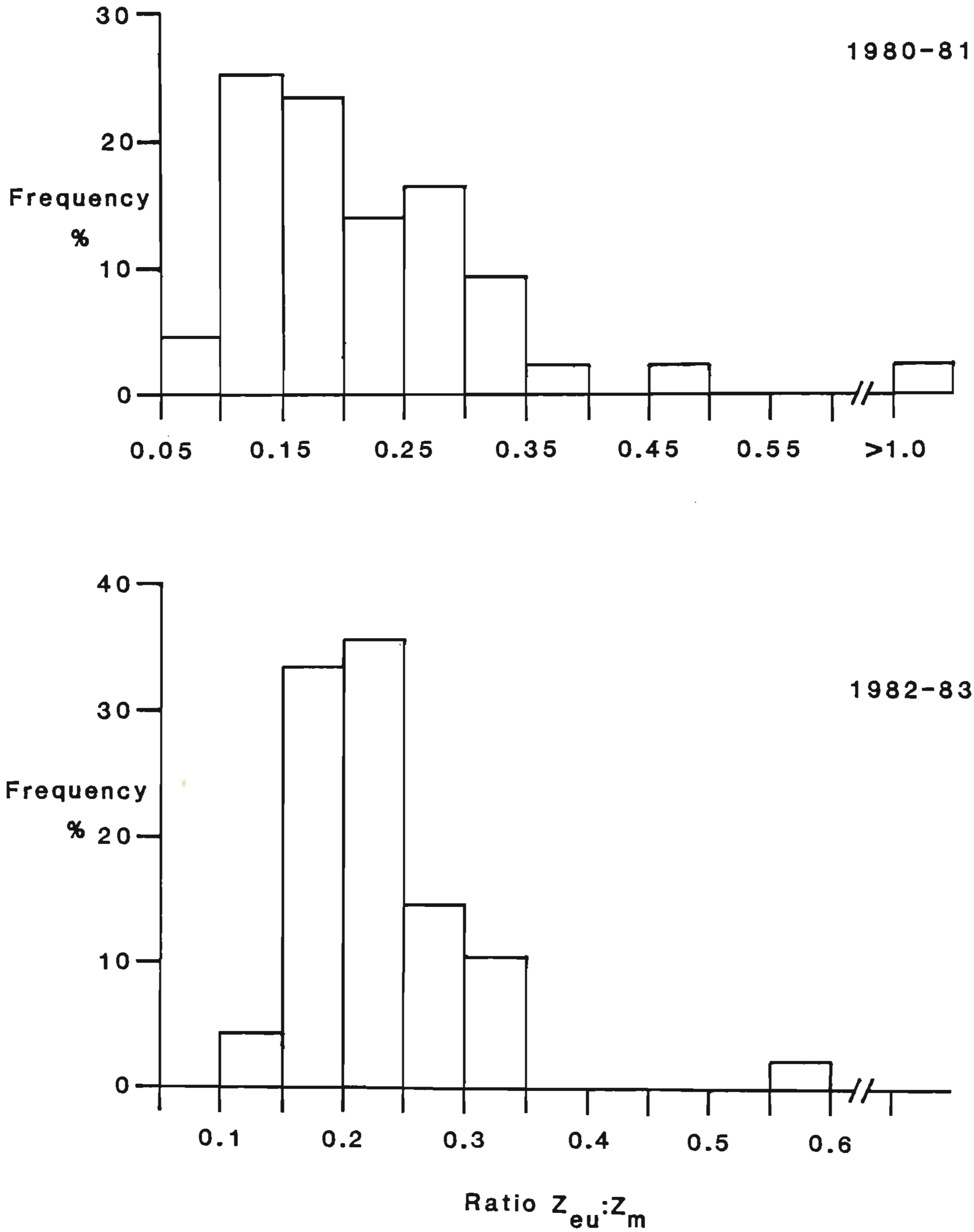

Figure 4.7. Histograms to show distribution of Z_{eu}:Z_m ratio values in 1980-81 and 1982-83.

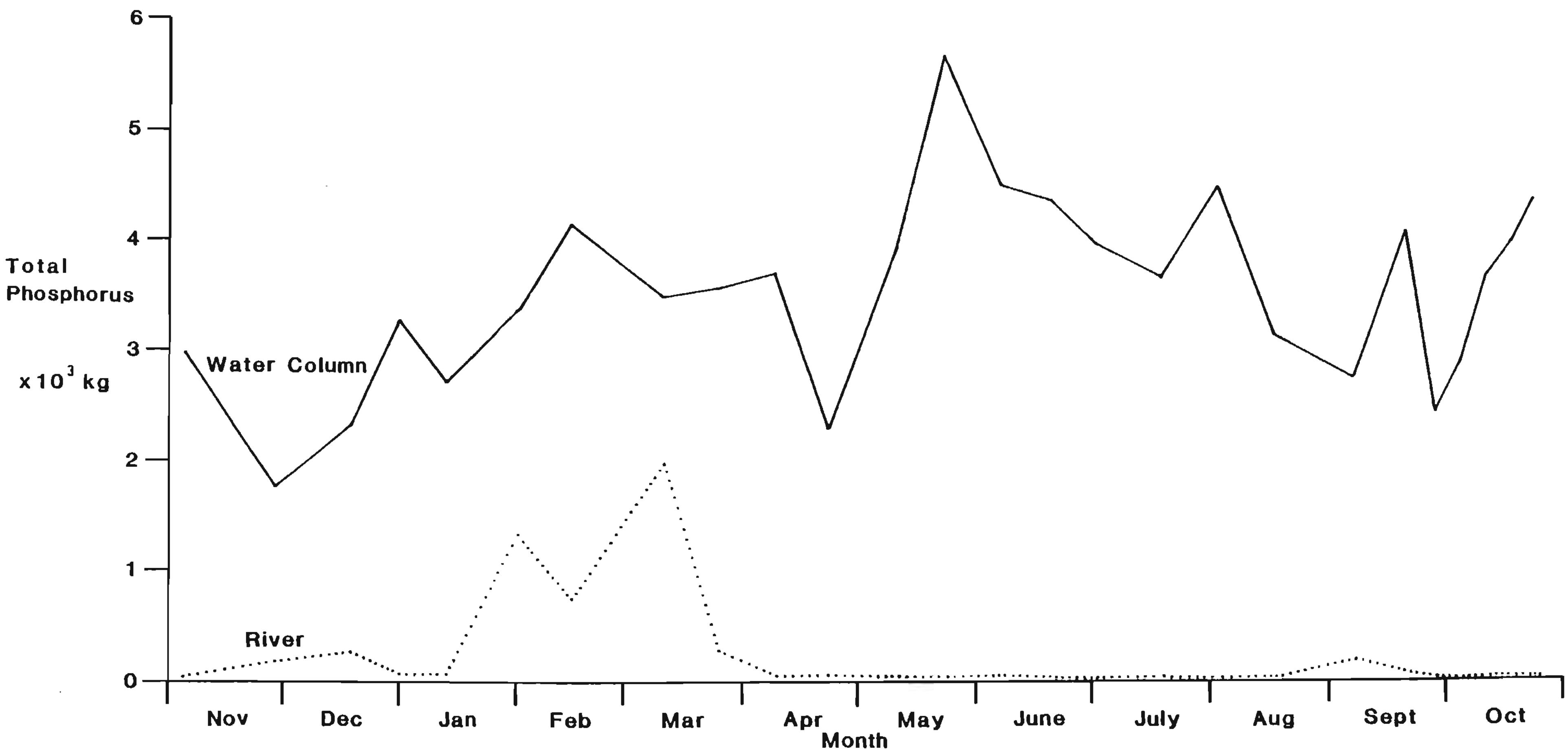

Figure 4.8. Annual variation in the total phosphorus content of the water column (solid line) and river inputs of total phosphorus (dotted line) for the period November 1980 to October 1981.

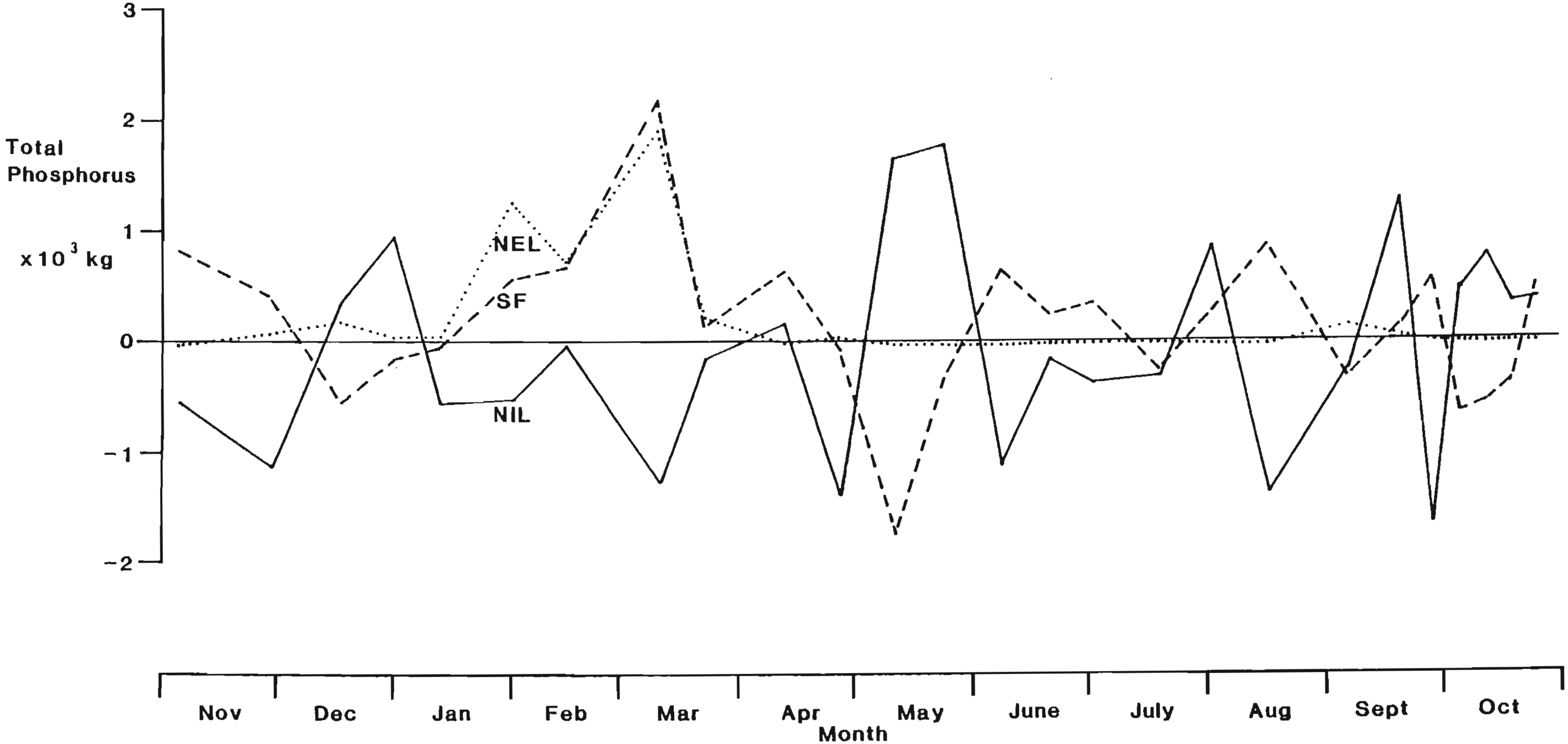

Figure 4.9. Annual variation in the net external load (NEL), sediment flux (SF) and net internal load (NIL) of total phosphorus for the period November 1980 to October 1981.

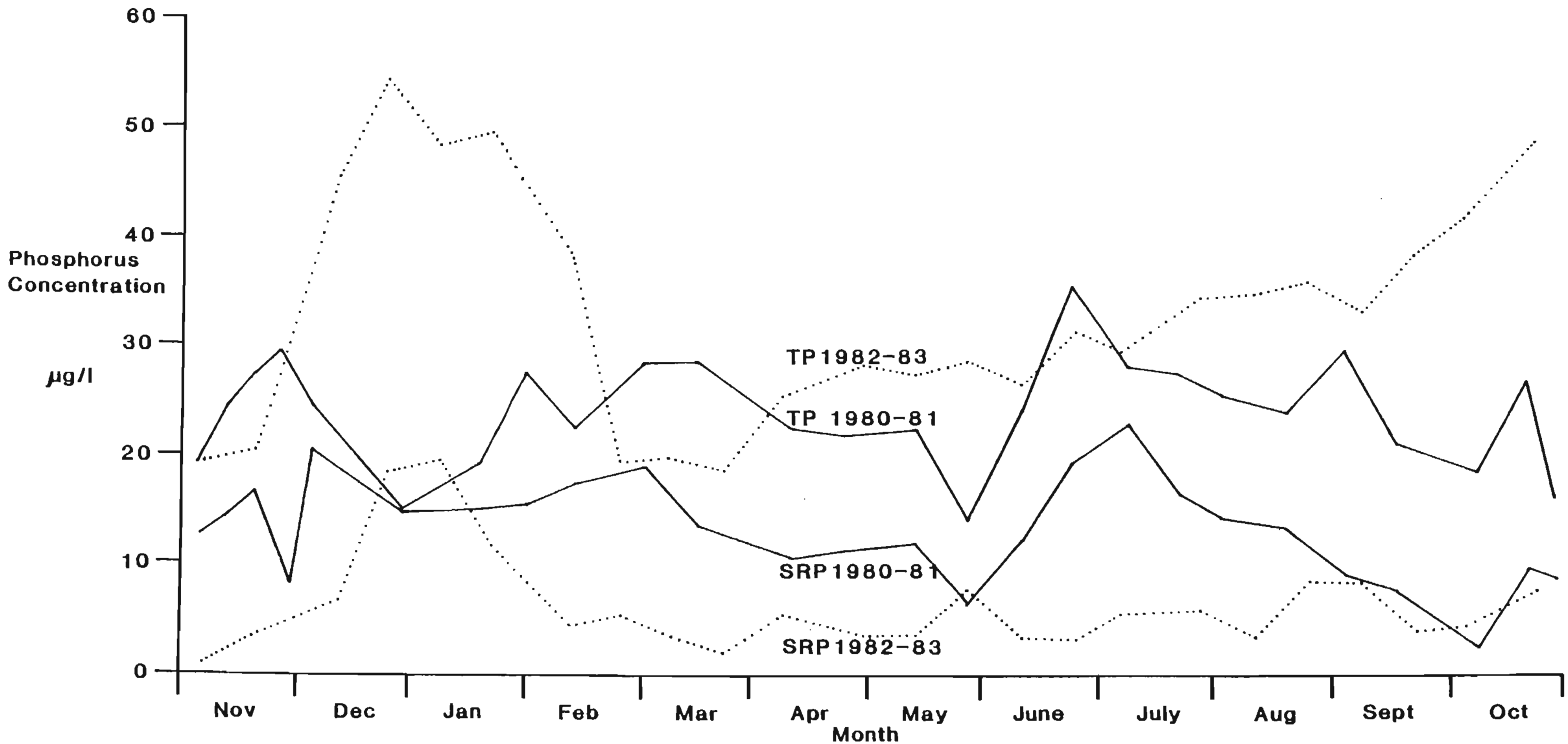

Figure 4.10. Annual variation in mean total phosphorus (TP) and soluble reactive phosphorus (SRP) concentrations in the water column for 1980-81 (solid lines) and 1982-83 (dotted lines).

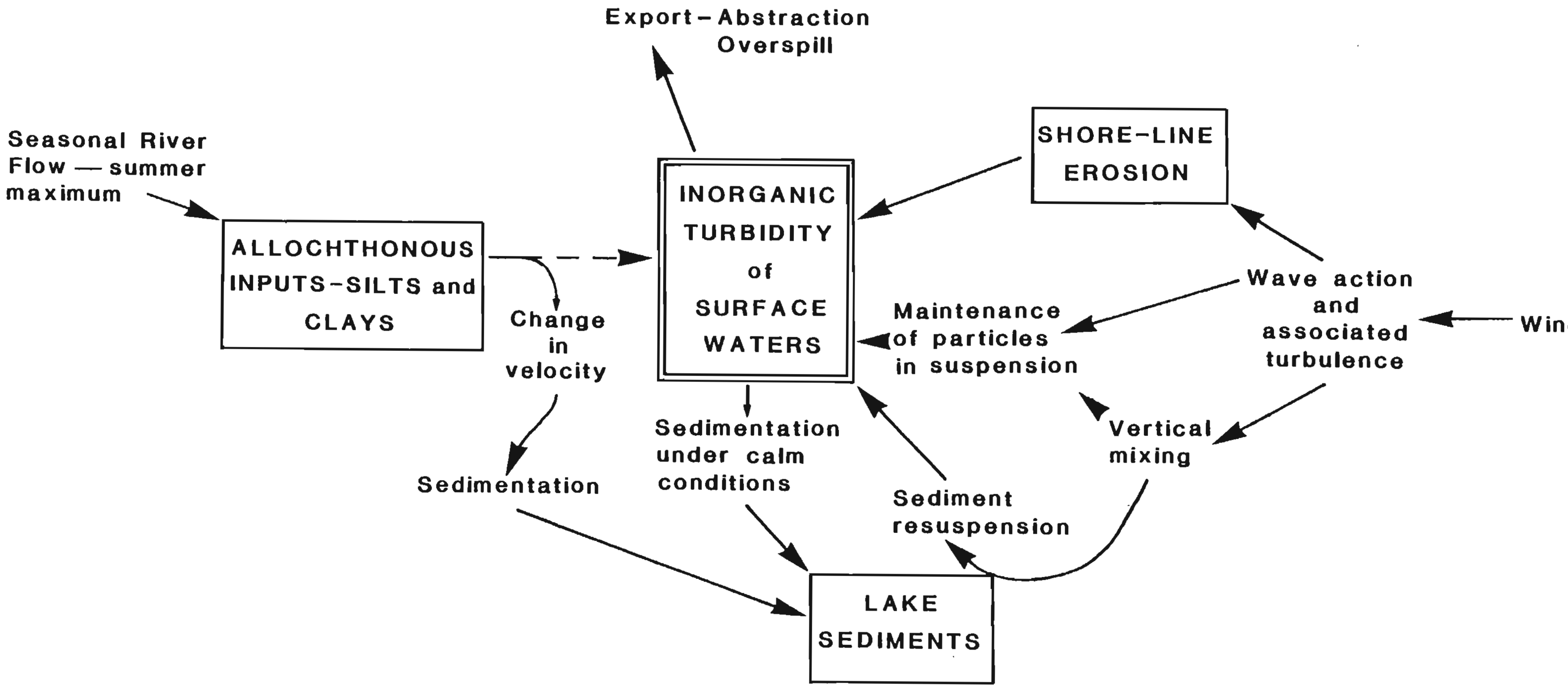

Figure 4.11. Sources of inorganic particulate material (solid boxes) and processes influencing inorganic turbidity in Lake Midmar.

Table 4.1. Mean, range and coefficients of variation (CV %) for the vertical attenuation coefficient for downwelling irradiance, K_d(PAR), and depth of the euphotic zone in 1980-81 and 1982-83.

Period	K_d(PAR) ln units/m			Euphotic zone depth m		
	Mean	Range	CV %	Mean	Range	CV %
1980 - 81						
October-March	1.69	1.11 - 2.33	18	2.72	2.07 - 3.83	15
April-September	2.19	1.31 - 4.26	31	2.19	1.39 - 3.43	24
1982 - 83						
October-March	1.98	1.16 - 3.17	28	2.54	1.37 - 3.8	28
April-September	3.47	1.62 - 5.78	38	1.22	0.78 - 1.95	29

Table 4.2. Regression constants for regression analysis of K_d(PAR) with phytoplankton standing crop (as B, mg Chl <u>a</u>/m^3, and ΣB, mg Chl <u>a</u>/m^2), total suspended solids and mean wind speed on the day before sampling.

Year	Variable	Variance ratio F	Significance	% variation accounted for
1980-81	B	0.02	n.s	-
	ΣB	7.97	< 0.001	18
	Wind	0.03	n.s	-
	River TSS	1.33	n.s	-
1982-83	B	0.5	n.s	-
	ΣB	11.61	< 0.001	29
	Wind	9.74	< 0.001	25
	Lake TSS	20.83	< 0.001	42
Step-wise Regression				
1982-83	Lake TSS	20.83	< 0.001	42
	Lake TSS+Wind	22.77	< 0.001	62 (Wind=20%)
	Lake TSS+Wind+ΣB	16.32	< 0.001	65 (ΣB=3%)

Table 4.3. Mean and range of vertical attenuation coefficients for downwelling blue, green and red light in 1981-82 and 1982-83.

Colour	Wavelength at mid-point of filter nm	Vertical attenuation coefficient ln units/m			
		1981 - 82		1982-83	
		Mean	Range	Mean	Range
Blue	443	2.93	1.43 - 6.36	7.59	2.53 - 13.95
Green	550	1.67	0.78 - 3.12	4.38	1.3 - 8.31
Red	670	1.35	0.73 - 1.99	2.68	1.17 - 6.16

Table 4.4. Planimetrically determined amounts of total phosphorus exchanged with sediments for the period November 1980 to October 1981. Determined from sediment flux and net internal load data presented in Figure 4.9.

Source	Amount of Phosphorus kg Total P/y	Direction of flow
Net internal load	376	To sediment
	210	To water column
Sediment flux	350	To sediment
	141	To water column

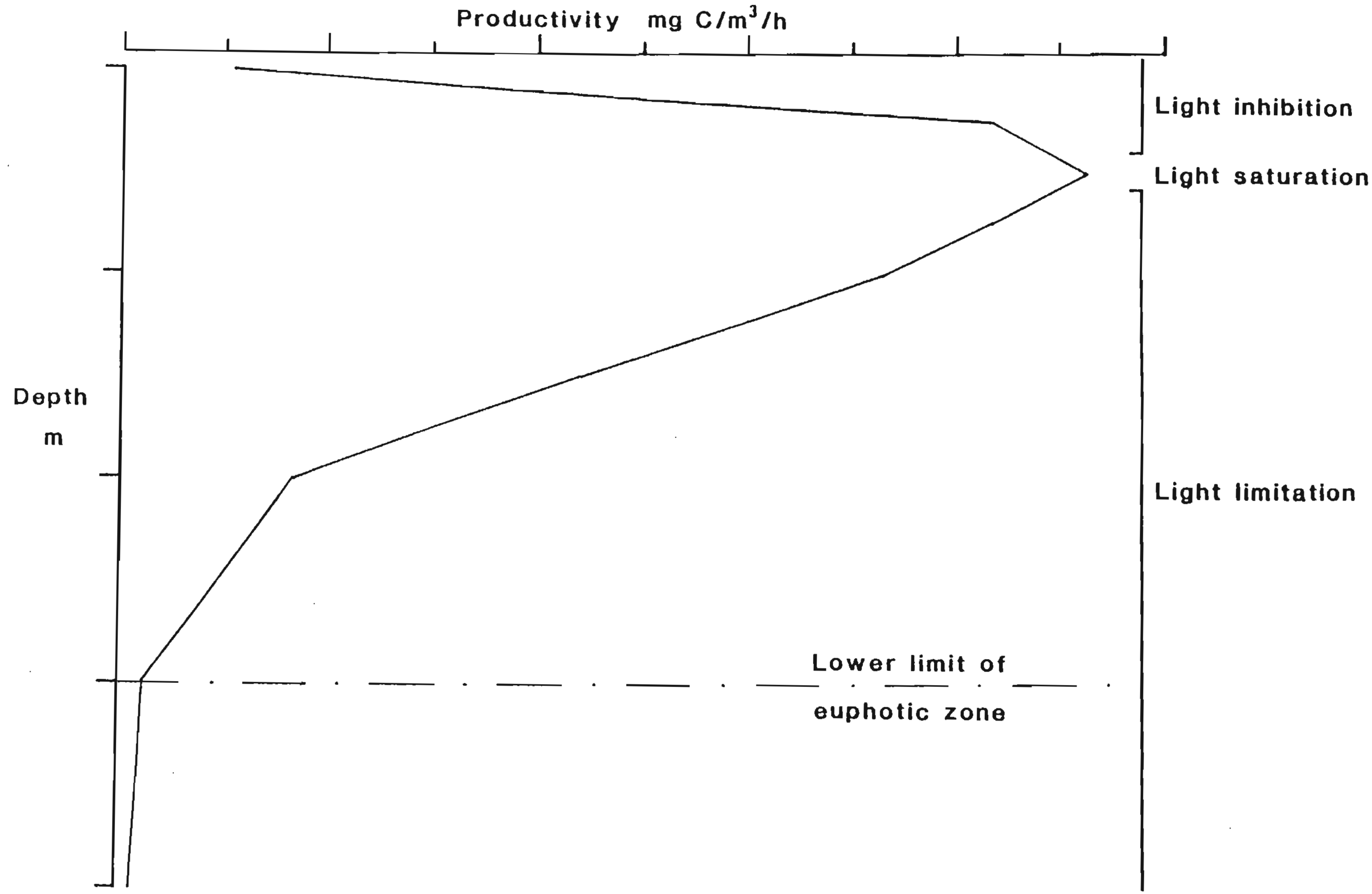

Figure 5.1 General form of productivity-depth profile in lakes.

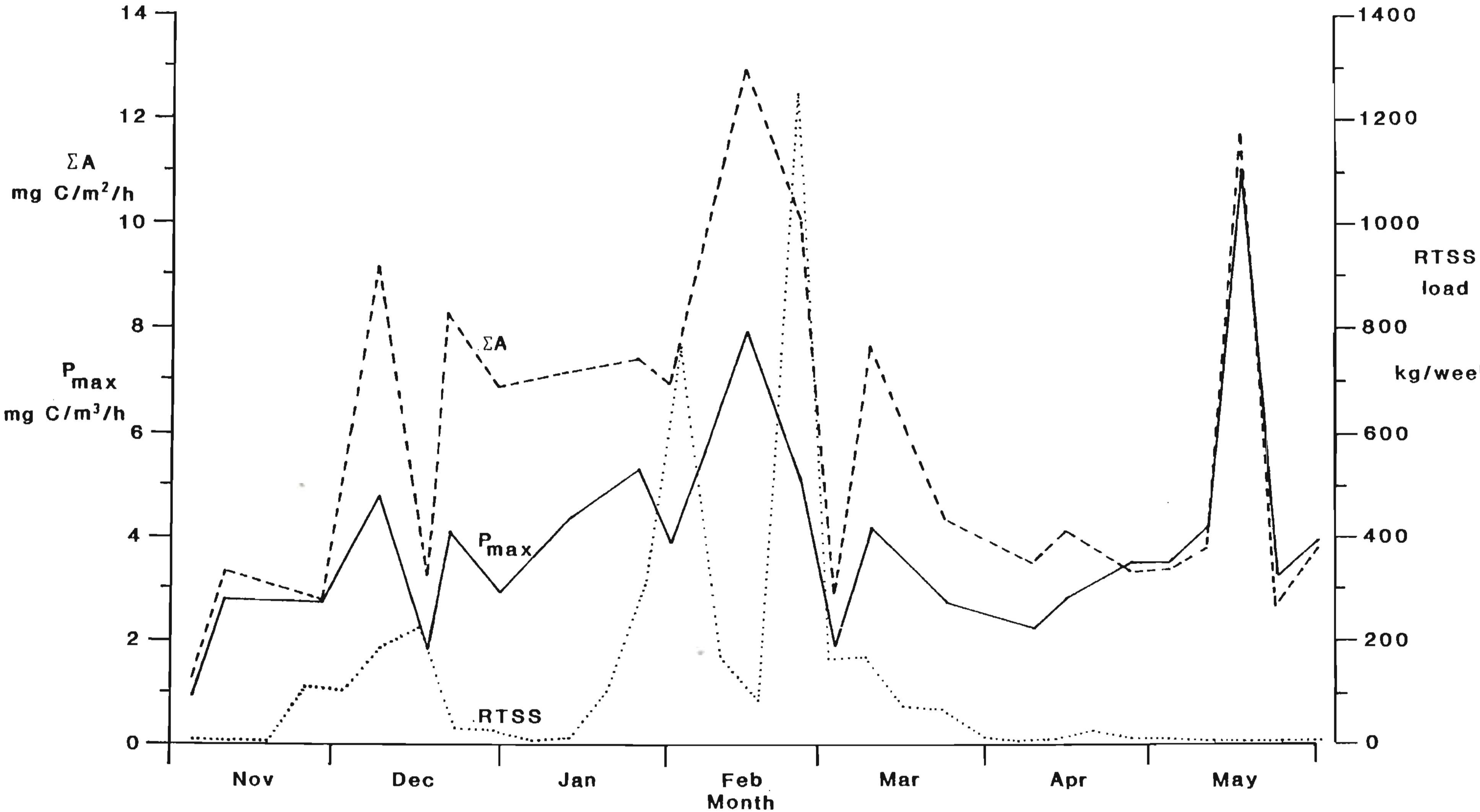

Figure 5.3. Changes in productivity parameters, P_{max} (the light saturated rate of production) and ΣA (planimetrically determined integral rate of production) in relation to changes in river inputs of suspended solids (TSS) for the period November 1980 to May 1981.

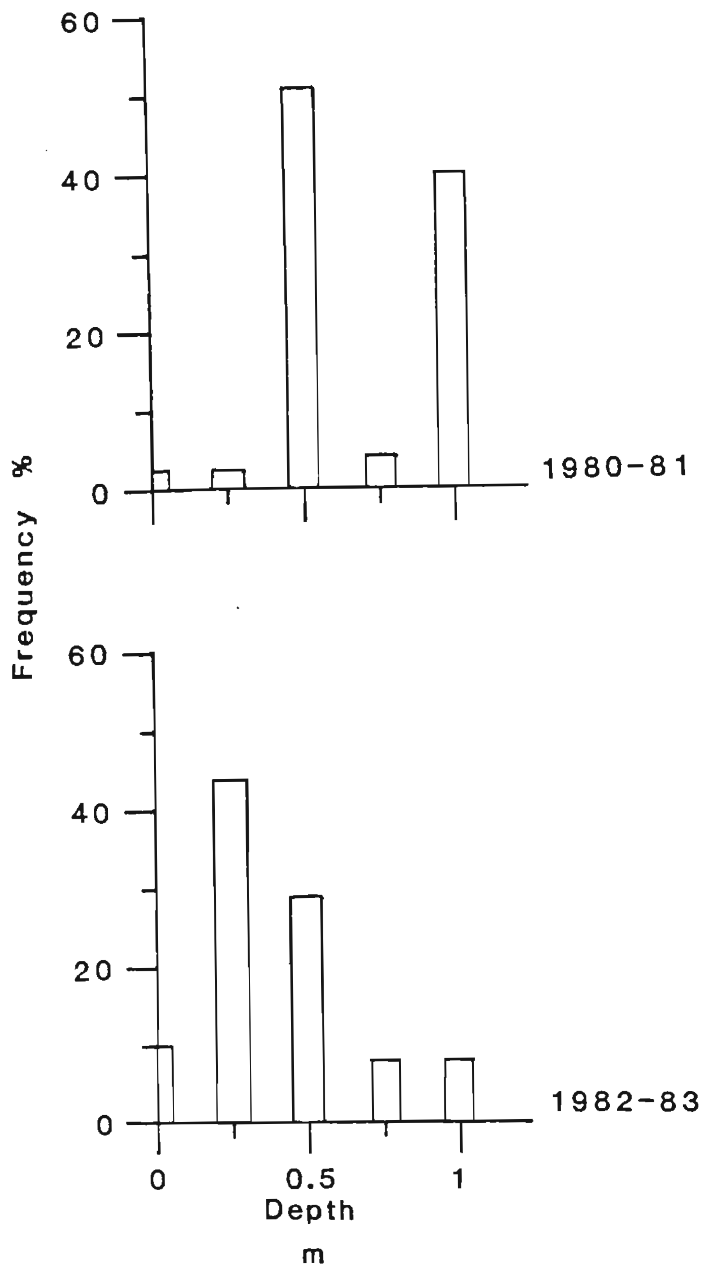

Figure 5.4. Histograms to show number of occasions (as frequency) when P_{max} was measured at a particular depth in 1980-81 and 1982-83.

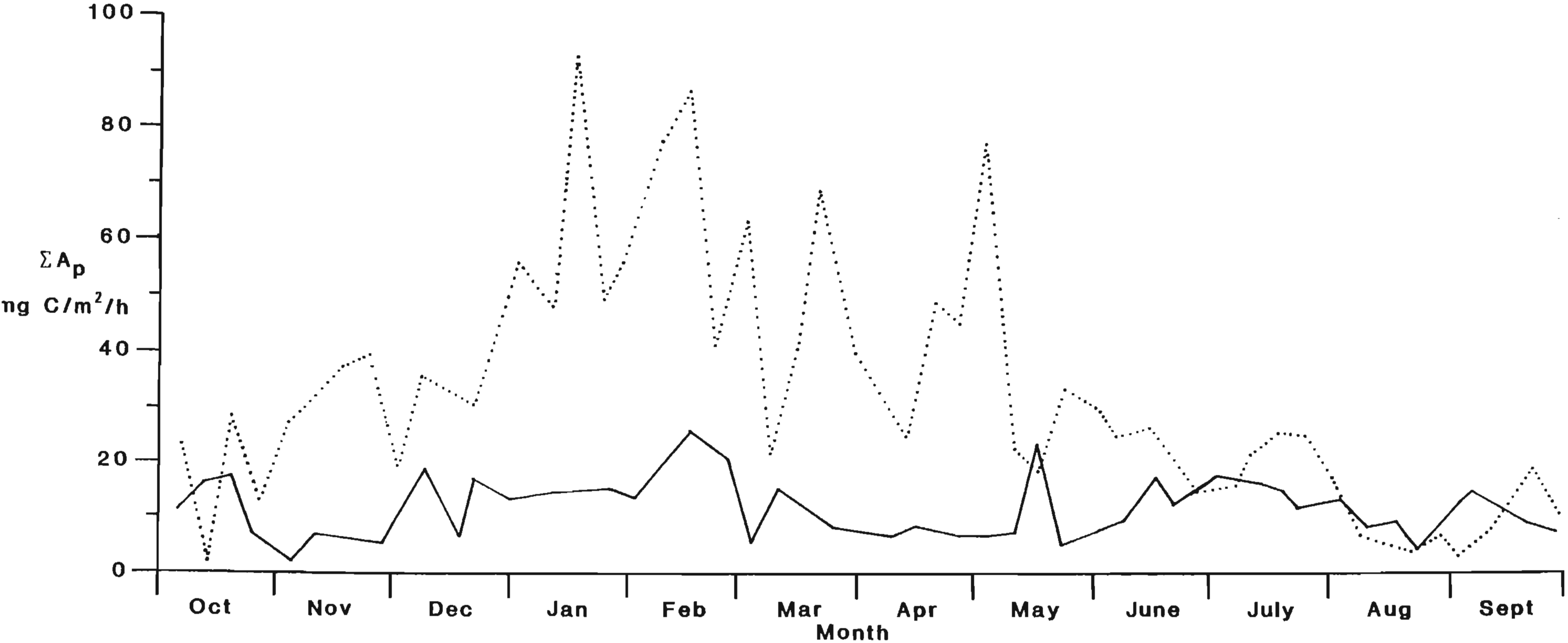

Figure 5.5. Annual variation in planimetrically determined values of ΣA (ΣA_p) in 1980-81 (solid line) and 1982-83 (dotted line).

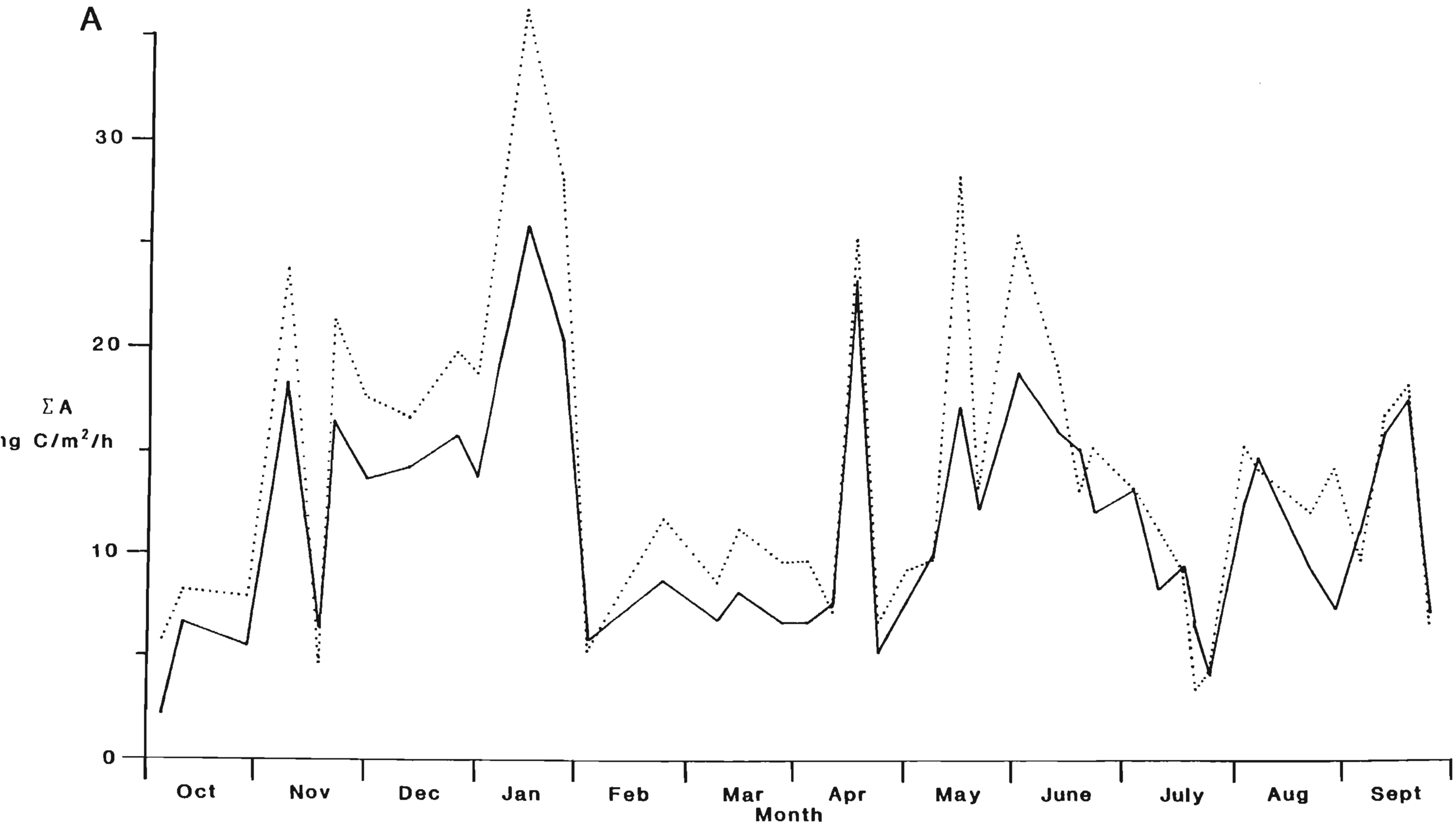

Figure 5.6. a) Annual variation in planimetrically determined values of ΣA (ΣA_p, solid line) and predicted values of ΣA, using Talling's model (ΣA_T, dotted line) in 1980-81.

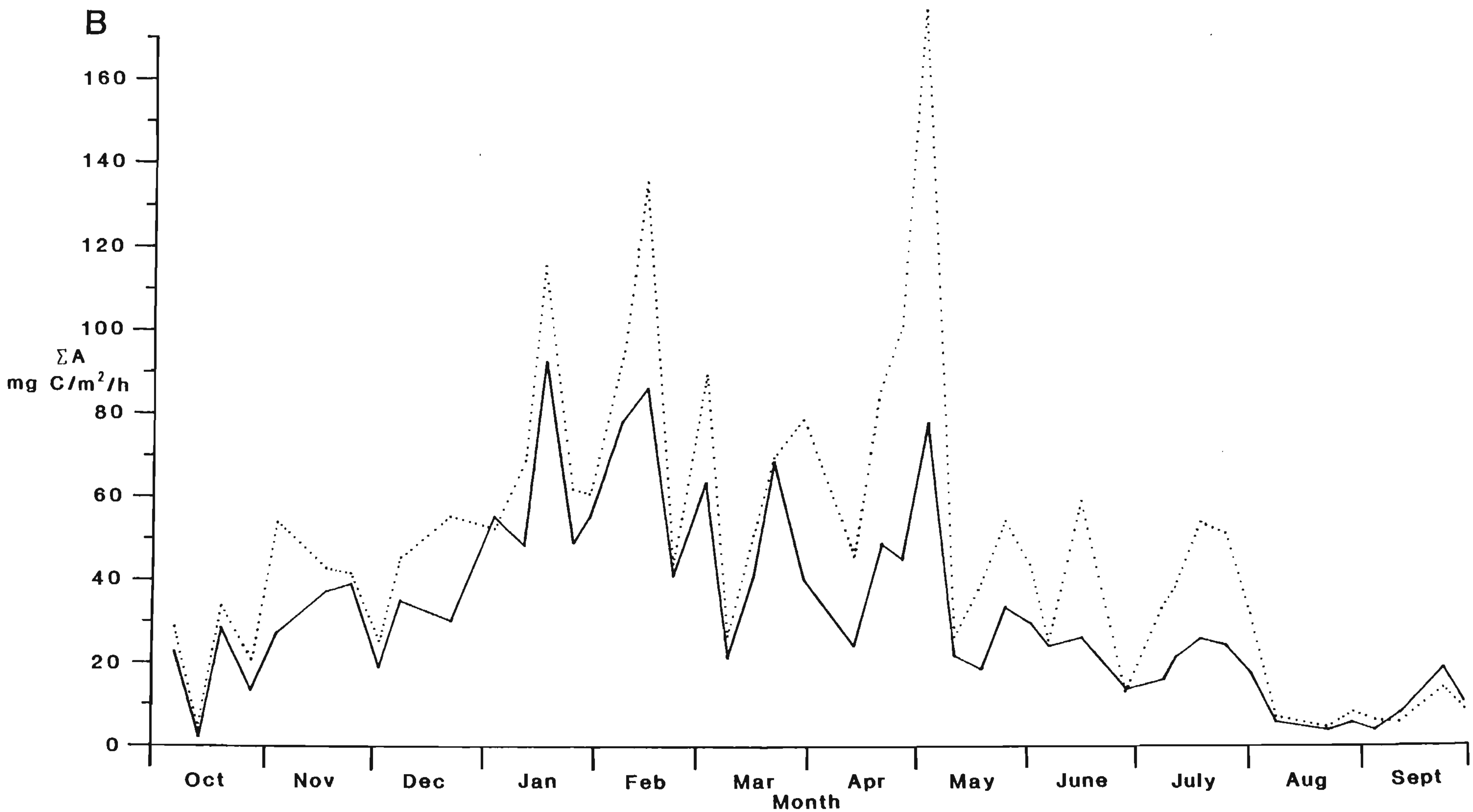

Figure 5.6. b) Annual variation in planimetrically determined values of ΣA (ΣA_p, solid line) and predicted values of ΣA, using Talling's model (ΣA_T, dotted line) in 1982-83.

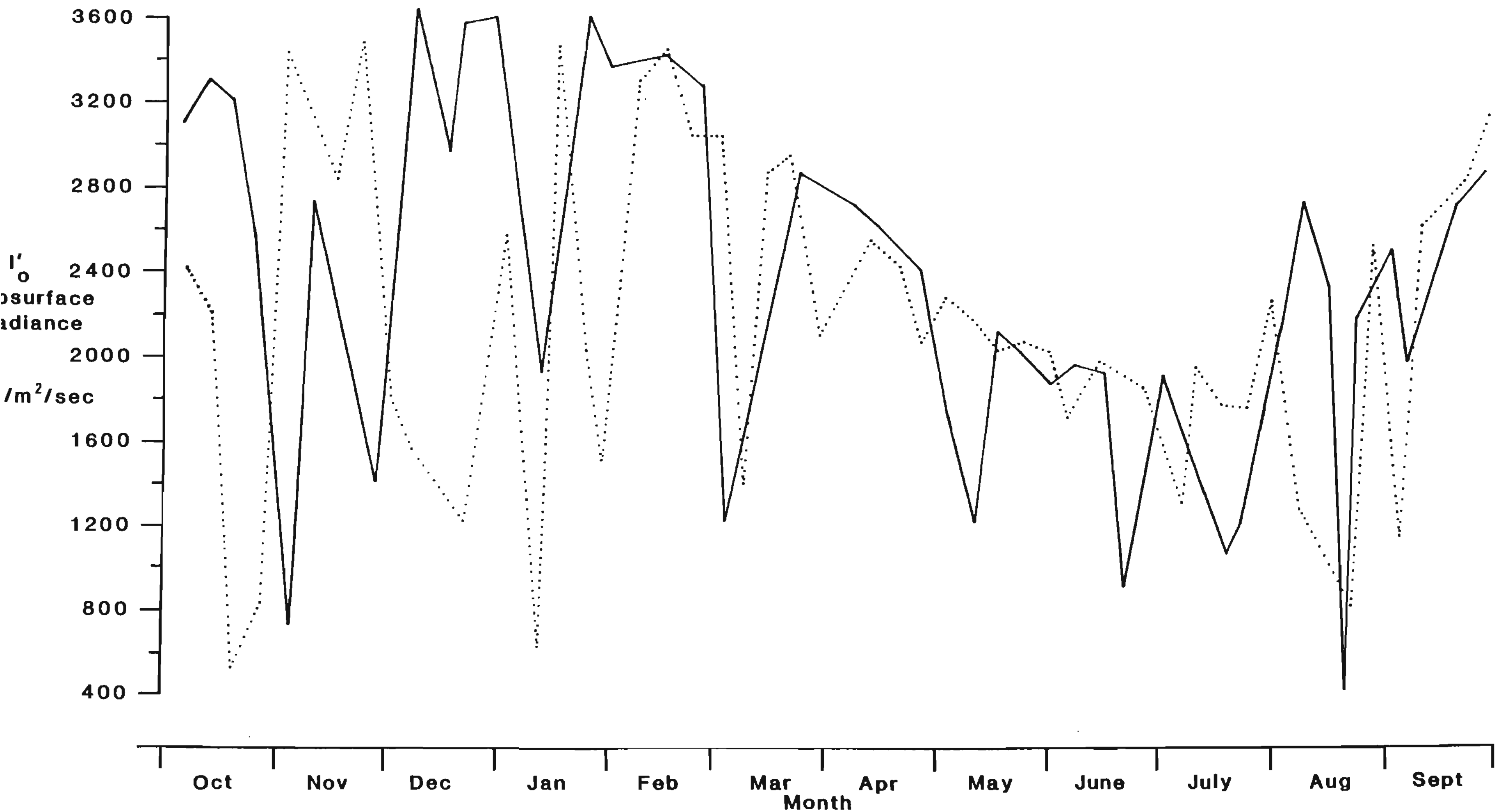

Figure 5.7. Annual variation in the subsurface irradiance (I'_o) during incubation period (10.00 to 14.00 hours) in 1980-81 (solid lines) and 1982-83 (dotted lines).

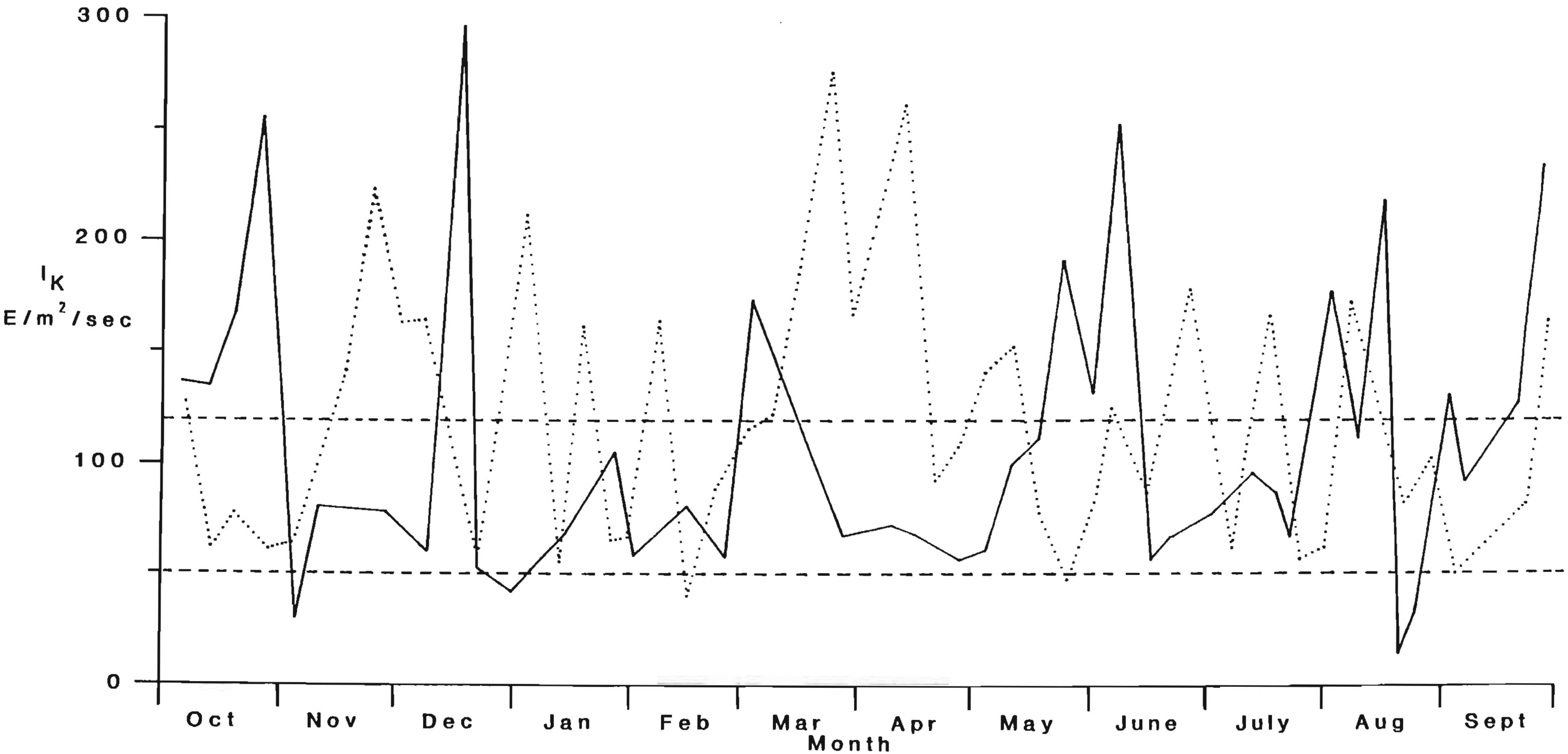

Figure 5.8. Annual variation in values of the photosynthetic saturation parameter (I_K) in 1980-81 (solid line) and 1982-83 (dotted line). Dashed horizontal lines range of I_K values reported by Harris (1978).

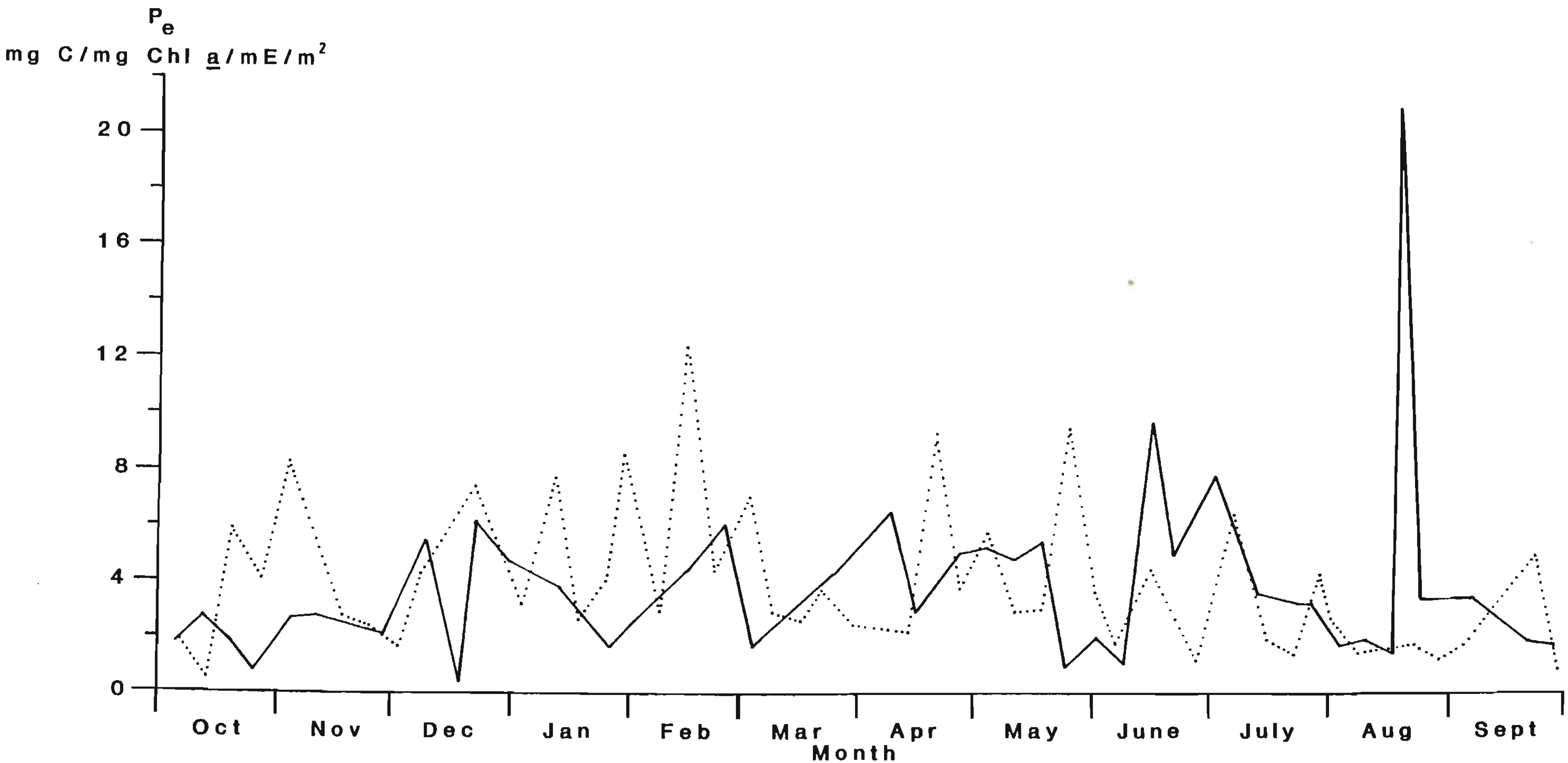

Figure 5.9. Annual variation in values of photosynthetic efficiency (P_e) in 1980-81 (solid lines) and 1982-83 (dotted line).

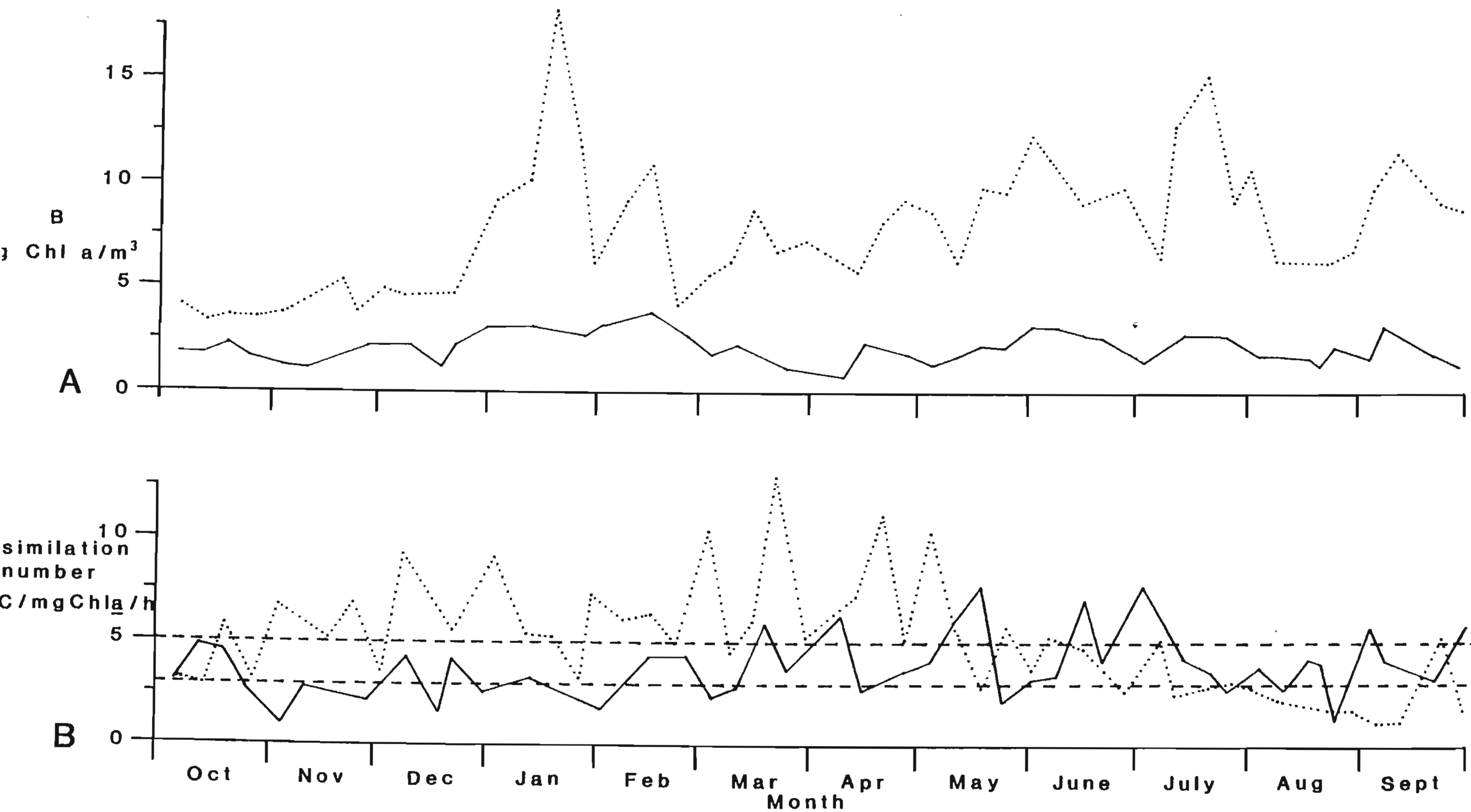

Figure 5.10. Annual variation in **a)** phytoplankton standing crop (as mean chlorophyll concentration in the euphotic zone, B);

b) assimilation number in 1980-81 (solid line) and 1982-83 (dotted line). Dashed horizontal lines Curl and Small's (1965) values of assimilation number indicating nutrient deficiency (lower line) and borderline nutrient deficiency (upper line).

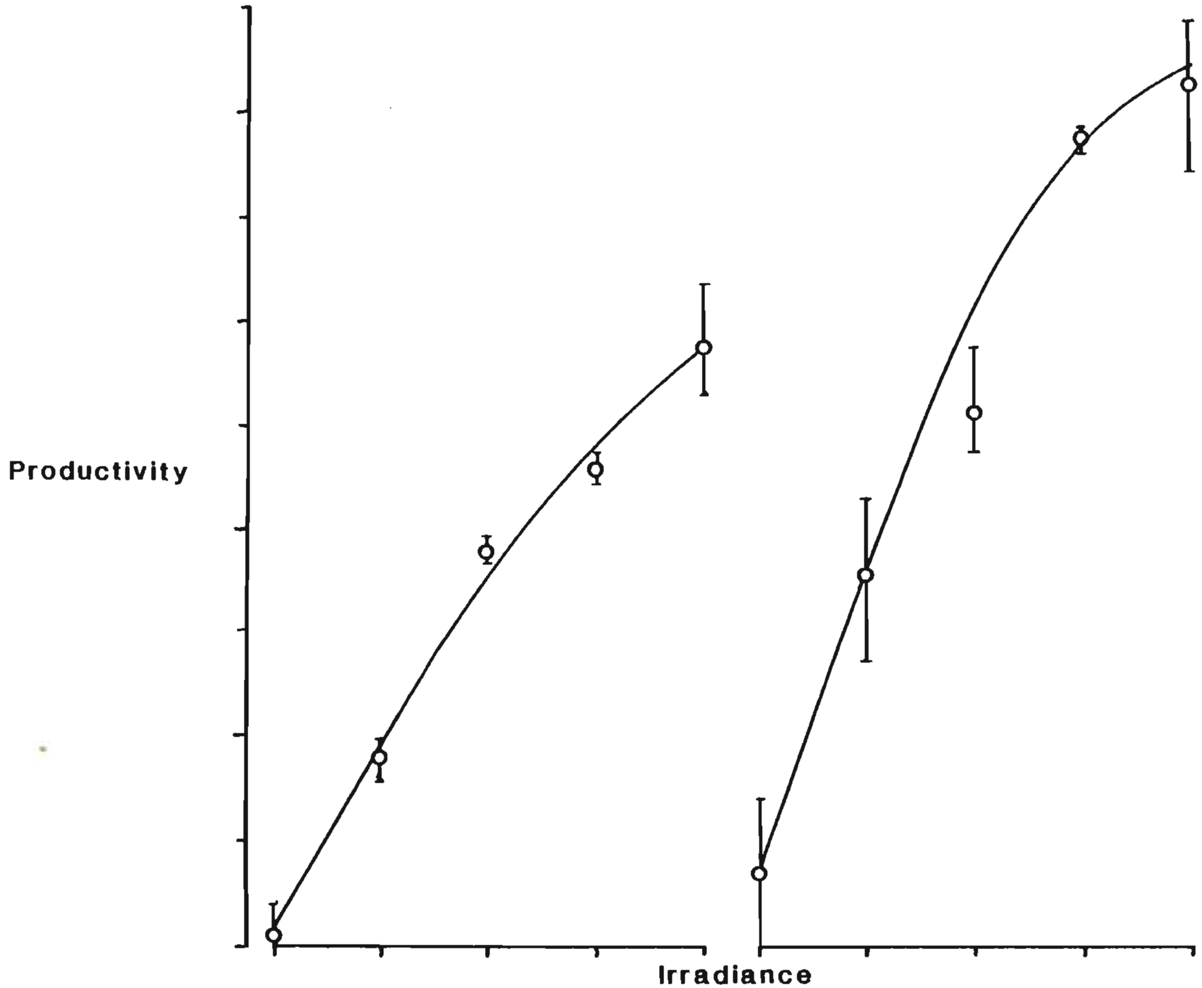

Figure 5.11. To show the relationship between productivity and irradiance determined by incubating samples collected at 5m, at 0.5m for different periods of time (one, two, three or four hours) on two different occasions.

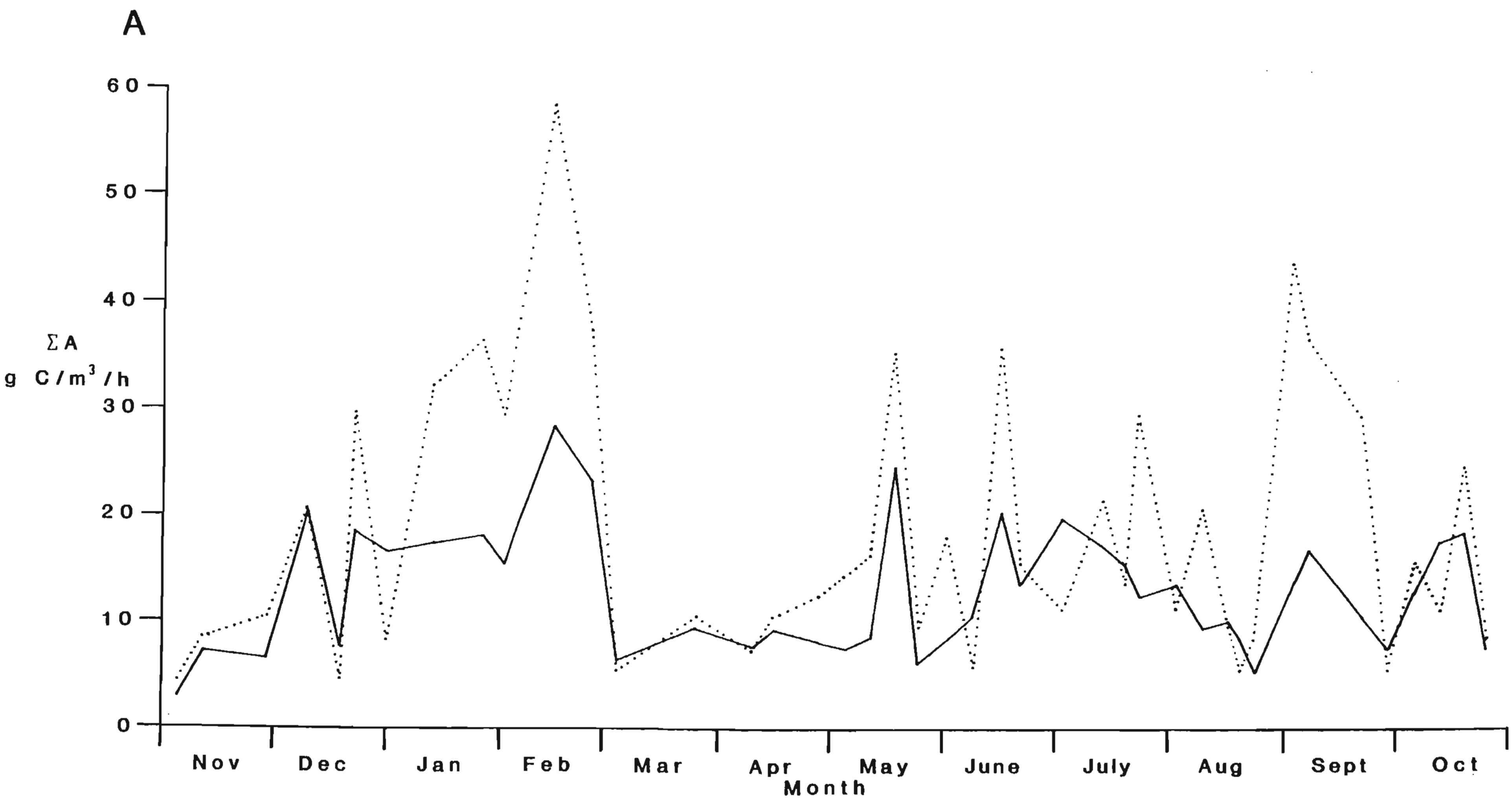

Figure 5.12. a) Annual variation in actual values of ΣA obtained using static incubation flasks (ΣA_p) (solid line) and calculated values for mixed samples (ΣA_{MIXED}) (dotted line) in 1980-81.

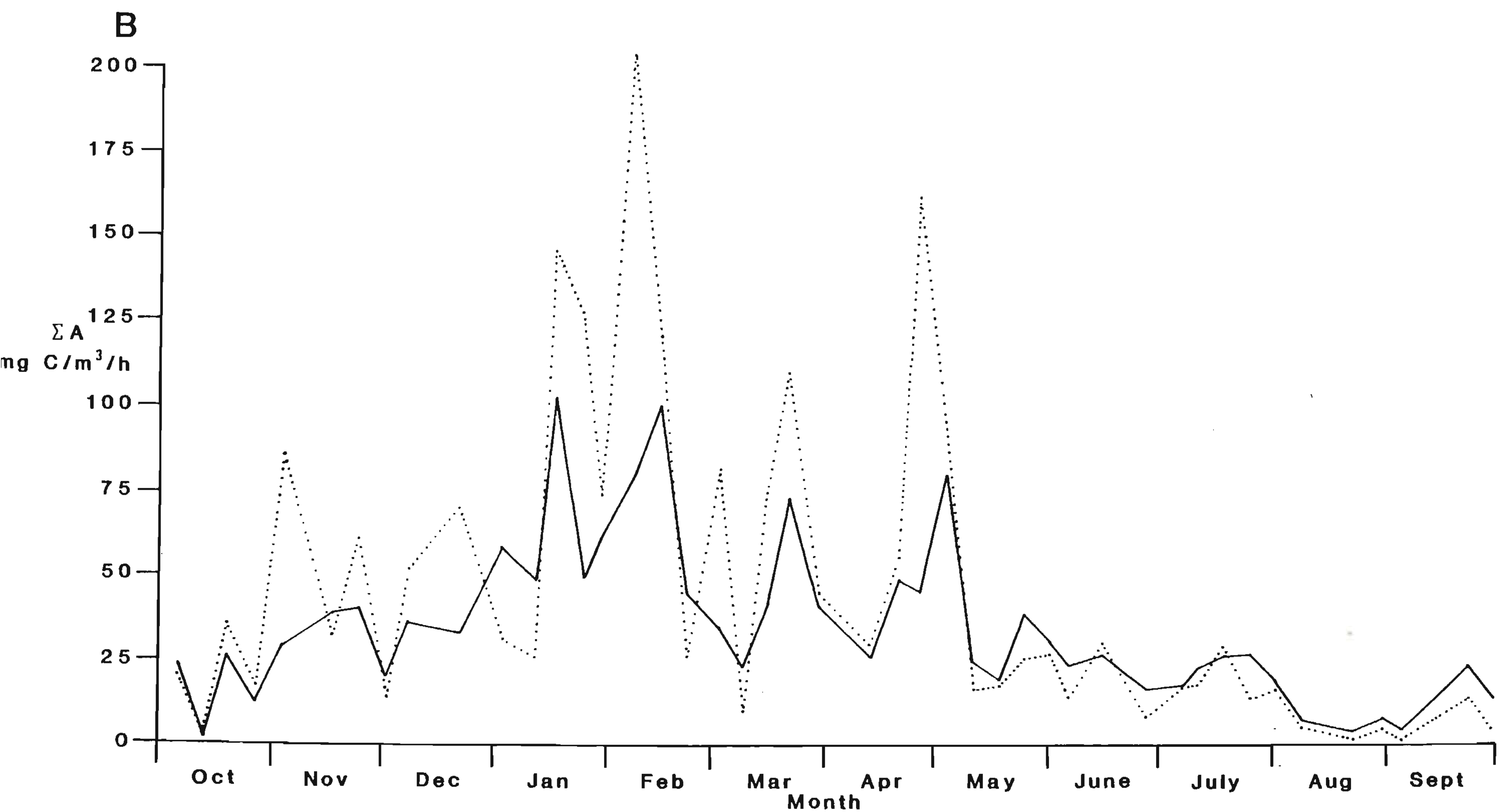

Figure 5.12. b) Annual variation in actual values of ΣA obtained using static incubation flasks (ΣA_p) (solid line) and calculated values for mixed samples (ΣA_{MIXED}) (dotted line) in 1982-83.

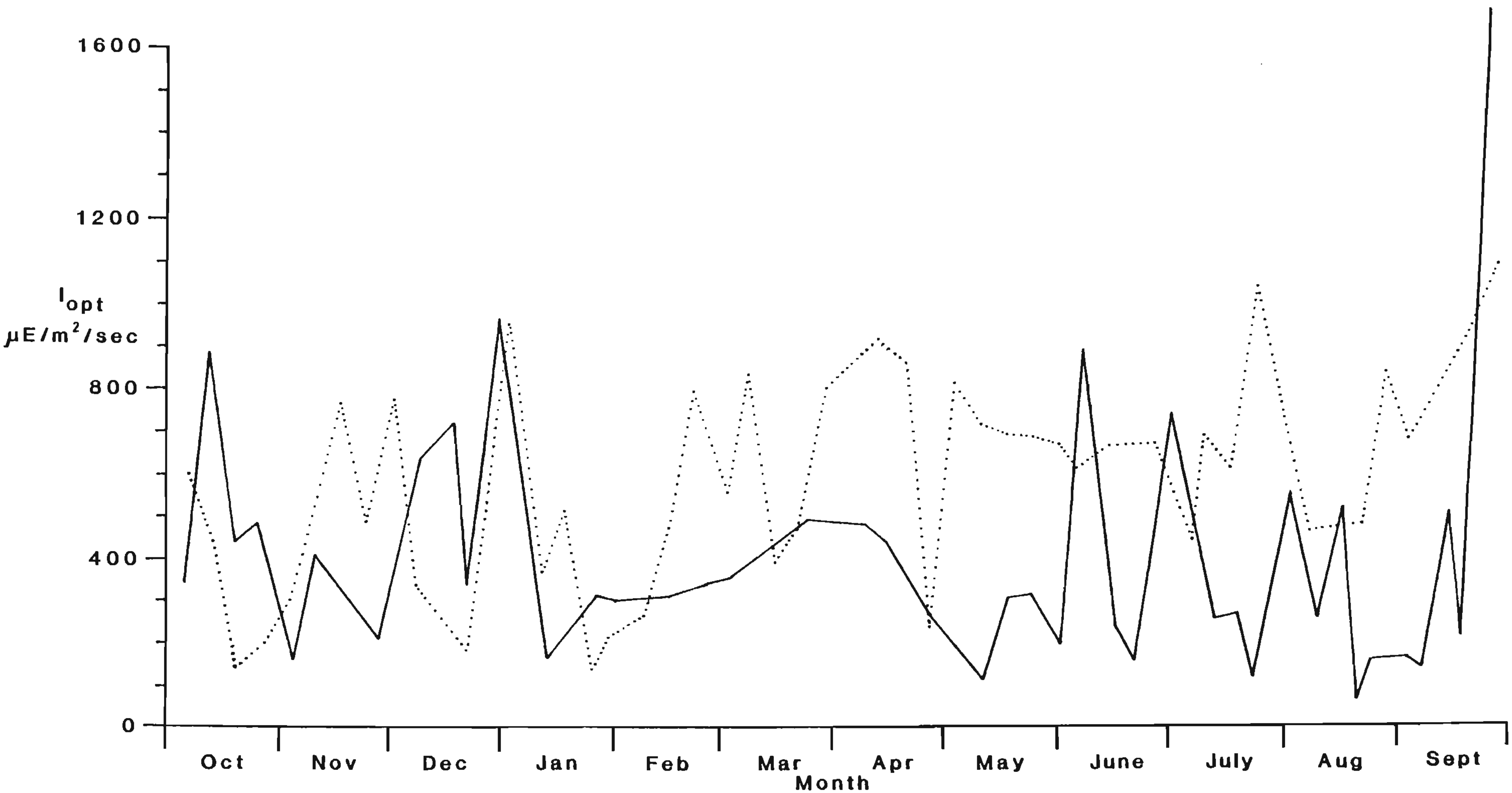

Figure 5.13. Annual variation in mean irradiance at depth where the light saturated rate of production was measured (I_{opt}) in 1980-81 (solid line) and 1982-83 (dotted line).

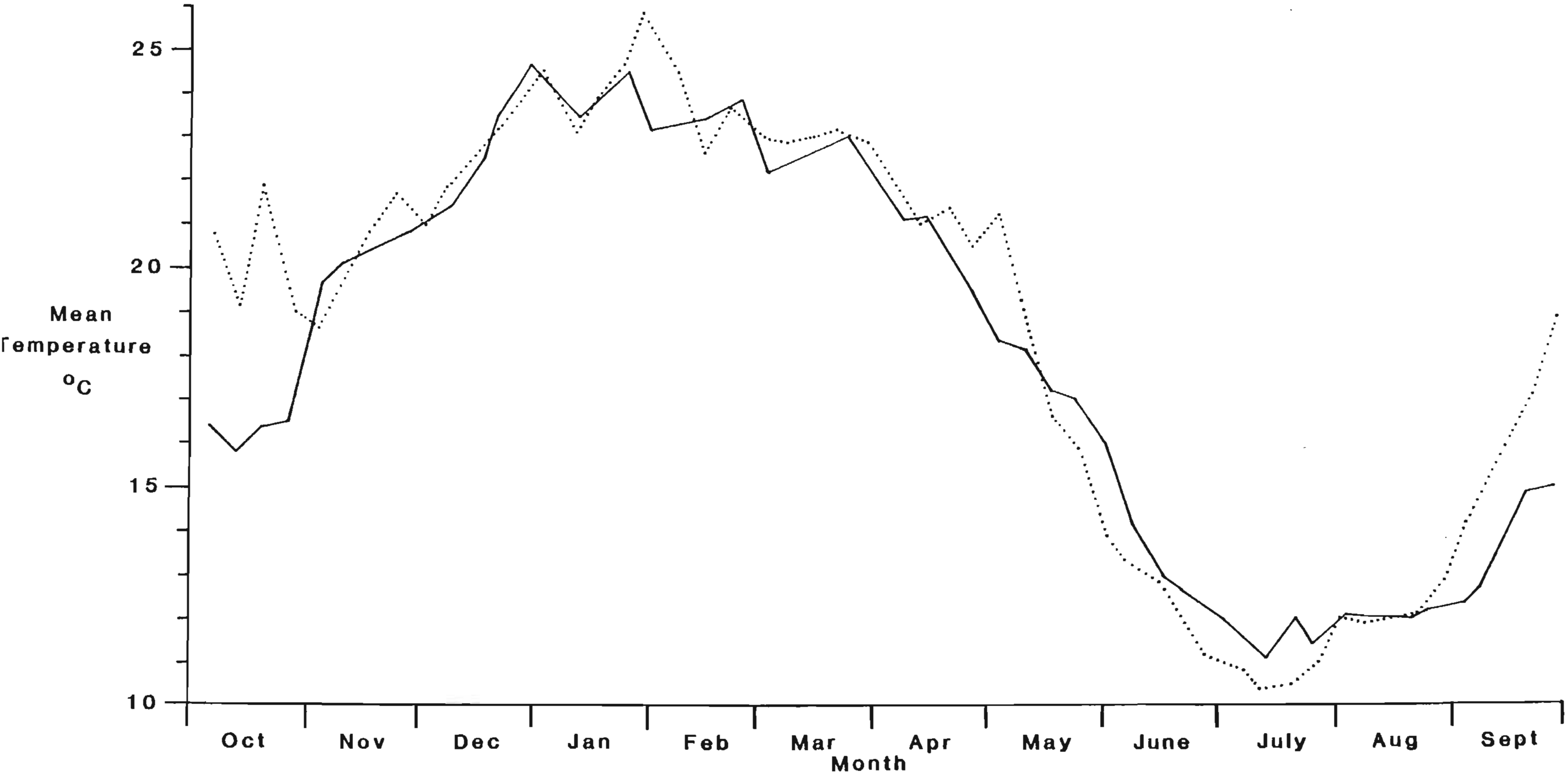

Figure 5.14. Annual variation in mean water temperature of the euphotic zone in 1980-81 (solid line) and 1982-83 (dotted line).

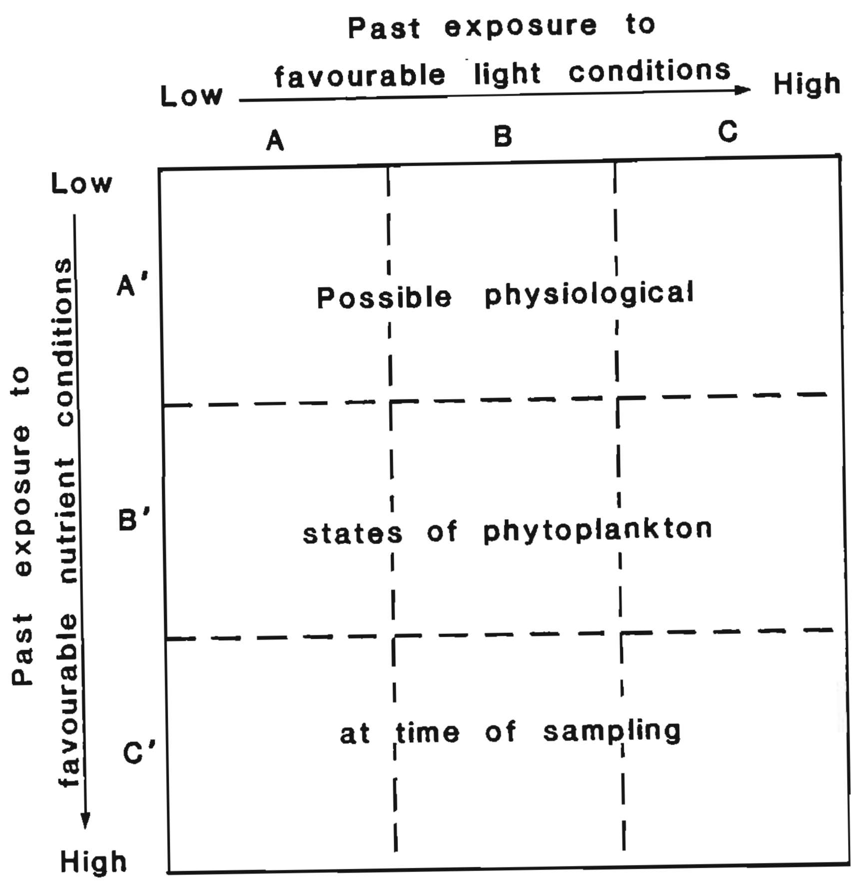

Figure 5.15. Matrix to show the range of possible physiological states in phytoplankton, on any sampling day, as a result of the influence of exposure to favourable light and/or nutrient conditions prior to sampling.

Table 5.1. Means, ranges and coefficients of variation (CV %) for the ratio Z_{eu}:Z_m and depth of the euphotic zone (Z_{eu}) in 1980-81 and 1982-83.

Year	$Z_{eu} : Z_m$			Z_{eu} metres		
	Mean	Range	CV %	Mean	Range	CV %
1980-81	0.24	0.1 - 1.28	78	2.47	1.39 - 3.83	22
1982-83	0.24	0.15 - 0.59	32	1.81	0.78 - 3.55	42

Table 5.2. Variation in predictive capability of Talling's model (as the ratio of predicted value of ΣA (ΣA_T) : actual value determined planimetrically (ΣA_P) in relation to I_K value on selected occasions.

Date	$\Sigma A_T : \Sigma A_P$	I_K $\mu E/m^2/s$
16.2.83	1.4	40.4
28.6.83	0.9	179.0
14.4.83	1.8	261.5
5.5.83	2.2	141.0

Table 5.3. Regression constants for regression analysis of I_K with P_e, assimilation number, mean irradiance during incubation (I_{IN}) and one day (I_{PRE1}), two (I_{PRE2}) or three (I_{PRE3}) days prior to estimation of I_K, and temperature in 1980-81 and 1982-83.

Simple regression

Year	Variable	Variance ratio F	Significance	% variation accounted for.
1980-81	P_e	18.2	< 0.05	31
	Assimilation number	0.17	n.s	0.4
	I_{IN}	0.6	n.s	1.5
	I_{PRE1}	3.3	n.s	8
	I_{PRE2}	5.3	< 0.05	12
	I_{PRE3}	5.5	< 0.05	12
	Temperature	1.2	n.s	3
1982-83	P_e	12.7	< 0.05	25
	Assimilation number	5.2	< 0.05	11.8
	I_{IN}	5.2	< 0.05	11.8
	I_{PRE1}	1.2	n.s	3
	I_{PRE2}	3.3	n.s	8
	I_{PRE3}	1.9	n.s	5
	Temperature	2.1	n.s	5

Stepwise Regression

1980-81	P_e	18.2	< 0.05	31.3
	P_e + I_{PRE2}	8.1	< 0.05	43.1
1982-83	P_e	12.7	< 0.05	24.6
	P_e + Assimilation number	89.5	< 0.05	77.5

Table 5.4. Regression constants for simple regression analysis of P_e with assimilation number, mean irradiance during incubation (I_{IN}) and one day (I_{PRE1}), two (I_{PRE2}) or three (I_{PRE3}) days prior to estimation of P_e, and temperature in 1980-81 and 1982-83.

Simple Regression

Year	Variable	Variance ratio F	Significance	% variation accounted for.
1980-81	Assimilation number	8.3	< 0.05	17
	I_{IN}	3.2	n.s	7.3
	I_{PRE1}	0.01	n.s	-
	I_{PRE2}	0	n.s	-
	I_{PRE3}	0.2	n.s	0.4
	Temperature	0.5	n.s	1
1982-83	Assimilation number	16.2	< 0.05	29
	I_{IN}	0.2	n.s	0.4
	I_{PRE1}	0.3	n.s	0.6
	I_{PRE2}	0.4	n.s	0.9
	I_{PRE3}	0.3	n.s	0.8
	Temperature	4.8	< 0.05	11

Table 5.5. Regression constants for stepwise regression analysis of predicted values of ΣA (ΣA_T) with individual components of Talling's model in 1980-81 and 1982-83.

Year	Variable	Variance ratio F	Significance	%variation accounted for.
1980-81	P_{max}	74.6	< 0.05	65.1
	P_{max} + [ln I'_o - ln 0.5 I_K]	28.0	< 0.05	79.7
	P_{max} + [ln I'_o - ln 0.5 I_K] + 1/ K_d(PAR)	71.6	< 0.05	93.0
1982-83	P_{max}	109.2	< 0.05	71.8
	P_{max} + 1/ K_d(PAR)	34.5	< 0.05	84.5
	P_{max} + 1/ K_d(PAR) + [ln I'_o - ln 0.05 I_K]	11.5	< 0.05	87.9

Table 5.6. Regression constants for stepwise regression analysis of the light saturated rate of production (P_{max}) with assimilation number and phytoplankton standing crop (as B, mean chlorophyll a concentration in the euphotic zone) in 1980-81 and 1982-83.

Year	Variable	Variance ratio F	Significance	% variation accounted for.
1980-81	Assimilation number	36.2	< 0.05	47.5
	Assimilation number + B	85.3	< 0.05	83.5
1982-83	Assimilation number	43.6	< 0.05	43.6
	Assimilation number + B	85.2	< 0.05	85.2

Table 5.7. Variation in predictive capability of Talling's model (as the ratio of predicted value of ΣA (ΣA_T) : actual value determined planimetrically (ΣA_P)) in relation to values of assimilation number, phytoplankton standing crop (as B, mean chlorophyll a concentration in the euphotic zone), I_K and K_d(PAR) on selected occasions.

$\Sigma A_T : \Sigma A_P$	Assimilation number mg C/mg Chl a/h	B mg Chl a/m^3	I_K $\mu E/m^2/s$	K_d(PAR) ln units/m
0.6	1.76	8.9	165.5	5.48
2.4	11.1	8.2	92.9	1.8
1.1	6.98	3.86	224.5	1.63
1.1	1.83	6.13	83.2	4.39
1.0	1.74	6.83	103.7	5.27
1.0	2.4	6.31	172.6	3.27
1.0	13.0	6.82	276.1	3.02
1.0	5.0	4.11	89.4	1.9
1.0	7.3	6.14	66.3	2.1

Table 5.8. Regression constants for simple regression analysis of assimilation number and mean irradiance at depth where P_{max} was measured (I_{opt}) with mean irradiance during incubation (I_{IN}) and one day (I_{PRE1}), two (I_{PRE2}) or three days (I_{PRE3}) prior to sampling, temperature and K_d(PAR) in 1980-81 and 1982-83.

Year	Variable	Variance ratio F	Significance	%variation accounted for.
1980-81	I_{IN}	0.02	n.s	-
	I_{PRE1}	0.9	n.s	2
	I_{PRE2}	4.0	< 0.05	9
	I_{PRE3}	2.3	n.s	6
	Temperature	3.4	n.s	8
	K_d(PAR)	0.4	n.s	1
1982-83	I_{IN}	4.7	< 0.05	11
	I_{PRE1}	0.2	n.s	-
	I_{PRE2}	1.4	n.s	3
	I_{PRE3}	1.0	n.s	2
	Temperature	22.7	< 0.05	37
	K_d(PAR)	5.9	< 0.05	13

Table 5.9. Regression constants for simple regression analysis of mean irradiance at depth where P_{max} was measured (I_{opt}) with mean irradiance during incubation (I_{IN}) and one day (I_{PRE1}), two (I_{PRE2}) or three days (I_{PRE3}) prior to sampling, in 1980-81 and 1982-83.

Year	Variable	Variance ratio F	Significance	%variation accounted for.
1980-81	I_{IN}	9	< 0.05	18
	I_{PRE1}	0.01	n.s	-
	I_{PRE2}	0.9	n.s	2
	I_{PRE3}	0.5	n.s	1
1982-83	I_{IN}	4.5	n.s	9
	I_{PRE1}	0.7	n.s	2
	I_{PRE2}	0.3	n.s	1
	I_{PRE3}	0.4	n.s	1

Table 5.10. A comparison of Lake Midmar primary productivity data (as values of P_{max} and ΣA) with a range of African lakes, for which there are comparable data

Lake	P_{max} mg $C/m^3/h$	ΣA mg $C/m^2/h$	Source
Chad (Chad)	66 - 336	61 - 318	Lemoalle(1973)
Crescent Island			
Crater (Kenya)	19 - 68	105 - 293	Melack(1979)
Hartbeespoort (S.Africa)	12 - 5916	46 - 3381	Robarts(1984)
McIlwaine (Zimbabwe)	155 - 653	248 - 653	Robarts(1979)
Midmar (S.Africa) 1980-81	2 - 22	3 - 29	This study
1982-83	1 - 104	3 - 103	This study
Naivasha (Kenya)	56 - 90	128 - 214	Melack(1979)
Oloiden (Kenya)	98 - 281	146 - 420	Melack(1979)
Swartvlei (S.Africa)	5 - 13	13 - 37	Robarts(1962)
Winam Gulf (Kenya)	86 - 240	150 - 341	Melack(1979)
Wuras (S.Africa)	45 - 420	19 - 192	Stegmann(1982)

Table 5.11. Regression constants for simple regression analysis of actual values of ΣA, assimilation number, the photosynthetic saturation parameter (I_K) and the photosynthetic efficiency (P_e) with $Z_{eu} : Z_m$ ratio and water column stability in 1980-81 and 1982-83.

Year	Variable	Variance ratio F	Significance	% variation accounted for.
		$Z_{eu} : Z_m$		
1980-81	ΣA	0.7	n.s	2
	Assimilation number	0.4	n.s	1
	I_K	-	n.s	-
	P_e	1.0	n.s	2
1982-83	ΣA	0.2	n.s	-
	Assimilation number	-	n.s	-
	I_K	-	n.s	-
	P_e	0.4	n.s	1
		Water column stability		
1980-81	ΣA	0.6	n.s	1
	Assimilation number	5.1	< 0.05	11
	I_K	1.0	n.s	3
	P_e	0.4	n.s	1
1982-83	ΣA	4.5	< 0.05	10
	Assimilation number	1.8	n.s	4
	I_K	0.2	n.s	1
	P_e	0.6	n.s	1

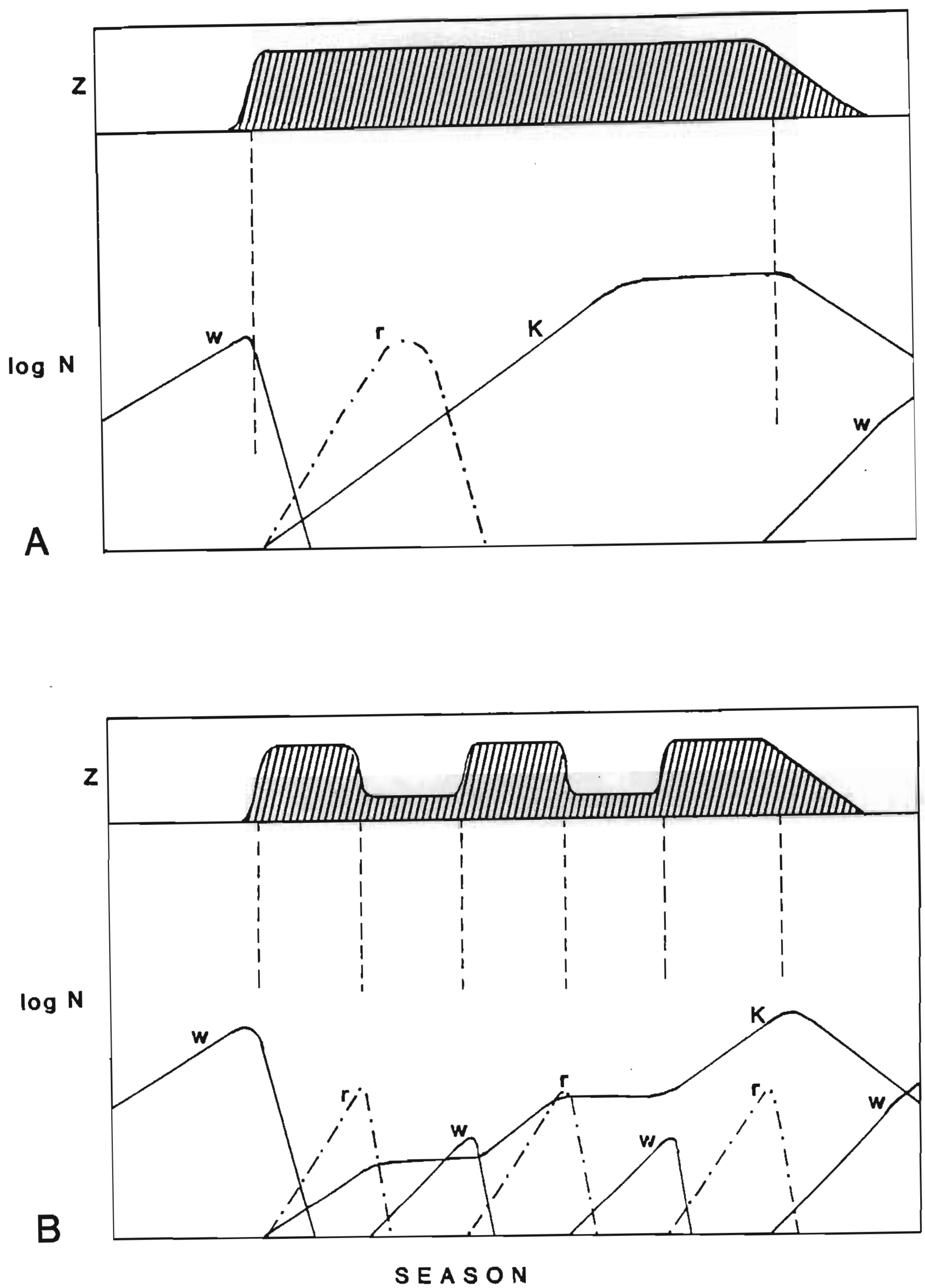

Figure 6.1. Stylised seasonal progression of change in standing populations (N) of three species of phytoplankton (w = diatom, representative of mixed conditions; r = relatively fast-growing, r - selected species and K = slow-growing, K-selected species) in relation to the cycle of stratification (shaded area) and destratification of the water column (Z) in **a)** a classicical stratified lake and **b)** a stratified lake exhibiting atelomixis. Modified from Reynolds <u>et</u> <u>al</u> (1983).

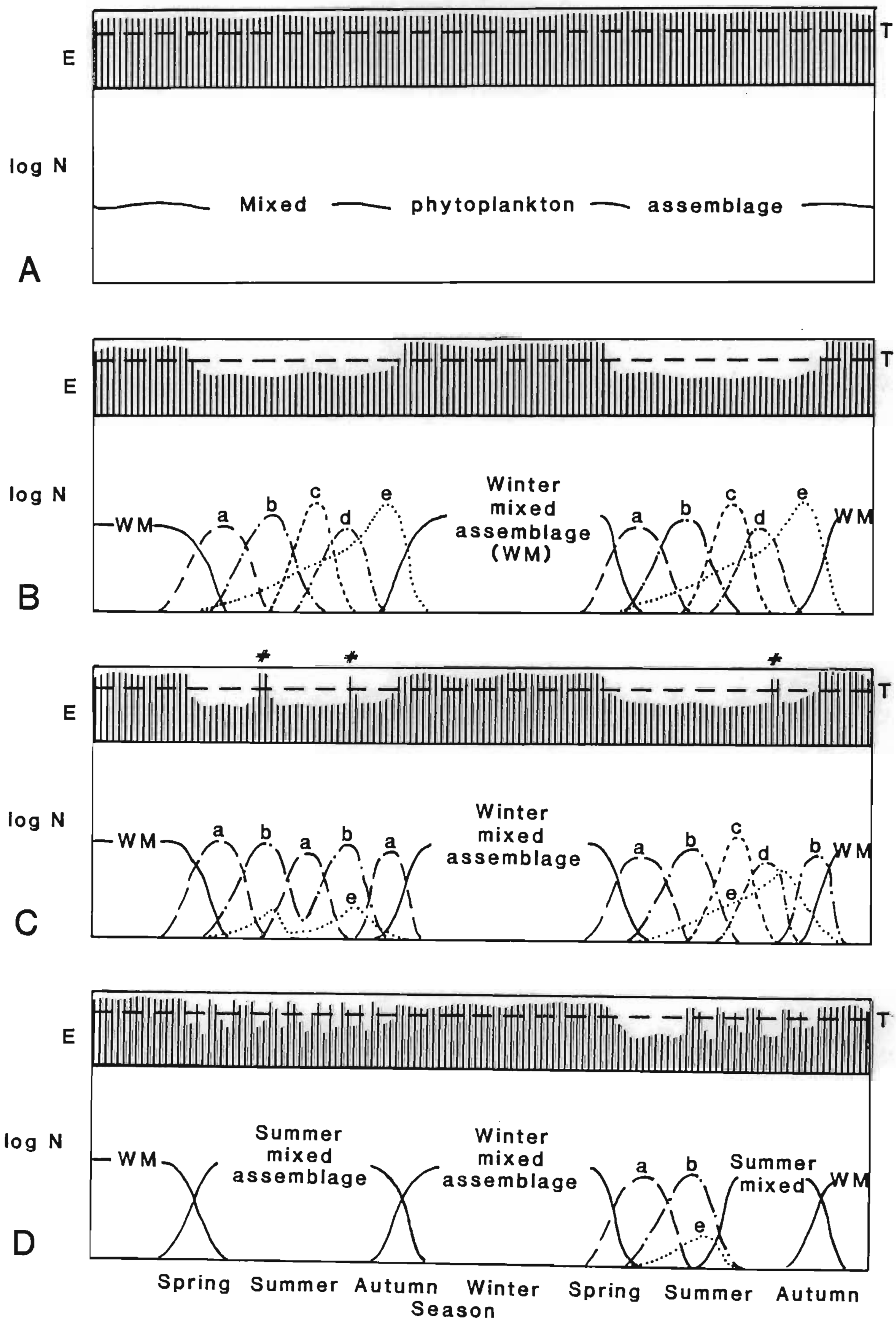
T
E
log N
Mixed phytoplankton assemblage
A
WM
a
b
c
d
e
Winter
mixed
assemblage
(WM)
B
C
Summer
mixed
assemblage
D
Summer
mixed
Spring
Summer
Autumn
Winter
Season

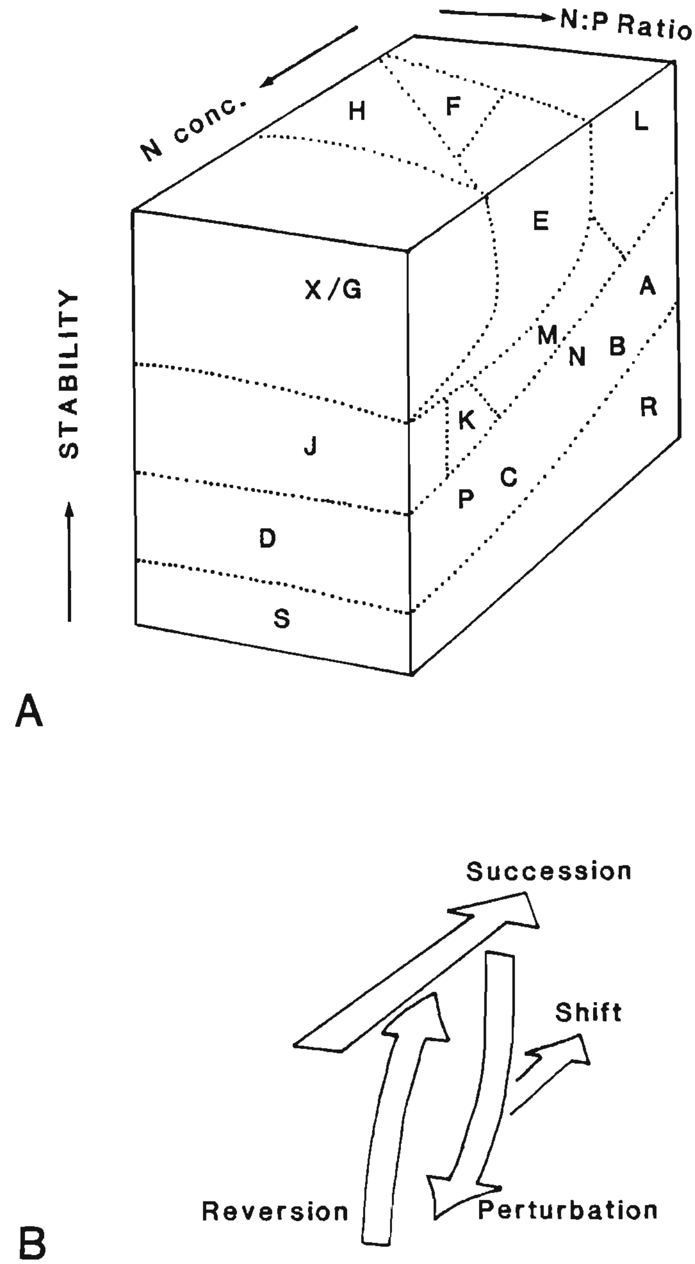

Figure 6.3. a) A hypothetical 3-D matrix with axes defined by i) mixing /stability, ii) the concentrations of nitrogen (N) and phosphorus (P) and iii) the N/P ratio which accommodates most phytoplankton assemblages (indicated by capital letters in matrix).

b) The three directions of periodic progression from one dominant assemblage to another: from given starting coordinates, autogenic successional changes are traced in the nutrient concentration/ratio plane; increased mixing ('perturbation') at any time, causes movements in all three planes to new coordinates from which a new 'shifted' succession may be initiated or, as the system becomes less mixed, a 'reversion' to a previous dominant assemblage may occur. From Reynolds (1984 b).

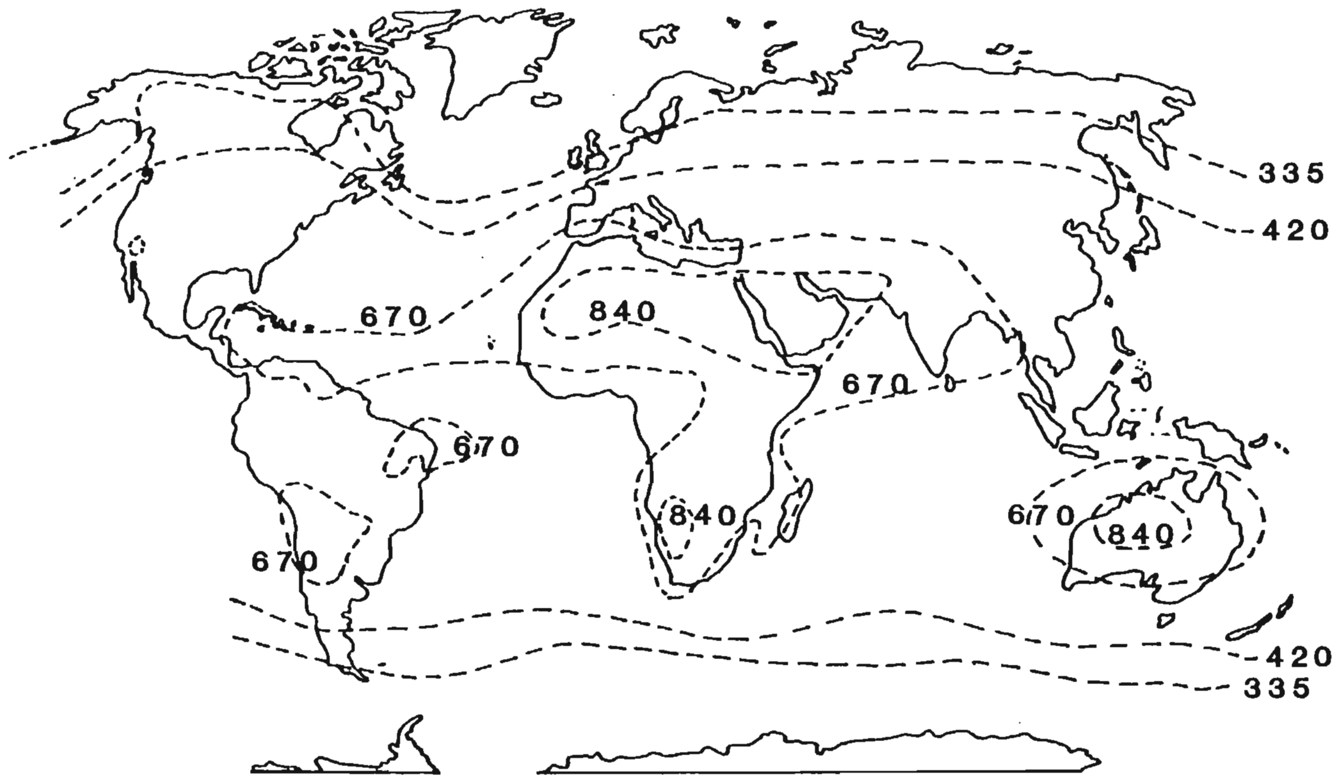

Figure 6.4 Annual average solar irradiance (300 - 2200nm, units x10^7 J/m^2/yr) reaching the earth's surface. From Geiger (1965, in Larcher (1975)).

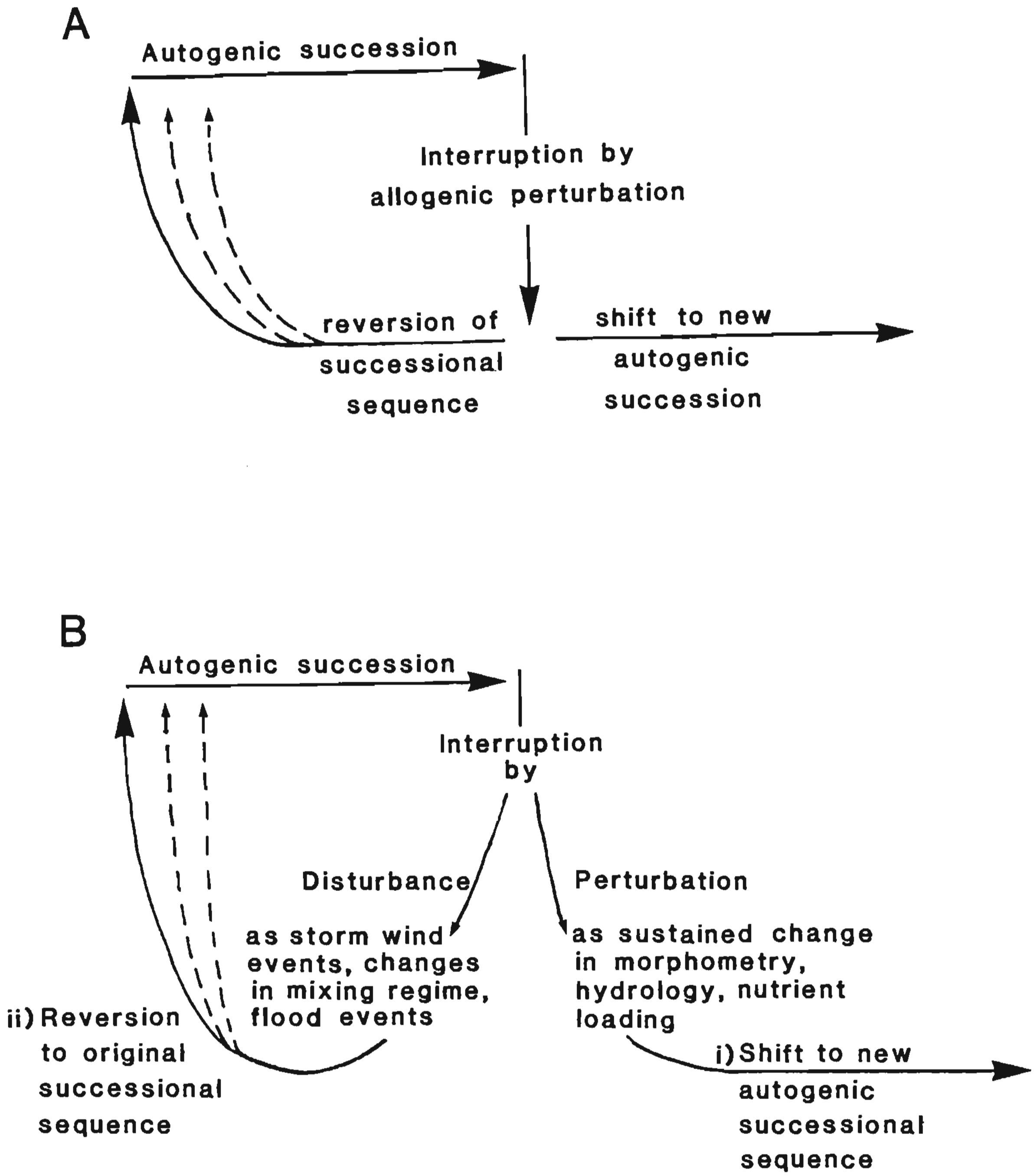

Figure 6.5. Diagrammatic representation of the three directions of periodic progression from one dominant phytoplankton assemblage to another.

a) Starting at a fixed coordinate, autogenic succession (temporal changes in phytoplankton species composition) proceeds until interrupted by allogenic perturbation, at the cessation of which the successional pattern may either: i) return to the original successional sequence or ii) shift to a new autogenic sequence, as proposed by Reynolds (1984 b). From: Ashton (1985).

b) Starting at a fixed coordinate, autogenic succession proceeds until interrupted by i) disturbance, short term modification of established environmental gradients, at the cessation of which there is reversion to the original successional sequence, or ii) perturbation, longer term (sustained) changes in environmental